



Tennessee Valley Authority, 1101 Market Street, Chattanooga, TN 37402

CNL-17-082

July 3, 2017

10 CFR 52, Subpart A

ATTN: Document Control Desk  
U.S. Nuclear Regulatory Commission  
Washington, DC 20555-0001

Clinch River Nuclear Site  
NRC Docket No. 52-047

Subject: Submittal of Supplemental Information Associated with Site Safety Analysis Report Section 2.5 in Support of the Clinch River Nuclear Site Early Site Permit Application

- References:
1. Letter from TVA to NRC, CNL-16-081, "Application for Early Site Permit for Clinch River Nuclear Site," dated May 12, 2016
  2. NRC Memorandum, "Audit Plan for Areas Covered in Section 2.5 of the Site Safety Analysis Report, Clinch River Nuclear Site Early Site Permit Application," issued April 19, 2017

By letter dated May 12, 2016 (Reference 1), Tennessee Valley Authority (TVA) submitted an application for an early site permit for the Clinch River Nuclear (CRN) Site in Oak Ridge, TN. Between May 8 and 9, 2017, the NRC conducted an audit of the geology, seismology, and geotechnical engineering information contained in the CRN Site Early Site Permit Application (ESPA) (Reference 2). During the face-to-face portion of the NRC audit held at the TVA offices in Knoxville, TN, and at the CRN Site, the NRC requested that TVA provide supplemental information associated with SSAR Section 2.5, "Geology, Seismology, and Geotechnical Engineering," to reflect the information that TVA provided during the NRC audit.

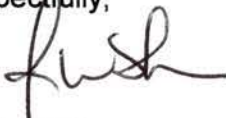
The enclosure to this letter provides supplemental information discussed during the NRC audit for geotechnical engineering (GE) information needs GE-01, GE-02, and GE-03. Attachments 1 and 2 of the enclosure provide copies of technical reports related to information needs GE-01 and GE-02. Attachment 3 of the enclosure provides SSAR markups for information needs GE-01, GE-02, and GE-03. The SSAR markups will be incorporated in a future revision of the early site permit application.

U.S. Nuclear Regulatory Commission  
CNL-17-082  
Page 2  
July 3, 2017

There are no new regulatory commitments associated with this submittal. If any additional information is needed, please contact Dan Stout at (423) 751-7642.

I declare under penalty of perjury that the foregoing is true and correct. Executed on this 3rd day of July 2017.

Respectfully,



J. W. Shea  
Vice President, Nuclear Regulatory Affairs & Support Services

Enclosure:

Supplemental Information Regarding Site Safety Analysis Report (SSAR) Section 2.5,  
"Geology, Seismology and Geotechnical Engineering"

cc (w/ Enclosure):

A. Fetter, Project Manager, Division of New Reactor Licensing, USNRC

cc (w/o Enclosure):

V. McCree, Executive Director of Operations, USNRC  
C. Haney, Regional Administrator, Region II, USNRC  
M. Johnson, Deputy Executive Director for Reactor and Preparedness Programs,  
USNRC  
V. Ordaz, Acting Director, Office of New Reactors, USNRC  
F. Akstulewicz, Director, Division of New Reactor Licensing, USNRC  
J. Donoghue, Acting Branch Chief, Division of New Reactor Licensing, USNRC  
M. Sutton, Project Manager, Division of New Reactor Licensing, USNRC  
P. Vokoun, Project Manager, Division of New Reactor Licensing, USNRC  
T. Dozier, Project Manager, Division of New Reactor Licensing, USNRC  
M. M. McIntosh, Regulatory Specialist, Eastern Regulatory Field Office,  
Nashville District, USACE

## ENCLOSURE

### **Supplemental Information Regarding Site Safety Analysis Report (SSAR) Section 2.5, "Geology, Seismology and Geotechnical Engineering"**

By letter dated May 12, 2016 (Reference 1), Tennessee Valley Authority (TVA) submitted an application for an early site permit for the Clinch River Nuclear (CRN) Site in Oak Ridge, TN. Between May 8 and 9, 2017, the NRC conducted an audit of the geology, seismology, and geotechnical engineering information contained in the CRN Site Early Site Permit Application (ESPA) (Reference 2). During the face-to-face portion of the NRC audit held at the TVA offices in Knoxville, TN, and at the CRN Site, the NRC requested that TVA provide supplemental information associated with SSAR Section 2.5, "Geology, Seismology, and Geotechnical Engineering," to reflect the information that TVA provided during the NRC audit.

This enclosure provides supplemental information discussed during the NRC audit for geotechnical engineering (GE) information needs GE-01, GE-02, and GE-03. Attachments 1 and 2 of this enclosure provide copies of technical reports related to information needs GE-01 and GE-02. Attachment 3 of this enclosure provides SSAR markups for information needs GE-01, GE-02, and GE-03. The SSAR markups included in Attachment 3 of this enclosure will be incorporated in a future revision of the ESPA.

#### References:

1. Letter from TVA to NRC, CNL-16-081, "Application for Early Site Permit for Clinch River Nuclear Site," dated May 12, 2016
2. NRC Memorandum from Mallecia Sutton to Allen Fetter, "Audit Plan for Areas Covered in Section 2.5 of the Site Safety Analysis Report, Clinch River Nuclear Site Early Site Permit Application," issued April 19, 2017
3. Letter from TVA to NRC, CNL-16-184, "Submittal of Additional Supplemental Information Related to Stability of Subsurface Materials and Foundation in Support of Early Site Permit Application for Clinch River Nuclear Site," dated December 15, 2016

#### Attachments:

1. Non-Proprietary Report Foundation Assessment Clinch River Nuclear Site, Revision 0
2. Addendum to Non-Proprietary Report Foundation Assessment Clinch River Nuclear Site Revision 0
3. Site Safety Analysis Report Subsection 2.5 Markups

### Supplemental Information Associated with NRC Audit Information Needs:

Following the face-to-face portion of the NRC audit, TVA is providing the following supplemental information associated with the referenced audit Information Need:

#### Supplemental Information associated with NRC Information Need GE-01

During the face-to-face discussions regarding the PLAXIS 2D analysis, the NRC requested a copy of the PLAXIS model report. A copy of the report, "Non-Proprietary Report, Foundation Assessment, Clinch River Nuclear Site," Revision 0, is provided in Attachment 1. In addition, TVA proposed a SSAR change to include a summary of and reference to the report. A summary and reference to the PLAXIS model is being added in new SSAR Subsection 2.5.4.13, "Foundation Assessment Model." This summary also adds new SSAR tables and figures. The current SSAR Subsection 2.5.4.13, "References," is being renumbered as SSAR Subsection 2.5.4.14. See the SSAR markup provided in Subsections 2.5.4.13 and 2.5.4.14 in Attachment 3.

#### Supplemental Information associated with NRC Information Need GE-02

Following face-to-face discussion regarding the bearing capacity and settlement packages, an assessment using PLAXIS 2D analysis software was performed to estimate the ultimate bearing capacity at the CRN Site. The assessment is documented as an addendum to the report provided in the Information Need GE-01 response. A copy of the addendum, "Addendum to Non-Proprietary Report, Foundation Assessment, Clinch River Nuclear Site," Revision 0, is provided in Attachment 2. A summary of the analysis has been included in the last paragraph of the SSAR Subsection 2.5.4.13. See the SSAR markup provided in Attachment 3.

#### Supplemental Information associated with NRC Information Need GE-03

Prior to the seismic audit, TVA had provided in Reference 3 a SSAR Subsection 2.5.1.2.3.4, "Estimation of Hypothetical Large Void," mark-up. After face-to-face discussions during the audit and because TVA established a critical void size as provided in the SSAR Subsection 2.5.4.13 markup provided in the supplemental information associated with NRC Information Need GE-01, SSAR Subsection 2.5.1.2.3.4 is being revised and renamed "Karst Evaluation." See the SSAR markup provided in Subsection 2.5.1.2.3.4 and 2.5.1.2.9 in Attachment 3.

**Attachment 1  
Non-Proprietary Report  
Foundation Assessment  
Clinch River Nuclear Site, Revision 0**

**NON-PROPRIETARY REPORT  
FOUNDATION ASSESSMENT  
CLINCH RIVER NUCLEAR SITE**

**PROJECT No. 16-5737  
REVISION 0  
JUNE 16, 2017**

**RIZZO ASSOCIATES  
PENN CENTER EAST, 500 PENN CENTER BLVD.  
BUILDING 5, SUITE 100  
PITTSBURGH, PENNSYLVANIA 15235  
TELEPHONE: (412) 856-9700  
TELEFAX: (412) 856-9749  
WWW.RIZZOASSOC.COM**





## CHANGE MANAGEMENT RECORD

**Project No.:** 16-5737

**Report Name:** Non-Proprietary Report  
Foundation Assessment  
Clinch River Nuclear Site

REVISION NO.	DATE	DESCRIPTIONS OF CHANGES/AFFECTED PAGES
0	June 16, 2017	Initial Submittal



# TABLE OF CONTENTS

	<b>PAGE</b>
LIST OF TABLES .....	7
LIST OF FIGURES .....	8
1.0 INTRODUCTION .....	13
1.1 PROJECT DESCRIPTION .....	13
1.2 GEOLOGIC CONDITIONS .....	15
1.2.1 Stratigraphy .....	15
1.2.2 Subsurface Material Properties .....	21
1.2.3 Other Critical Geologic Features Influencing Engineering Conditions .....	21
1.2.4 Engineering Considerations Related to Critical Geologic Features .....	25
2.0 FINITE ELEMENT MODELING OF FOUNDATION CONDITIONS .....	29
2.1 MODEL LAYERING .....	29
2.1.1 Discontinuity and Shear Fracture Zone Cases Considered .....	30
2.1.2 Stress Conditions .....	38
2.1.3 2-D PLAXIS Models for Site A and Site B .....	38
3.0 RESULTS .....	59
3.1 CAVITY DIAMETERS .....	59
3.2 CAVITY DEPTHS .....	61
3.3 CAVITY LOCATIONS .....	62
3.4 EMBEDMENT DEPTHS .....	64
3.5 OVERALL MODEL LOADING RESULTS .....	65
4.0 SUMMARY AND RECOMMENDATIONS .....	76
5.0 REFERENCES .....	78



## TABLE OF CONTENTS (CONTINUED)

### APPENDICES:

APPENDIX A	STRATIGRAPHIC UNIT DEPTHS IN INDIVIDUAL CLINCH RIVER NUCLEAR SITE BORINGS
APPENDIX B	BEST ESTIMATE ENGINEERING PROPERTIES VALUES FOR CLINCH RIVER NUCLEAR SITE STRATIGRAPHIC UNITS
APPENDIX C	GEOLOGIC CROSS SECTIONS OF THE CRBRP EXCAVATION AND SLOPES
APPENDIX D	CAVITIES IN INDIVIDUAL CLINCH RIVER NUCLEAR SITE BORINGS



## LIST OF TABLES

TABLE NO.	TITLE	PAGE
TABLE 1-1	STRATIGRAPHIC UNITS ENCOUNTERED AT THE CLINCH RIVER NUCLEAR SITE.....	16
TABLE 1-2	AVERAGE TRUE AND APPARENT STRATIGRAPHIC UNIT THICKNESS (FROM SSAR TABLE 2.5.4-26).....	19
TABLE 1-3	PRIMARY AND SECONDARY JOINTING OBSERVED IN ATV DATA LOGS (ADAPTED FROM SSAR SECTION 2.5.1.2.4.3.3).....	22
TABLE 2-1	ANALYZED CASES FOR SITE A .....	36
TABLE 2-2	ROCK MASS PROPERTIES FOR SITES A AND B USED IN FE MODELING .....	42
TABLE 2-3	DISTURBED ROCK MASS PROPERTIES (D=0.7).....	43
TABLE 3-1	MODEL RESULTS IN LOADING PHASES FOR SITES A AND B.....	67



## LIST OF FIGURES

FIGURE NO.	TITLE	PAGE
FIGURE 1-1	LOCATION MAP FOR THE CLINCH RIVER NUCLEAR SITE .....	14
FIGURE 1-2	GEOLOGIC CROSS SECTION FOR THE CLINCH RIVER NUCLEAR SITE .....	17
FIGURE 1-3	JOINT ZONE HEIGHT AND DEPTH DISTRIBUTION (ADAPTED FROM SSAR TABLE 2.5.1-16).....	23
FIGURE 1-4	BAR GRAPH OF SHEAR FRACTURE ZONE THICKNESSES IN SITE BORINGS (ADAPTED FROM SSAR TABLE 2.5.1-17).....	24
FIGURE 1-5	BAR GRAPH OF CAVITIES IN SITE BORINGS (ADAPTED FROM SSAR TABLE 2.5.1-11).....	26
FIGURE 1-6	SHEAR FRACTURE ZONE THICKNESS AND DEPTH DISTRIBUTION (ADAPTED FROM SSAR FIGURE 2.5.1-60).....	27
FIGURE 1-7	CAVITY HEIGHT AND DEPTH DISTRIBUTION FOR CRN SITE BORINGS (ADAPTED FROM SSAR FIGURE 2.5.1-52) .....	28
FIGURE 2-1	GEOLOGIC CROSS SECTION A-A' FOR SITE A.....	31
FIGURE 2-2	GEOLOGIC CROSS SECTION E-E' FOR SITE A.....	32
FIGURE 2-3	GEOLOGIC CROSS SECTION B-B' FOR SITE B.....	33
FIGURE 2-4	GEOLOGIC CROSS SECTION F-F' FOR SITE B .....	34
FIGURE 2-5	LOCATION OF SECTIONS USED IN SITE A AND SITE B MODELS .....	35
FIGURE 2-6	FOUNDATION EVALUATION CASES CONSIDERED FOR SITE A .....	37
FIGURE 2-7	FOUNDATION EVALUATION CASES CONSIDERED FOR SITE B.....	37
FIGURE 2-8	A TYPICAL MODEL WITH REFINED MESH .....	44
FIGURE 2-9	TYPICAL MODEL INTERFACE ELEMENT LOCATED ALONG A BEDDING PLANE.....	45
FIGURE 2-10	SITE A, CROSS SECTION: A-A', CAVITY DIAMETER: 15FT, EMBEDMENT DEPTH: 40FT, CAVITY DEPTH: 5FT BELOW FOUNDATION, CAVITY LOCATION: CENTER OF NI.....	47



**TABLE OF FIGURES  
(CONTINUED)**

<b>FIGURE NO.</b>	<b>TITLE</b>	<b>PAGE</b>
FIGURE 2-11	SITE A, CROSS SECTION: A-A', CAVITY DIAMETER: 15FT, EMBEDMENT DEPTH: 40FT, CAVITY DEPTH: 30FT BELOW FOUNDATION, CAVITY LOCATION: CENTER OF COMMON BASEMAT .....	48
FIGURE 2-12	SITE A, CROSS SECTION A-A' SITE A, CROSS SECTION: A-A', CAVITY DIAMETER: 15FT, EMBEDMENT DEPTH: 40FT, CAVITY DEPTH: 30FT BELOW FOUNDATION, CAVITY LOCATION: EDGE OF COMMON BASEMAT, ON BEDDING PLANE .....	48
FIGURE 2-13	SITE A, CROSS SECTION: A-A', CAVITY DIAMETER: 15FT, EMBEDMENT DEPTH: 40FT, CAVITY DEPTH: 30FT BELOW FOUNDATION CAVITY LOCATION: EDGE OF COMMON BASEMAT, ON BEDDING PLANE, TWO SHEAR JOINT INTERFACES BASED ON BORING LOGS AND WEAK SILTSTONE REPRESENTATION.....	49
FIGURE 2-14	SITE A, CROSS SECTION: A-A', CAVITY DIAMETER: 15FT, EMBEDMENT DEPTH: 90FT, CAVITY LOCATION: 30FT BELOW EDGE OF COMMON BASEMAT, BEDDING PLANE, SHEAR JOINT INTERFACE.....	49
FIGURE 2-15	SITE A, CROSS SECTION: A-A', CAVITY DIAMETER: 15FT, EMBEDMENT DEPTH: 140FT, CAVITY DEPTH: 5FT BELOW FOUNDATION, CAVITY LOCATION: EDGE OF COMMON BASEMAT, ON BEDDING PLANE, SHEAR JOINT INTERFACE .....	50
FIGURE 2-16	SITE A, CROSS SECTION: E-E', CAVITY DIAMETER: 15FT, EMBEDMENT DEPTH: 40FT, CAVITY DEPTH: 5FT BELOW FOUNDATION, CAVITY LOCATION: CENTER OF COMMON BASEMAT .....	50
FIGURE 2-17	SITE A, CROSS SECTION: E-E', CAVITY DIAMETER: 15FT, EMBEDMENT DEPTH: 40FT, CAVITY DEPTH: 30FT BELOW FOUNDATION, CAVITY LOCATION: CENTER OF COMMON BASEMAT .....	51
FIGURE 2-18	SITE A, CROSS SECTION: E-E', CAVITY DIAMETER: 15FT, EMBEDMENT DEPTH: 90FT, CAVITY DEPTH: 5FT BELOW FOUNDATION, CAVITY LOCATION: CENTER OF COMMON BASEMAT .....	51



## TABLE OF FIGURES (CONTINUED)

FIGURE NO.	TITLE	PAGE
FIGURE 2-19	SITE A, CROSS SECTION: E-E', CAVITY DIAMETER: 15FT, EMBEDMENT DEPTH: 90FT, CAVITY DEPTH: >30FT BELOW FOUNDATION, CAVITY LOCATION: EDGE OF COMMON BASEMAT, ON THE BEDDING PLANE.....	52
FIGURE 2-20	SITE A, CROSS SECTION: E-E', CAVITY DIAMETER: 15FT, EMBEDMENT DEPTH: 140FT, CAVITY DEPTH: 30FT BELOW FOUNDATION, CAVITY LOCATION: EDGE OF COMMON BASEMAT.....	52
FIGURE 2-21	SITE B, CROSS SECTION: B-B', CAVITY DIAMETER: 15FT, EMBEDMENT DEPTH: 40FT, CAVITY DEPTH: 5FT BELOW FOUNDATION, CAVITY LOCATION: CENTER OF COMMON BASEMAT .....	53
FIGURE 2-22	SITE B, CROSS SECTION: B-B', CAVITY DIAMETER: 15FT, EMBEDMENT DEPTH: 40FT, CAVITY DEPTH: 30FT BELOW FOUNDATION, CAVITY LOCATION: CENTER OF COMMON BASEMAT .....	54
FIGURE 2-23	SITE B, CROSS SECTION: B-B', CAVITY DIAMETER: 15FT, EMBEDMENT DEPTH: 40FT, CAVITY DEPTH: 30FT BELOW FOUNDATION, CAVITY LOCATION: EDGE OF COMMON BASEMAT WITH SHEAR FRACTURE ZONE INTERFACE.....	54
FIGURE 2-24	SITE B, CROSS SECTION: B-B', CAVITY DIAMETER: 15FT, EMBEDMENT DEPTH: 90FT, CAVITY DEPTH: 5FT BELOW FOUNDATION, CAVITY LOCATION: CENTER OF COMMON BASEMAT WITH SHEAR FRACTURE ZONE INTERFACE.....	55
FIGURE 2-25	SITE B, CROSS SECTION: B-B', CAVITY DIAMETER: 15FT, EMBEDMENT DEPTH: 90FT, CAVITY DEPTH: 5FT BELOW FOUNDATION, CAVITY LOCATION: EDGE OF COMMON BASEMAT WITH SHEAR FRACTURE ZONE INTERFACE .....	55
FIGURE 2-26	SITE B, CROSS SECTION: B-B', CAVITY DIAMETER: 15FT, EMBEDMENT DEPTH: 140FT, CAVITY DEPTH: 5FT BELOW FOUNDATION, CAVITY LOCATION: ON BEDDING PLANE WITH SHEAR FRACTURE ZONE INTERFACE.....	56
FIGURE 2-27	SITE B, CROSS SECTION: F-F', CAVITY DIAMETER: 15FT, EMBEDMENT DEPTH: 40FT, CAVITY DEPTH:	



## TABLE OF FIGURES (CONTINUED)

FIGURE NO.	TITLE	PAGE
	5FT BELOW FOUNDATION CAVITY LOCATION: CENTER OF COMMON BASEMAT .....	56
FIGURE 2-28	SITE B, CROSS SECTION: F-F', CAVITY DIAMETER: 15FT, EMBEDMENT DEPTH: 40FT, CAVITY DEPTH: 30FT BELOW FOUNDATION, CAVITY LOCATION: CENTER OF COMMON BASEMAT .....	57
FIGURE 2-29	SITE B, CROSS SECTION: F-F', CAVITY DIAMETER: 15FT, EMBEDMENT DEPTH: 90FT, CAVITY DEPTH: 5FT BELOW FOUNDATION, CAVITY LOCATION: CENTER OF COMMON BASEMAT WITH SHEAR FRACTURE ZONE INTERFACE .....	57
FIGURE 2-30	SITE B, CROSS SECTION: F-F', CAVITY DIAMETER: 15FT, EMBEDMENT DEPTH: 90FT, CAVITY DEPTH: 30FT BELOW FOUNDATION, CAVITY LOCATION: EDGE OF COMMON BASEMAT ON THE BEDDING PLANE WITH SHEAR FRACTURE ZONE INTERFACE.....	58
FIGURE 2-31	SITE B, CROSS SECTION: F-F', CAVITY DIAMETER: 15FT, EMBEDMENT DEPTH: 140FT, CAVITY DEPTH: 5FT BELOW FOUNDATION, CAVITY LOCATION: ON THE BEDDING PLANE WITH SHEAR FRACTURE ZONE INTERFACE .....	58
FIGURE 3-1	EXAMPLE RELATIVE SHEAR VALUE RESULTS FOR 15 FT (LEFT), 10 FT (CENTER), AND 5 FT (RIGHT) CAVITY HEIGHTS .....	60
FIGURE 3-2	EXAMPLE VERTICAL DEFORMATION VALUE RESULTS FOR 15 FT (LEFT), 10 FT (CENTER), AND 5 FT (RIGHT) CAVITY HEIGHTS .....	60
FIGURE 3-3	EXAMPLE RELATIVE SHEAR VALUE RESULTS FOR CAVITY DEPTHS OF 5 FT (LEFT) AND 30 FT (RIGHT) BELOW FOUNDATION BASEMAT .....	61
FIGURE 3-4	EXAMPLE VERTICAL DEFORMATION RESULTS FOR CAVITY DEPTHS OF 5 FT (LEFT) AND 30 FT (RIGHT) BELOW FOUNDATION BASEMAT .....	62
FIGURE 3-5	EXAMPLE RELATIVE SHEAR VALUE RESULTS FOR CAVITY LOCATIONS 5 FT BELOW FOUNDATION BASEMAT (LEFT) AND ON A BEDDING PLANE DISCONTINUITY (RIGHT).....	63
FIGURE 3-6	EXAMPLE VERTICAL DEFORMATION RESULTS FOR CAVITY LOCATIONS 5 FT BELOW	



**TABLE OF FIGURES  
(CONTINUED)**

<b>FIGURE NO.</b>	<b>TITLE</b>	<b>PAGE</b>
	FOUNDATION BASEMAT (LEFT) AND ON A BEDDING PLANE DISCONTINUITY (RIGHT).....	63
FIGURE 3-7	EXAMPLE RELATIVE SHEAR VALUE RESULTS FOR FOUNDATION EMBEDMENT DEPTHS OF 40 FT (LEFT), 90 FT (CENTER), AND 140 FT (RIGHT) .....	64
FIGURE 3-8	EXAMPLE RESULTS FOR VERTICAL DEFORMATIONS FOR FOUNDATION EMBEDMENT DEPTHS OF 40 FT (LEFT), 90 FT (CENTER), AND 140 FT (RIGHT) .....	65
FIGURE 3-9	SITE A CROSS SECTION A-A' FOUNDATION DEPTH 40 FT CAVITY (15 FT) ON THE BEDDING PLANE INTERFACE RELATIVE SHEAR=0.85.....	68
FIGURE 3-10	SITE A CROSS SECTION A-A' FOUNDATION DEPTH 90 FT CAVITY (15 FT) ON THE BEDDING PLANE INTERFACE RELATIVE SHEAR=0.90.....	69
FIGURE 3-11	SITE A CROSS SECTION A-A' FOUNDATION DEPTH 140 FT CAVITY (15 FT) ON THE BEDDING PLANE INTERFACE RELATIVE SHEAR=0.85.....	70
FIGURE 3-12	SITE B CROSS SECTION B-B' FOUNDATION DEPTH 40 FT CAVITY (15 FT) LOCATED 30 FT BELOW EDGE OF COMMON BASEMAT RELATIVE SHEAR=0.95 .....	71
FIGURE 3-13	SITE B CROSS SECTION B-B' FOUNDATION DEPTH 90 FT CAVITY (15 FT) LOCATED 5 FT BELOW EDGE OF COMMON BASEMAT RELATIVE SHEAR=0.90 .....	72
FIGURE 3-14	SITE B CROSS SECTION B-B' FOUNDATION DEPTH 140 FT CAVITY (15 FT) LOCATED 5 FT BELOW CENTER OF COMMON BASEMAT ON BEDDING PLANE INTERFACE RELATIVE SHEAR=0.92.....	73
FIGURE 3-15	EFFECT OF INTERFACE ON SITE B RESPONSE CROSS SECTION B-B', CAVITY 30 FT BELOW EDGE OF COMMON BASEMAT, ON SHEAR ZONE INTERFACE MAXIMUM VERTICAL DEFORMATION = -9.34E-3 FT .....	74
FIGURE 3-16	EFFECT OF INTERFACE ON SITE B RESPONSE CROSS SECTION B-B' CAVITY 30 FT BELOW EDGE OF COMMON BASEMAT, ON SHEAR ZONE INTERFACE MAXIMUM VERTICAL DEFORMATION = -6.27E-3 FT (RIGHT).....	75



# NON-PROPRIETARY REPORT FOUNDATION ASSESSMENT CLINCH RIVER NUCLEAR SITE

## 1.0 INTRODUCTION

This Report discusses a foundation assessment for proposed Small Modular Reactors (SMRs) at the Tennessee Valley Authority (TVA) Clinch River Nuclear (CRN) Site, in support of TVA's Early Site Permit (ESP) Application for the SMRs. This assessment involves finite element (FE) modeling, using PLAXIS 2D analysis software, to determine potential karstic cavity impacts on SMR foundations.

### 1.1 PROJECT DESCRIPTION

Proposed development of the CRN Site includes four SMRs configured as pairs (Units 1&2 and Units 3&4) in a northwest to southeast orientation. Units 1&2, located to the north, are identified as SMR Site A as shown on *Figure 1-1*. Units 3&4, in a more southerly location, are identified as SMR Site B.

In general, information on foundation loads, foundation dimensions, foundation thicknesses, and deformation limits (e.g., angular distortion or differential settlement) are required in a PLAXIS 2D or similar analysis to determine the minimum size of an undetected cavity that could adversely affect foundation performance. These parameters are technology dependent. Since an SMR technology has not yet been selected for the CRN Site, the structures in the PLAXIS 2D model presented here reflect a typical nuclear power plant layout. In the model, the major safety related structures are assumed to rest on a common basemat. A Final Plant Grade at EL 821 feet (ft) North American Vertical Datum of 1988 (NAVD88) is used for the common basemat area. Multiple foundation embedment depths (40 ft, 90 ft, and 140 ft below the ground surface) were considered.



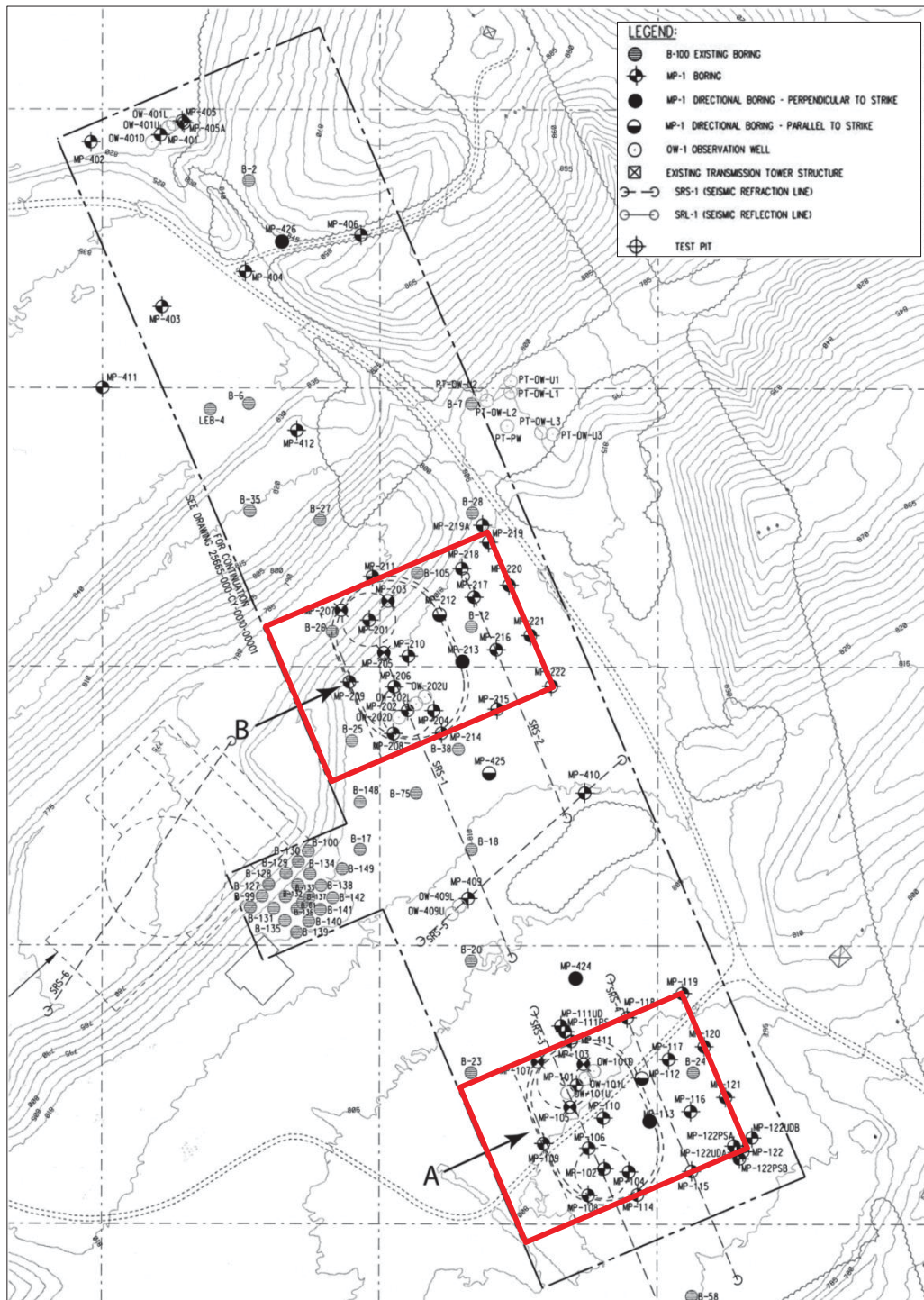


**FIGURE 1-1  
LOCATION MAP FOR THE CLINCH RIVER NUCLEAR SITE**



The site is characterized as having karst features that include open and clay filled cavities, and weathered and fractured zones with dissolution. Cavities are encountered primarily in the Rockdell Formation and the Eidson Formation, and in smaller numbers in near surface exposures (to depths of approximately 100 ft below ground surface) of the Benbolt Formation and Blackford Formations. Using PLAXIS 2D FE modeling, critical CRN Site karst cavity sizes and locations were evaluated. In particular, three different cavity sizes (5 ft, 10 ft, and 15 ft diameters) and two different cavity depths below foundation level (5 ft and 30 ft) were evaluated, as were multiple cavity locations (namely on the edge of the Nuclear Island (NI), the center of the NI, and along bedding planes) for both Site A and Site B with static stress conditions.

## 1.2 GEOLOGIC CONDITIONS

Detailed information related to the physical geography (physiography) and geology of the CRN Site is provided in Section 2.5.1.2 of the ESP Application Site Safety Analysis Report (SSAR). Stratigraphic relationships and geologic features and geologic engineering conditions critical to modeling of safety-related foundations at the CRN Site are summarized hereinafter in **Section 1.2.1 and Section 1.2.2**, respectively using information from the CRN Site ESP SSAR and from published studies on geologic conditions in eastern Tennessee and wider CRN Site area, including data from Site geotechnical investigations.

### 1.2.1 Stratigraphy

Surface exposed stratigraphic units in the proposed location of Site A and Site B power block areas include (from northwest to southeast and oldest to youngest) undifferentiated Kingsport Formation and Mascot Dolomite (Newala Formation) rocks of the Knox Group, and rock masses assigned to the Blackford Formation, Eidson and Fleanor members of the Lincolnshire Formation, and Rockdell and Benbolt Formations of the Chickamauga Group, as summarized in **Table 1-1** and shown on **Figure 1-2**. In general, Newala Formation rocks are estimated as lower Ordovician in age (488.3 mega-annum [Ma] to 471.8 Ma). Unconformable Chickamauga Group rocks are middle Ordovician in age (471.8 Ma to 460.9 Ma).



**TABLE 1-1  
STRATIGRAPHIC UNITS ENCOUNTERED AT THE  
CLINCH RIVER NUCLEAR SITE**

GROUP <sup>(1)</sup>	AGE <sup>(2)</sup>	FORMATION <sup>(3)</sup>	
Chickamauga Group	Middle Ordovician	Moccasin Formation	
		Witten Formation	
		Bowen Formation	
		Benbolt Formation	
		Rockdell Formation	
		Lincolnshire Formation	Fleanor Member
			Eidson Member
Knox Group	Lower Ordovician	Blackford Formation	
		Newala Formation	Mascot Dolomite
			Kingsport Formation

**Notes:**

- (1) Newala Formation rock represents only the uppermost component of the Knox Group in the larger Clinch River Site region.
- (2) Estimated age.
- (3) Moccasin Formation and Witten Formation rocks do not specifically crop out in Site A and Site B power block areas and consequently are not discussed here. Also, the Mascot Dolomite and Kingsport Formation are generally not differentiated at the Clinch River Site.

Deformation related to the Alleghanian Orogeny (*ca.* 330 Ma to 265 Ma) has resulted in a relatively uniform strike and dip directions (i.e., structural orientations) in Knox and Chickamauga Group rocks underlying Site A and Site B power block locations. In particular, acoustic televiewer (ATV) logging data suggest a prominent 063° strike and 33° (southeast) dip to bedding planes under the proposed locations of Units 1&2 and 3&4 (SSAR Section 2.5.1.2.4.3.2) (*Figure 1-2*).

Strike and dip directions estimated from borehole orientations for Fleanor Member and Rockdell Formation upper contacts (i.e., upper bound) similarly suggest a 051° to 053° strike and southeast (32° to 36°) dip to Site A and Site B rock (Bechtel, 2014). Detailed geologic mapping and inspection in northern and southern portions of the Clinch River Breeder Reactor Plant



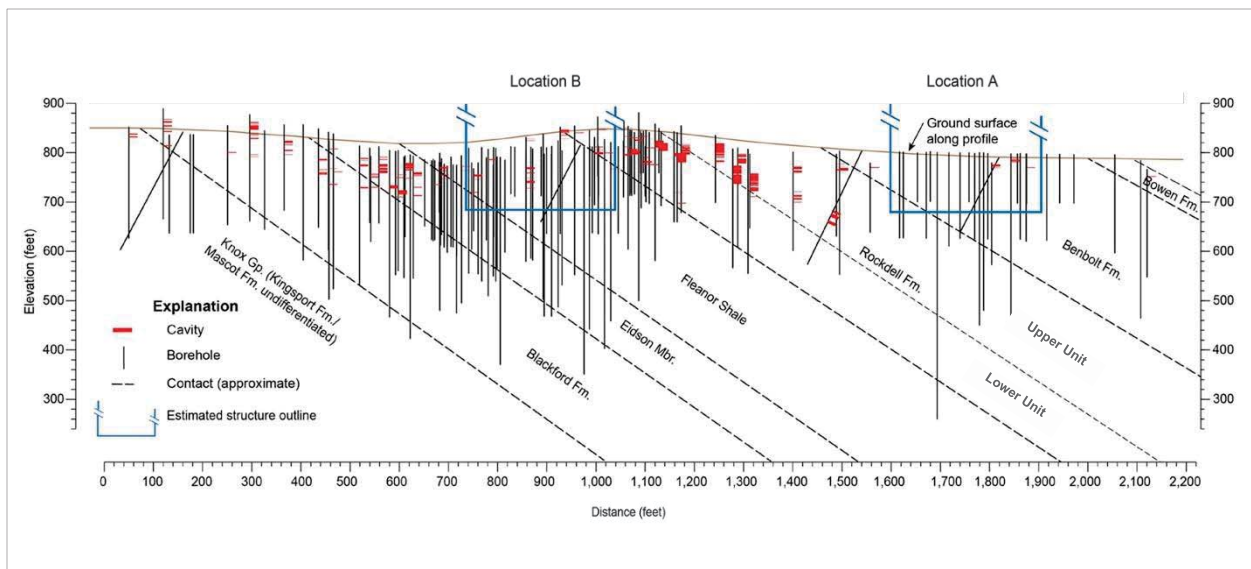


**FIGURE 1-2  
GEOLOGIC CROSS SECTION FOR THE CLINCH RIVER NUCLEAR SITE**

CRBRP Nuclear Island (NI), and CRBRP equalization basin excavations adjacent to Site A and Site B also revealed average bedding strike and dip orientations of 060° and 33° southeast, 053° and 33° southeast, and 053° 35° southeast, respectively (Drakulich, 1984).

It is important to note that excavations for SMR Units 1&2 (Site A) and 3&4 (Site B) at the CRN Site are expected to be located entirely in Chickamauga Group formations. Nevertheless, bedding orientations are expected to expose different Chickamauga Group strata at power block excavation levels in Site A and Site B. Specifically, Units 1&2 are expected to be founded on Benbolt Formation rock mass, whereas Units 3&4 are expected to be founded on rock ascribed to the Fleanor Member of the Lincolnshire Formation.

Each of the stratigraphic units exposed at the CRN Site (as shown on *Figure 1-2*) or encountered in the core (per *Appendix A*) is described in more detail, below, in *Section 1.2.1.1 through Section 1.2.1.5*.

### 1.2.1.1 Newala Formation (Knox Group)

Both the Kingsport Formation and Mascot Dolomite (i.e., undifferentiated Newala Formation) are primarily composed of medium-gray to light-gray, fine-grained to medium-grained dolomite



(Hatcher et al., 1992). Fine-grained pale-pink to grayish-pink dolomite is also common in the uppermost Kingsport Formation, and in the Mascot Dolomite. Massively bedded calcilutite (lime mudstone) is similarly common in the lowermost Kingsport Formation, but is less common in the Mascot Formation.

Hatcher et al. (1992) have suggested that Mascot Dolomite thickness ranges from 250 feet (ft) to 500 ft in CRN Site areas, owing to erosional topographic relief on the unconformable contact with the overlying Blackford Formation, as further described hereinafter in **Section 1.2.1.2**. Kingsport Formation rocks, in turn are reportedly 300 ft to 500 ft thick in the greater CRN Site area (Hatcher et al., 1992).

Data from borings positioned near Site A and Site B (i.e., data specific to Units 1&2 and 3&4) do not provide information on the full extent of the Mascot Dolomite or Kingsport Formation, as no SMR project related borings fully penetrated Newala Formation rocks at the CRN Site (*Appendix A*).

#### **1.2.1.2 Blackford Formation (Chickamauga Group)**

Unconformably overlying Newala Formation rock units, the Blackford Formation includes a lowermost pale-olive limestone and a purplish-maroon dolomitic limestone overlain by a relatively thick upper sequence of purplish to maroon siltstone, pale-olive limestone, and (Hatcher et al., 1992). SSAR Section 2.5.1.2.3.3 similarly describes a Lower Blackford Formation rock unit containing moderately to thickly bedded gray micritic limestone, and an Upper Blackford Formation containing gray, laminated to moderately bedded, calcareous siltstone.

Total Blackford Formation thickness in the greater CRN Site area has been estimated to range from 230 ft to 260 ft (Hatcher et al., 1992). The average apparent thickness of the Blackford Formation under Units 1&2 and 3&4 (Sites A and B) is estimated to be approximately 254 ft (*Table 1-2*).



**TABLE 1-2  
AVERAGE TRUE AND APPARENT STRATIGRAPHIC UNIT THICKNESS  
(FROM SSAR TABLE 2.5.4-26)**

UNIT <sup>(1)</sup>	THICKNESS <sup>(2)</sup>	UNITS 1&2 <sup>(3)</sup>			UNITS 3&4 <sup>(4)</sup>		
		THICKNESS	TOP		THICKNESS	TOP	
	DEPTH		ELEVATION	DEPTH		ELEVATION	
	(ft)	(ft)	(ft bgs)	(ft)	(ft)	(ft bgs)	(ft)
Benbolt	330 (277)	147	41	780	-	-	-
Rockdell	287 (241)	287	188	633	-	-	-
Fleanor	257 (216)	257	475	346	128	41	780
Eidson	102 (86)	102	732	89	102	169	652
Blackford	254 (213)	254	834	-13	254	271	550
Newala	-	-	1,088	-267	-	525	296

**Notes:**

ft = feet

ft bgs = ft below ground surface

- (1) Stratigraphic unit. Rocks of the Benbolt Formation, the Rockdell Formation, the Fleanor and Eidson members of the Lincolnshire Formation, and the Blackford Formation are considered part of the larger Chickamauga Group in the CRN Site area. Newala Formation rock represents the uppermost component of the Knox Group.
- (2) The average apparent vertical thickness and true thickness (parenthetical value) for critical stratigraphic units in the CRN Site area. According to SSAR Section 2.5.4.1.1, the apparent (vertical) thickness of each stratigraphic unit was estimated from projections of contacts between stratigraphic units assuming an average bedding plane dip of 33° (see also **Section 1.2.1**, herein). True stratigraphic unit thickness is calculated as the product of the apparent thickness and the cosine of the 33° average bedding plane dip (0.83867) (SSAR Section 2.5.4.1.1).
- (3) The stratigraphic unit vertical thickness and top depth and elevation under SMR Units 1&2 (Site A). The thickness and top depth and elevation for the Benbolt Formation are estimated for a truncated subsurface profile considering only sound rock.
- (4) The stratigraphic unit vertical thickness and top depth and elevation under SMR Units 3&4 (Site B). The thickness and top depth and elevation for the Fleanor Formation are estimated for a truncated subsurface profile considering only sound rock. Benbolt Formation and Rockdell Formation rock are not exposed in Site B.

Laboratory and field material testing suggest no significant difference in lower and Upper Blackford Formation physical properties (SSAR Section 2.5.4.2.1.9). As a result, from an overall engineering characterization standpoint, both the lower and Upper Blackford Formation can be considered as a single unit.

### 1.2.1.3 Lincolnshire Formation (Chickamauga Group)

Across most of eastern Tennessee, the Lincolnshire Formation includes three distinct lithologies identified as the Eidson, Fleanor, and Hogskin members, although only Eidson Member and



Fleanor Member rocks are exposed in CRN Site areas (Hatcher et al., 1992). Rock of the Eidson and Fleanor members is specifically expected to be exposed in Site B (Units 3&4) power block excavations (*Figure 1-2*).

Hatcher et al. (1992) described Eidson Member rock in CRN Site areas as a massive to nodular limestone containing bedded and nodular cherts, and indicated a laterally variable average thickness of 65 ft for the unit. In CRN Site borings, Eidson Member rock maintains an average apparent thickness of approximately 102 ft (*Table 1-2*) and is described as a gray colored, laminated to thinly-bedded, argillaceous, micritic limestone (SSAR Sections 2.5.1.2.3.3).

Fleanor Member rock in turn is described in CRN Site borings as a red (or maroon) calcareous siltstone containing gray limestone interbeds (SSAR Section 2.5.1.2.3.3). Lowermost and uppermost portions of the Fleanor Member have been described as including a distinct olive-gray calcareous siltstone (Hatcher et al., 1992).

The average apparent thickness of the Fleanor Member of the Lincolnshire Formation is estimated to be approximately 257 ft in the overall CRN Site area (*Table 1-2*) (SSAR Section 2.5.4.2.1.7).

#### **1.2.1.4 Rockdell Formation (Chickamauga Group)**

Overlying the Eidson and Fleanor members of the Lincolnshire Formation, the Rockdell Formation is a thick (approximately 260 ft to 280 ft) limestone mass that grades upward from light-gray calcarenite, dark-gray calcareous siltstone, and fossiliferous nodular and micritic limestone to dense calcarenite containing abundant bedded and nodular chert (Hatcher et al., 1992).

Based on recent field investigations, SSAR Section 2.5.1.2.3.3 describes the lowermost Rockdell Formation as a gray to bluish-gray to dark-gray thinly to moderately bedded limestone containing some thin calcareous siltstone interbeds and chert beds, lenses, and nodules, and the uppermost Rockdell Formation as a light-brownish-gray, gray, bluish-gray, or dark-gray laminated to moderately bedded micritic limestone containing minimal calcareous siltstone interbeds and few chert beds and lenses.

The average apparent thickness of the Rockdell Formation (based on recent borings) is estimated to be approximately 287 ft (*Table 1-2*) (SSAR Section 2.5.4.2.1.6).



### 1.2.1.5 Benbolt Formation (Chickamauga Group)

Hatcher et al. (1992) described the Benbolt Formation as an interbedded mass of fossiliferous nodular limestone, un-fossiliferous amorphous micrite in a dark-gray siltstone matrix, more massive dark-gray siltstone, and un-fossiliferous calcarenite. SSAR Sections 2.5.1.2.3.3 and 2.5.4.2.1.5 describe the Benbolt Formation (in core) as a gray to bluish- to dark bluish-gray, very thinly- to thinly-bedded nodular limestone. Borings also indicate two distinct calcareous siltstone interbeds located approximately 16 ft and 44 ft above the Benbolt Formation's contact with the underlying Rockdell Formation.

The apparent vertical thickness of the Benbolt Formation based on recent borings is approximately 330 ft (*Table 1-2*). Hatcher et al. (1992) similarly suggested that the Benbolt Formation is roughly 360 ft to 380 ft in thick.

### 1.2.2 Subsurface Material Properties

Best estimate engineering properties values for Newala Formation, Blackford Formation, Eidson and Fleanor members of the Lincolnshire Formation, and Rockdell Formation and Benbolt Formation rock masses are provided in *Appendix B*, as based on field investigation and material testing data presented in SSAR Section 2.5.4.

It should be noted that Appendix B includes material properties weathered rock and existing fill and residual soil expected to be excavated from Site A and Site power block areas prior to foundation construction. Accordingly, Appendix B materials properties are not entirely relevant to the FE modeling. Instead, rock mass properties based on the Geological Strength Index (GSI) are used in the PLAXIS 2D models for Sites A and B, and thus include considerations for bedding plane discontinuities, joints, shear fractures, and other structures, as described below, in *Section 1.2.3*. Specific details related to GSI-based rock mass properties are provided in *Section 2.0*.

### 1.2.3 Other Critical Geologic Features Influencing Engineering Conditions

Other critical geologic features in Site A and Site B power block areas potentially influencing SMR Units 1&2 and 3&4 foundation performance include bedding planes and joints, deformation (shear fracture) zones, and potential karst features (i.e., cavities). Brief discussions of each geologic structure are provided hereinafter, in *Section 1.2.3.1 through Section 1.2.3.3*.



Corresponding implications for subsurface stability (resulting from geologic features) are in turn discussed in *Section 1.2.4*.

### 1.2.3.1 Bedding Planes and Joints/Fractures (Discontinuities)

As described in *Section 1.2.1*, field mapping and ATV logging data indicate that bedding planes under Units 1&2 and 3&4 (i.e., in Site A and Site B) and in other CRN Site areas strike predominantly from 050° to 065° and dip roughly 30° to 40° southeast.

ATV logs also indicate two principal fracture (i.e., joint) sets in CRN Site areas, one set oriented (on average) parallel to bedding plane strike and perpendicular to bedding plane dip, striking 240° and dipping 59° north-northwest, and another set oriented parallel to both bedding plane strike and dip, on average striking 060° and dipping 38° southeast (*Table 1-3*). Secondary joint sets observed in ATV logs are reported as near vertical (73° to 74°, on average) and oriented both parallel and normal to bedding plane strike. In core, most joints are described as hairline or open joints, and characterized as planar, discontinuous, or irregular.

It should be noted that ATV data indicate that joints occur in highest frequency in the upper 100 ft of rock under Site A and Site B (as shown on *Figure 1-3*). Per SSAR Section 2.5.4.1.3.1, primary joint sets (Sets 1 and 2 in *Table 1-3*) occur in each stratigraphic unit. Secondary joint sets (Sets 3, 4, and 5) in contrast are observed primarily in the Newala Formation.

**TABLE 1-3  
PRIMARY AND SECONDARY JOINTING OBSERVED IN ATV DATA LOGS  
(ADAPTED FROM SSAR SECTION 2.5.1.2.4.3.3)**

JOINT SET <sup>(1)</sup>	STRIKE <sup>(2)</sup>	DIP <sup>(3)</sup>	DIP DIRECTION <sup>(4)</sup>
1	240°	59°	330°
2	060°	38°	150°
3	060°	73°	-
4	140°	74°	-
5	322°	73°	-

**Notes:**

- (1) Joint sets 1 and 2 are described in SSAR Section 2.5.1.2.4.3.3 as primary joint (fracture) sets. Sets 3, 4, and 5 represent secondary joint sets.
- (2) As reported in SSAR Section 2.5.1.2.4.3.3.
- (3) As reported in SSAR Section 2.5.1.2.4.3.3.
- (4) As reported in SSAR Figure 2.5.1-38, Sheet 5. Secondary joint dip directions were not directly reported and are not provided here.



CRBRP related excavation mapping per Drakulich (1984) and Kummerle and Benvie (1987) likewise indicated major bedding plane joints striking 052° and 050° and dipping 37° southeast and 58° northwest, respectively, similar to Joint Sets 1 and 2 in *Table 1-3*. Drakulich (1984) and Kummerle and Benvie (1987) also identified joint sets striking 335° and 295° and dipping 80° southwest and 75° northeast, respectively.

Excluding bedding separation related joints, Drakulich (1984) ascribed joint formation primarily to syndepositional settlement, or syndeformational (synorogenic) compression and tension.

### 1.2.3.2 Shear Fracture Zones

Previous CRBRP drilling investigations provided evidence for multiple slickensided joint and bedding surfaces in CRN Site areas, including a prominent re-healed shear zone in Eidson Member (Lincolnshire Formation) rock from 37 borings, ranging from 19 ft to 46 ft in total thickness (SSAR Section 2.5.1.2.4.3.4 and CRBRP PSAR Section 2.5.1.2.4.3).

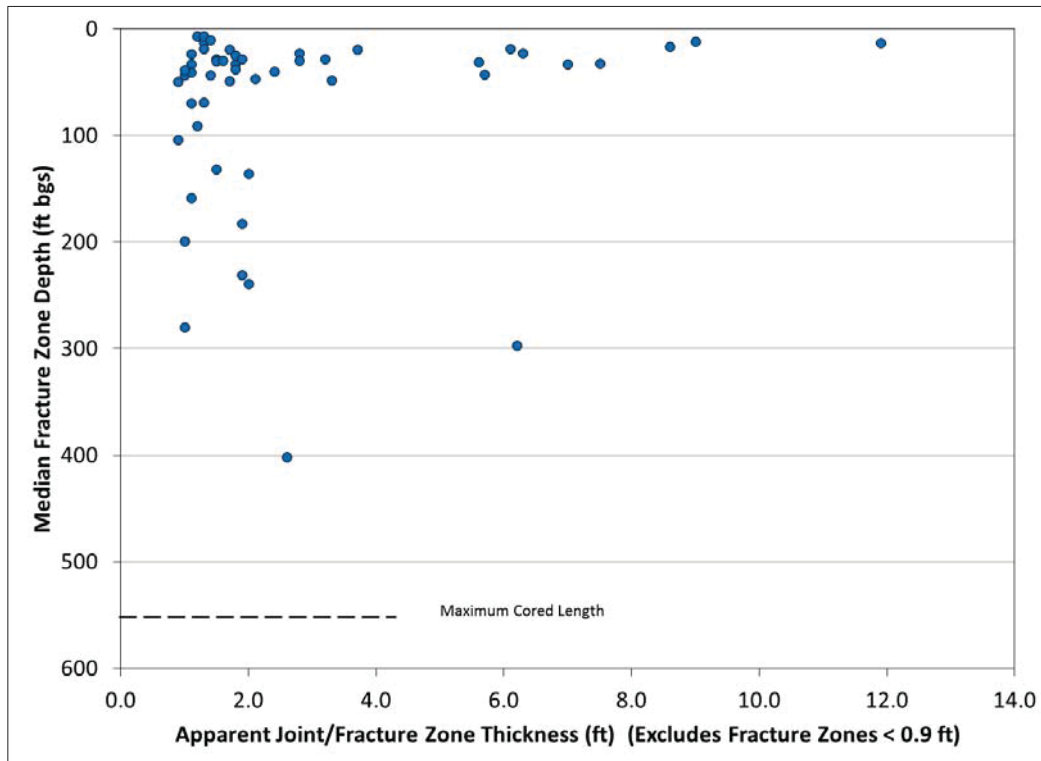


**FIGURE 1-3  
JOINT ZONE HEIGHT AND DEPTH DISTRIBUTION  
(ADAPTED FROM SSAR TABLE 2.5.1-16)**



Drakulich (1984) similarly identified shear fracture zones in CRBRP foundation excavations, but suggested that the aforementioned deformation in Eidson Member limestone units extended into Blackford Formation siltstone (*Appendix C*). Drakulich (1984) also mapped a prominent shear zone in Rockdell Formation exposures. According to Drakulich (1984), both zones provide evidence for bedding plane slips that transition to upright or overturned folds and small-scale thrust or reverse faults.

Similar structures (multiple zones of bedding-parallel, closely spaced calcite-healed fractures) were identified in the core from the Eidson Member of the Lincolnshire Formation and in the core from the Rockdell and Benbolt formations during field investigations specific to SMR Units 1&2 and 3&4 (*Figure 1-4*) (SSAR Sections 2.5.1.2.4.3.4, 2.5.1.2.6.4, and 2.5.4.1.3.2). Eidson Member deformational zones (i.e., shear fracture zones) range in thickness from 1 ft to 18 ft, and average 4 ft. Shear joint zone thickness in the Rockdell and Benbolt formations ranges from 1 ft to 7 ft (and average 3 ft).

It should be noted that the most significant (thickest) shear fracture zone reported in Eidson Member core collected from SMR Units 1&2 and 3&4 areas is interpreted to be the same structure observed in CRBRP drilling and excavation mapping.

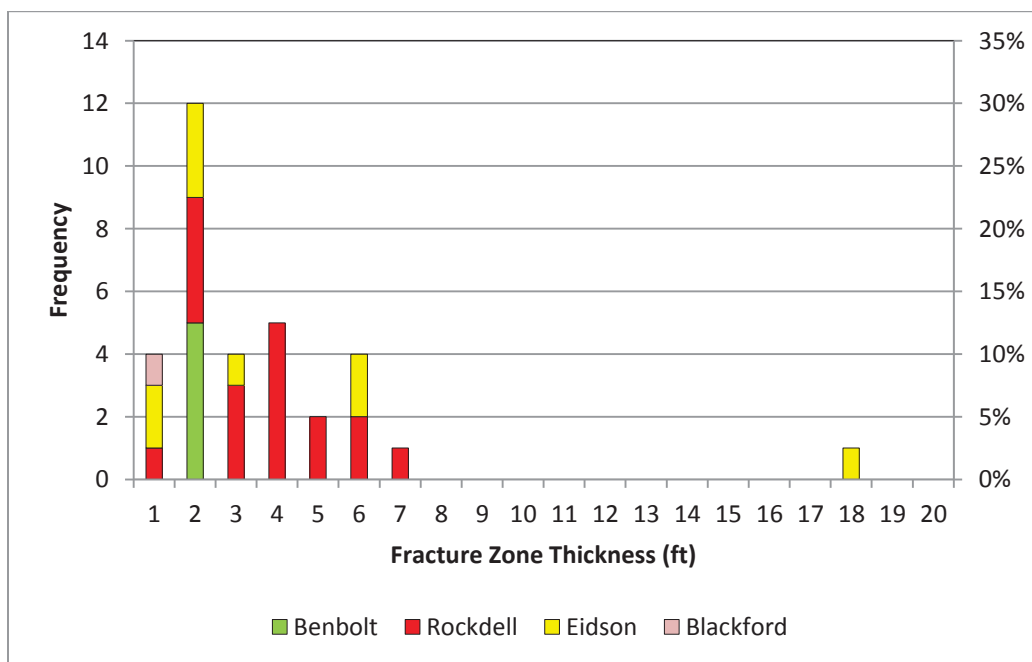


**FIGURE 1-4**  
**BAR GRAPH OF SHEAR FRACTURE ZONE THICKNESSES IN SITE BORINGS**  
**(ADAPTED FROM SSAR TABLE 2.5.1-17)**



### 1.2.3.3 Karst Features

In general, cavity systems in Knox Group rocks in the greater CRN Site area are well developed and extensive. Cavities in Chickamauga Group rocks are less extensive, but have been reported in each stratigraphic unit underlying Site A and Site B. More relevant to SMR Sites A and B, Drakulich (1984) reported a general absence of cavities in Chickamauga Group exposures at bedrock depths greater than 75 ft in CRBRP foundation excavations, but suggested that rock cavities could be found at almost any depth in the underlying Knox Group. Nevertheless, Drakulich (1984) did note cavities in Eidson Member equivalent rock units, and in Rockdell Formation equivalent rock.

Field investigations for SMR Units 1&2 and 3&4 similarly suggest that cavities are present in each of the stratigraphic units at the CRN Site, but occur most frequently in the Rockdell Formation and Eidson Member of the Lincolnshire Formation (*Figure 1-5*). Most cavities in Site A and Site B area borings (75 percent of the cavities identified in borings) are estimated or interpreted to be less than 1.6 ft in height, and rarely exceed 5.0 ft in height. Excepting one 6.3 ft cavity in the Newala Formation, larger cavities (in excess of 5.0 ft, but less than 17 ft) occur only in borings from the Rockdell Formation and Eidson Member.

### 1.2.4 Engineering Considerations Related to Critical Geologic Features

Kummerle and Benvie (1987) previously suggested that the intersection of bedding planes and/or joint sets and excavations in general created potential failure planes for CRBRP foundations. However, Drakulich (1984) noted that fractures in CRBRP excavations became actual detachment surfaces only on direct physical impact (namely blasting). In particular, excavation damage was described as only slight displacements of rock blocks bounded by discontinuities (e.g., fracture/joint sets). Sub-horizontal rock surfaces (i.e., CRBRP excavation bases and floors) and rock surfaces sloping normal to (opposite in direction to) bedding was also apparently blasted effectively without damage, excepting some large over-breaks.



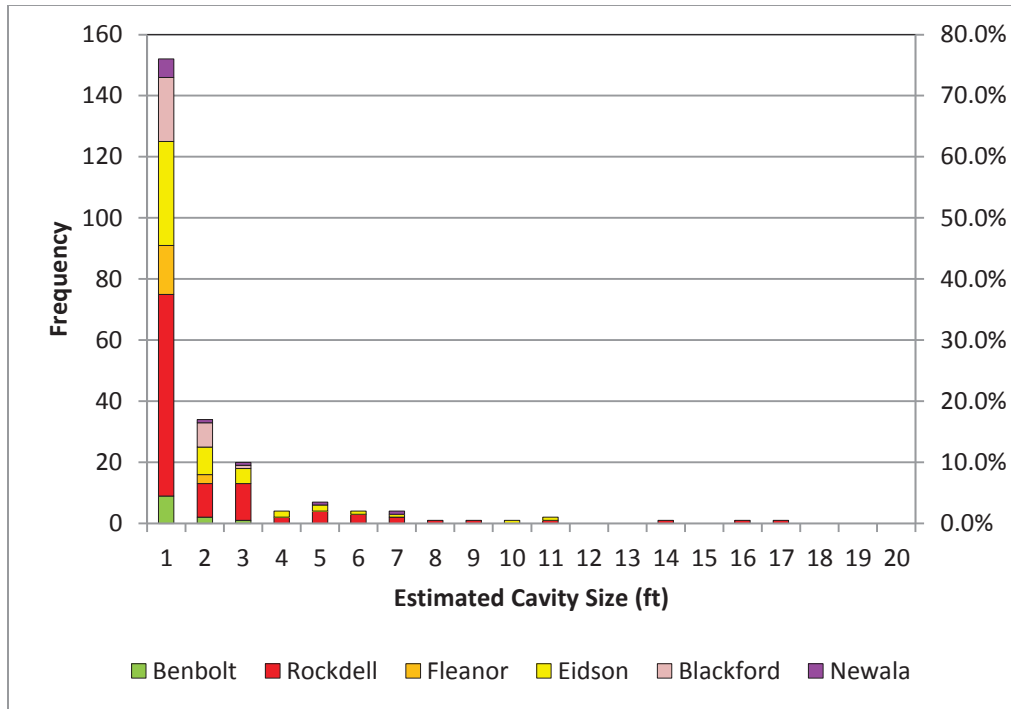


**FIGURE 1-5  
BAR GRAPH OF CAVITIES IN SITE BORINGS  
(ADAPTED FROM SSAR TABLE 2.5.1-11)**

Notwithstanding the above, Drakulich (1984) indicated that bedding separation represented the most frequent rock discontinuity in CRBRP excavations, and suggested that most beds in excavation areas were detached via partings. Accordingly, bedding surface slip is plausible in Site A and Site B, in particular, due to reactivation (opening or shearing) of the significant shear fracture zones located on or near the Blackford Formation and Eidson Member contact and in the Rockdell Formation (as shown in *Appendix C*).

As previously noted in *Section 1.2.3.2*, a conspicuous shear fracture zone was also identified in Rockdell Formation exposures during CRBRP foundation excavations, and is evident in CRN Site borings. Depth distributions of shear fracture zones specifically suggest generalized clusters of sheared rock centered on (roughly) depths of 150 ft and 300 ft in the Rockdell Formation, and at 160 ft in the Eidson Member of the Lincolnshire Formation and 50 ft and 150 ft in the Benbolt Formation (*Figure 1-6*).

Aforementioned shallower (50 ft, 150 ft, and 160 ft) shear zones in the Rockdell and Benbolt formations and Eidson Member roughly coincide with alternatively proposed 40 ft, 90 ft and 150 ft foundation excavation levels for Site A and Site B, and could present potential foundation



failure planes. However, it should be noted that SSAR Section 2.5.4.10.1.2 dismissed general shear failure of the foundation (including sliding along bedding and/or fracture planes) given expected net decreases in bearing pressures (i.e., unloading) at foundation levels. Unloading is expected to result from net changes in pressure from overburden removal during excavation, relative to foundation load (SSAR Section 2.5.4.10.1.2).

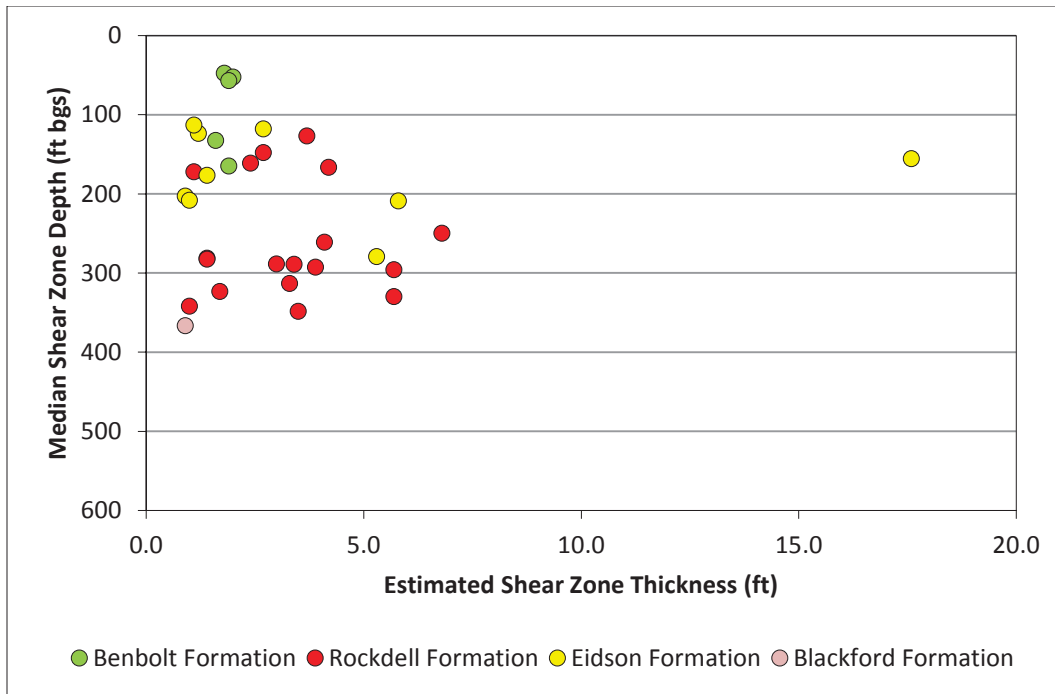


**FIGURE 1-6  
SHEAR FRACTURE ZONE THICKNESS AND DEPTH DISTRIBUTION  
(ADAPTED FROM SSAR FIGURE 2.5.1-60)**

Cavities in Site A and Site B areas also present potential failure loci for SMR Units 1&2 and 3&4 foundations. Numerous cavities occur in Rockdell Formation, Eidson Member, and Blackford Formation rock (10 or more cavities in each of the aforementioned units) at depth equivalents near the proposed 40 ft foundation excavation levels for SMR Units 1&2 and 3&4 (i.e., at 30 ft to 50 ft depths) (*Figure 1-7*). Fewer cavities occur at depths proximal to the alternatively proposed 90 ft foundation level, and include only six cavities each in the Eidson Member of the Lincolnshire Formation and the Blackford Formation, and four in the Rockdell Formation. Only one cavity (in the Rockdell Formation) is inferred for depths between 130 ft and 150 ft (generally equivalent to the proposed 140 ft Units 1&2 and 3&4).



Cavity development in CRN Site areas is generally limited to the most markedly weathered zone immediately below ground surface (to depths less than 100 ft) (**Figure 1-7**). To wit, 75 percent of the reported cavities in CRN Site borings occurred at depths less than approximately 55 ft (**Appendix D**). Consequently, cavity-related failure potential is likely greatest at relatively shallow depth, perhaps to a depth less than about 30 ft.

It should be noted that rock weathering depth limits in Units 1&2 and 3&4 areas, and in CRBRP foundation excavations in particular, have previously been attributed to the general imperviousness of Chickamauga Group siltstone sequences (Drakulich, 1984). Interstitial porosity in the siltstone sequences is considered to be effectively negligible, and much groundwater flow is confined to bedrock discontinuities, namely bedding plane separations and joints and fractures. In the Rockdell Formation, for example, larger cavities in more massive limestone layers appear to be aligned to bedding, in particular at contacts with calcareous siltstone interbeds (SSAR Section 2.5.1.2.5.1.2).

Given the aforementioned conditions, the geologic engineering condition most critical to SMR Units 1&2 and 3&4 safety-related foundations is likely potential cavities located on or along bedding planes, especially more impervious siltstone interbed contacts.

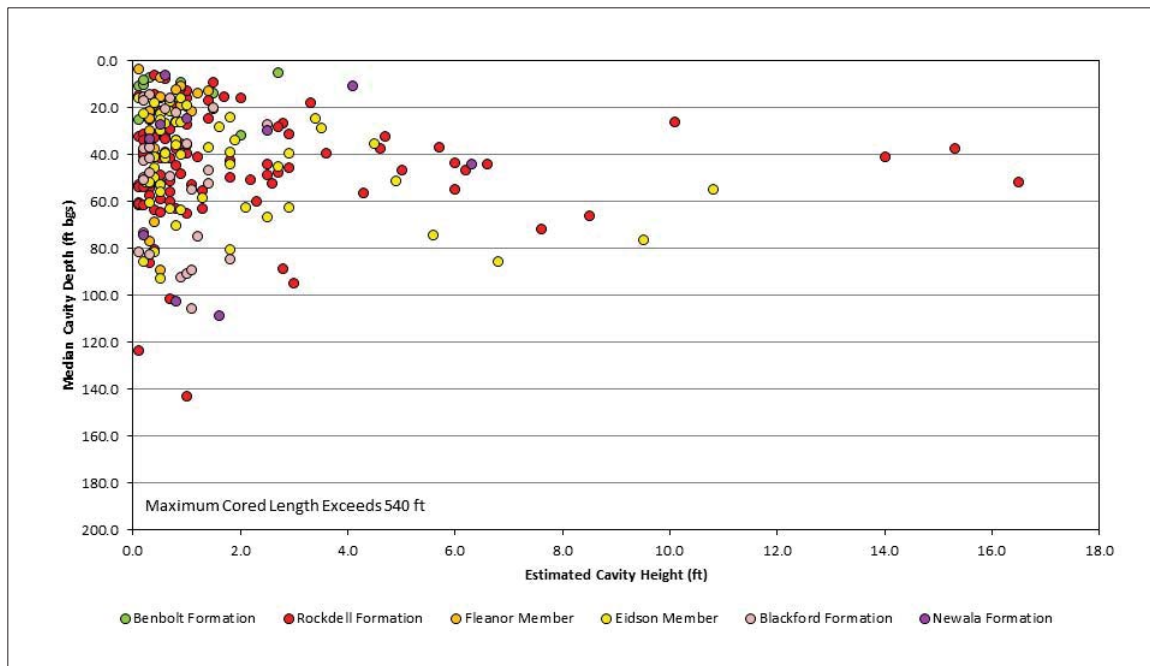


**FIGURE 1-7**  
**CAVITY HEIGHT AND DEPTH DISTRIBUTION FOR CRN SITE BORINGS**  
**(ADAPTED FROM SSAR FIGURE 2.5.1-52)**



## 2.0 FINITE ELEMENT MODELING OF FOUNDATION CONDITIONS

As described in *Section 1.2.4*, potential cavities located on or along bedding planes or in shear fracture zones are considered to be the most critical safety-related engineering conditions for CRN Site SMR Units 1&2 and 3&4. Accordingly, the impact of various cavity sizes and locations on SMR foundation performance were evaluated using PLAXIS 2D FE modeling.

Specifically, the following cavity size and location scenarios were considered in Site A and Site B FE models, for foundation embedment depths of 40 ft, 90 ft, and 140 ft:

- Cavity diameters of 5 ft, 10 ft, and 15 ft;
- Cavity depths of 5 ft and 30 ft below foundation embedment depths; and
- Cavity locations on the edge of the common basemat, the center of the common basemat, and along bedding planes conservatively assumed to feature shear fracture zones or significant discontinuities.

Analyzed cavity diameters were selected based on preliminary analyses that show what size is likely to fail, and observed cavity sizes at the Site.

Model scenarios assumed plane strain in two-dimensional space, static loading conditions, and circular cavity geometries. Conservatively, cavities were modeled as infinitely long tunnels. On the other hand, CRN Site cavities more likely have finite lengths and more ellipsoidal shapes (elongated perpendicular to groundwater flow) owing to phreatic origin.

### 2.1 MODEL LAYERING

As previously indicated in Section 1.2.1, excavations for SMR Site A and Site B are expected to be located entirely in Chickamauga Group formations. However, bedding orientations are expected to expose different Chickamauga Group strata at power block excavation levels in Sites A and B. Specifically, Units 1&2 (Site A) are expected to be founded on Benbolt Formation rock, whereas Units 3&4 (Site B) are expected to be founded on rock ascribed to the Fleanor Member of Lincolnshire Formation.

Bedding plane orientations (i.e., dips) and formation thicknesses used in FE models for Sites A and B were specifically derived from four geologic sections provided in SSAR Section 2.5.4



supporting calculations, as shown on **Figure 2-1 through Figure 2-4** (from Bechtel, 2014). Locations of the cross sections in plant north-south and east-west directions are shown on **Figure 2-5**.

### 2.1.1 Discontinuity and Shear Fracture Zone Cases Considered

As described in **Section 1.2.3.2**, multiple zones of bedding-parallel, closely spaced calcite-healed fractures were identified in core from the Eidson Member of the Lincolnshire Formation and in core from the Rockdell and Benbolt formations during field investigations specific to Site A and Site B. Development of such shear fracture zones in Site A and Site B strata, identified via slickensided surfaces and/or severely warped or brecciated rock, suggests differential movement resulting from regional-scale folding and faulting.

Significant shear fracture zones and arguably less significant bedding plane or general rock mass discontinuities (bedding plane coincident fracture zones, zones of slightly to highly weathered jointing, etc.) were evaluated in the PLAXIS 2D FE analyses by introducing model interface elements. Specifically, these modeled interface elements allow for delineation of potentially weaker planes (strata) in the subsurface, and application of rock strength or stiffness reduction factors to the modeled strata located immediately above or below potential shear fracture zones or bedding discontinuities (assuming fair to poor quality rock).

In particular, PLAXIS 2D modeling for Site A included simulation of discrete interface element located long the Rockdell Formation and Benbolt Formation contact, and simulation of a second interface element approximately 15 ft above the Rockdell and Benbolt formations contact, as summarized in **Table 2-1 and Figure 2-6**. It should be noted that the second (latter) interface element was designed to simulate the lowermost of two potentially weaker calcareous siltstone layers identified in Benbolt Formation cores, as described in **Section 1.2.1.5**.



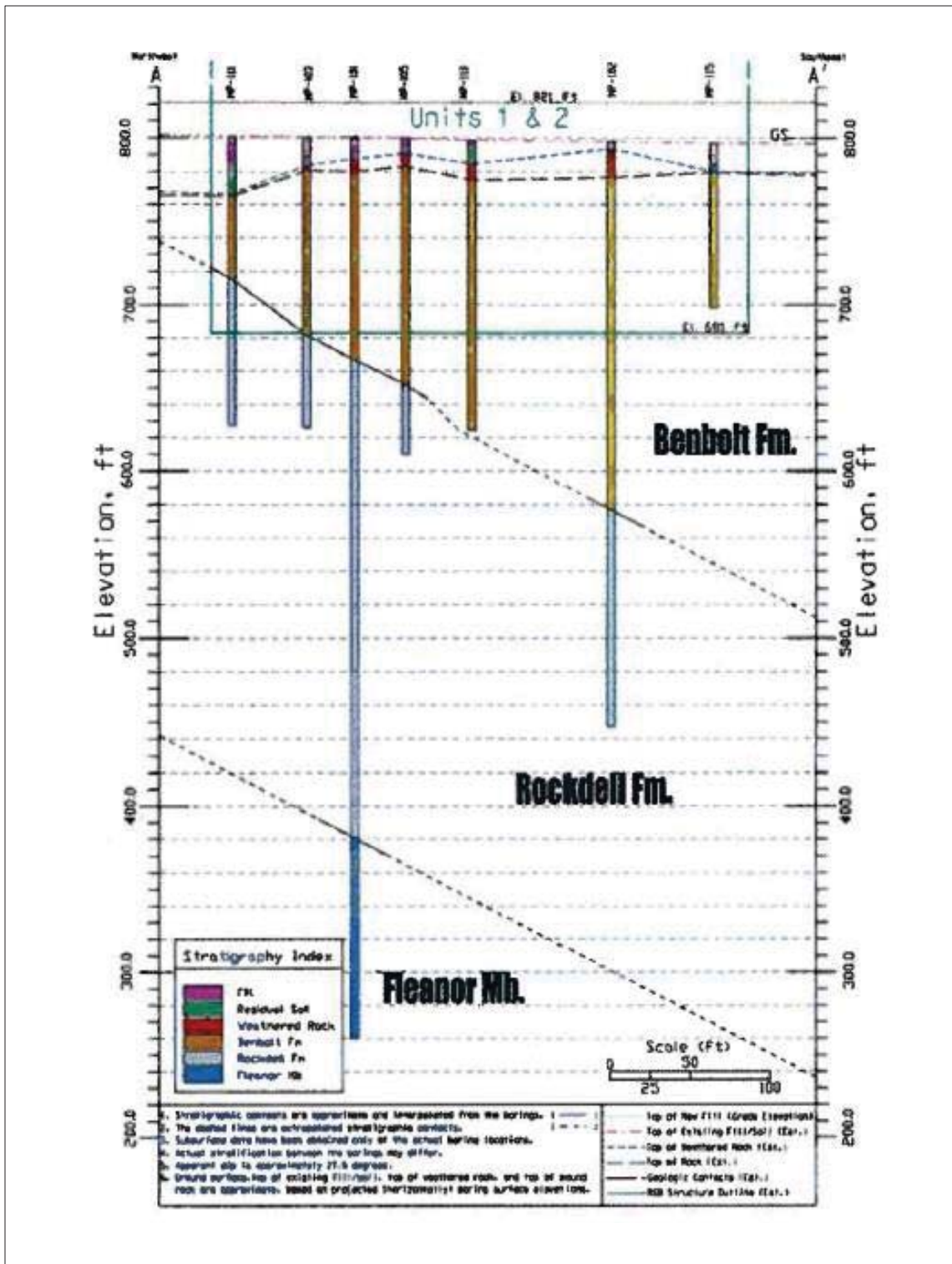


FIGURE 2-1  
GEOLOGIC CROSS SECTION A-A' FOR SITE A



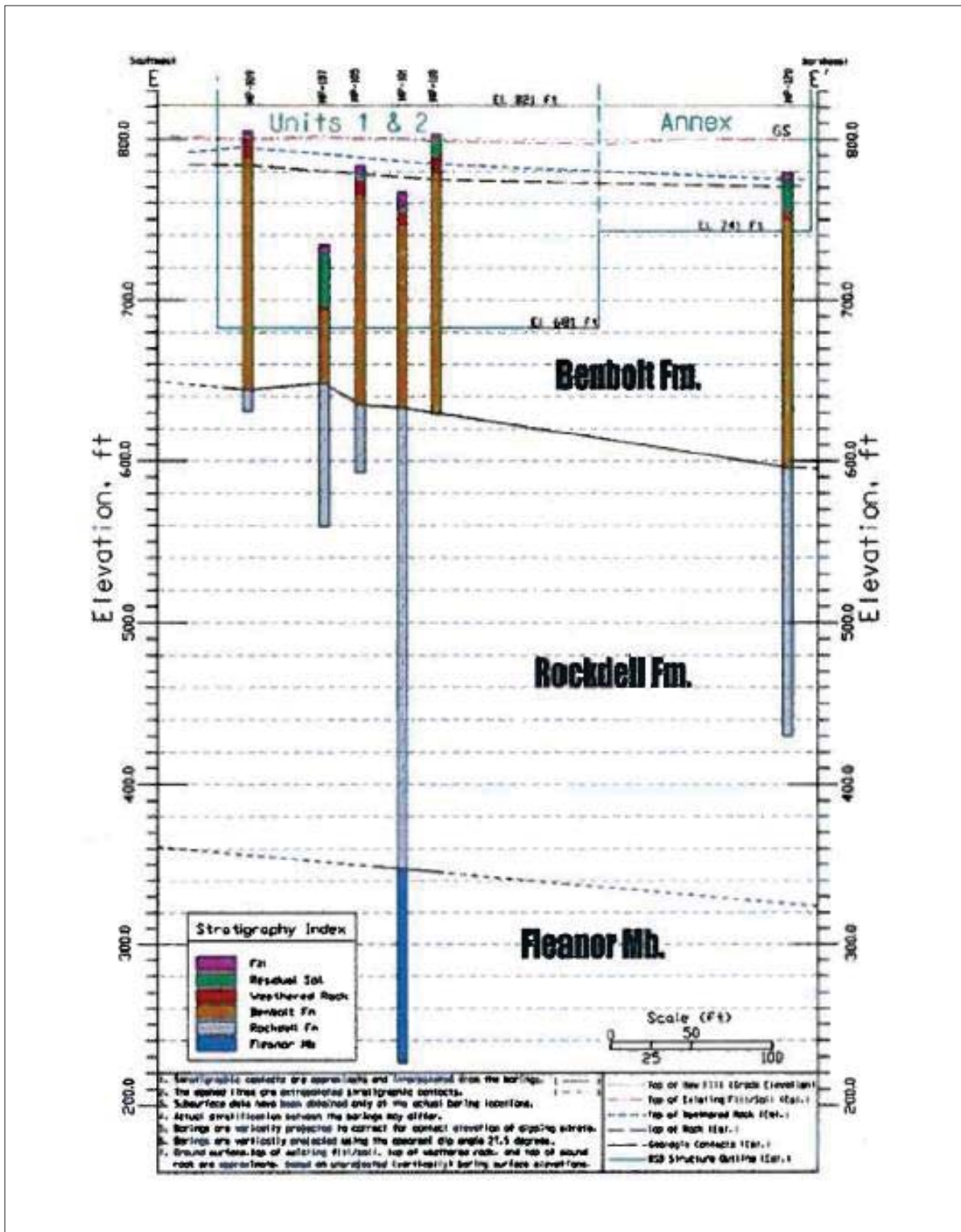


FIGURE 2-2  
GEOLOGIC CROSS SECTION E-E' FOR SITE A



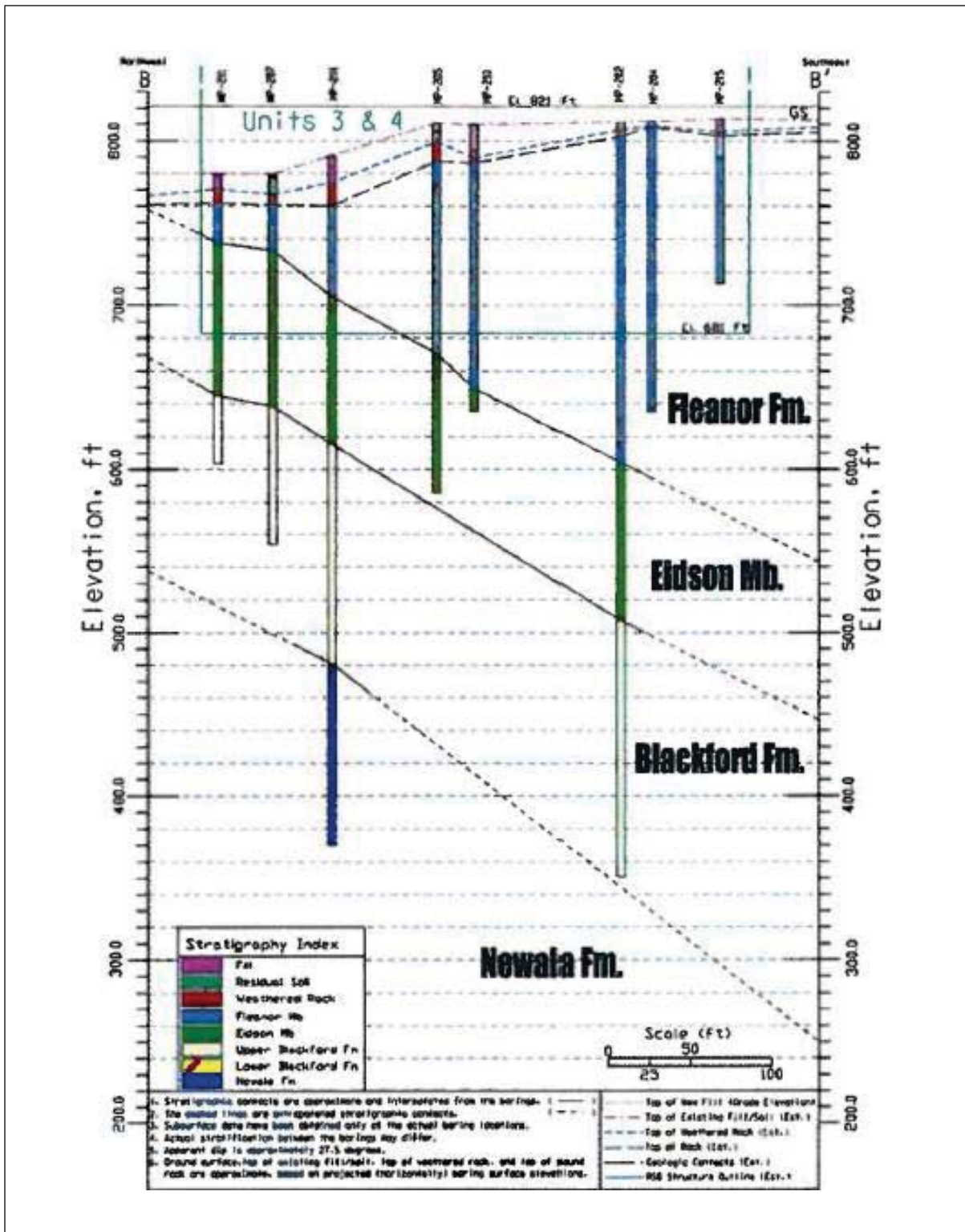


FIGURE 2-3  
 GEOLOGIC CROSS SECTION B-B' FOR SITE B



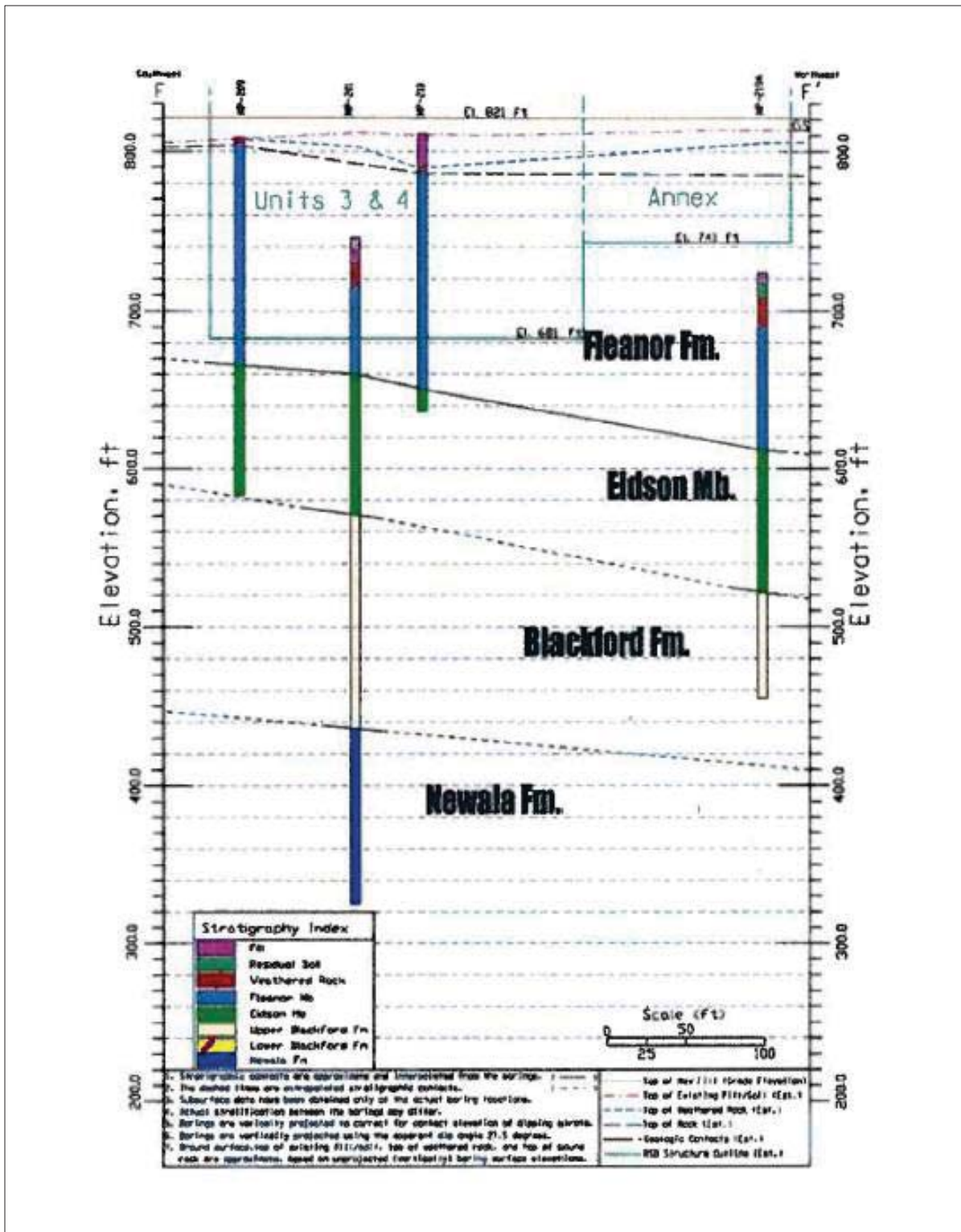
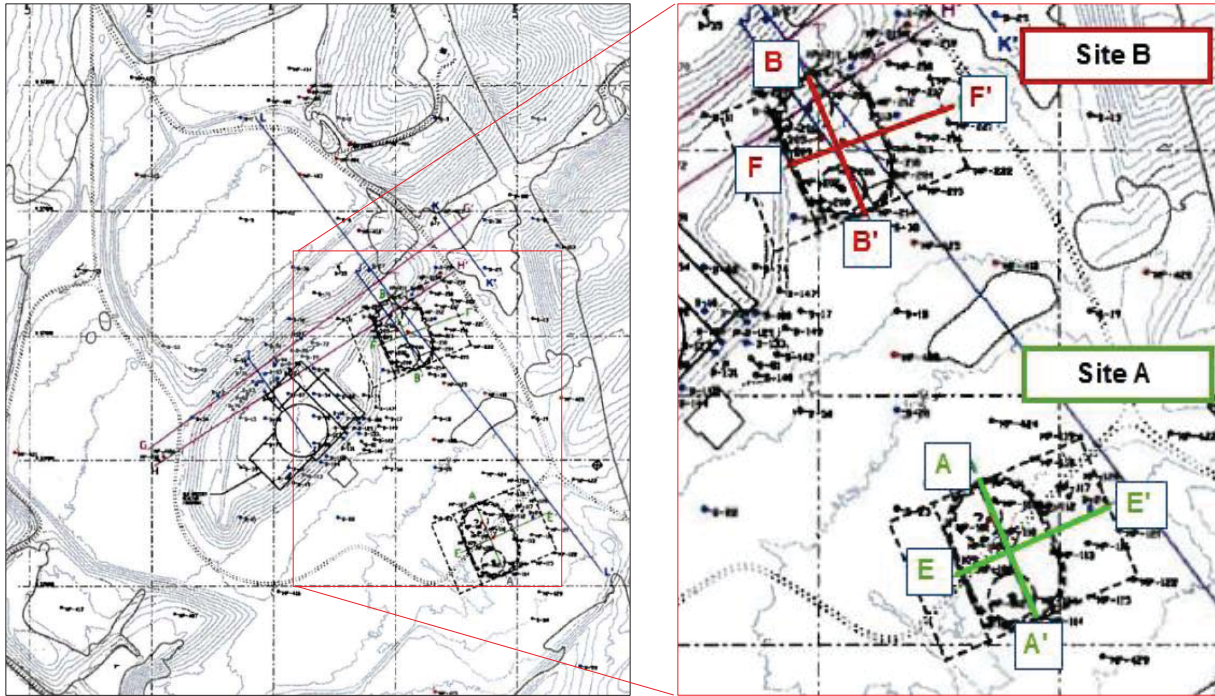


FIGURE 2-4  
GEOLOGIC CROSS SECTION F-F' FOR SITE B





**FIGURE 2-5  
LOCATION OF SECTIONS USED IN SITE A AND SITE B MODELS**

For Site B, as summarized in *Table 2-1 and Figure 2-7*, an interface element was included along the bedding plane separating the Fleanor and Eidson members of the Lincolnshire Formation to simulate the shear zone identified in CRN Site borings and CRBRP borings and foundation excavations, as previously described in *Section 1.2.3.2*. Although inferred to extend into Lower Blackford Formation rock, Site B FE foundation models included this prominent shear zone at the contact of the Eidson and Fleanor members, in order to more conservatively simulate shear zone coincidence with the common basemat for Units 3&4.

More detailed descriptions of interface element implementation and corresponding reduction factors are provided in *Section 2.1.3.3*.



**TABLE 2-1  
ANALYZED CASES FOR SITE A**

SITE <sup>(1)</sup>	SECTION <sup>(2)</sup>	FOUNDATION DEPTH <sup>(3)</sup>	CAVITY SIZE <sup>(4)</sup>	CAVITY LOCATION <sup>(5)</sup>	REMARKS <sup>(6)</sup>
		(ft)	(ft)		
A	A-A'	40	5,10,15	Center of common basemat	5 ft below basemat
				Center of common basemat	30 ft below basemat
				Bedding (Benbolt-Rockdell)	1 Interface
		Bedding (Benbolt-Rockdell)	2 interfaces		
		Edge of common basemat	5 ft below basemat		
		Center of common basemat	5 ft below basemat		
	90	5,10,15	Bedding (Benbolt-Rockdell)	1 Interface	
			Bedding (Benbolt-Rockdell)	1 Interface	
	E-E'	40	5,10,15	Center of common basemat	5 ft below basemat
				Center of common basemat	30 ft below basemat
				Center of common basemat	5 ft below basemat
		90	5,10,15	Bedding (Benbolt-Rockdell)	1 Interface
Bedding (Benbolt-Rockdell)				1 Interface	
B		B-B'	40	5,10,15	Center of common basemat
	Center of common basemat				30 ft below basemat
	Bedding (Fleanor-Eidson)				1 Interface
	Edge of common basemat		5 ft below basemat		
	90		5,10,15	Center of common basemat	5 ft below basemat
				Bedding (Fleanor-Eidson)	1 Interface
	140	5,10,15	Bedding (Fleanor-Eidson)	1 Interface	
			Bedding (Fleanor-Eidson)	1 Interface	
	F-F'	40	5,10,15	Center of common basemat	5 ft below basemat
				Center of common basemat	30 ft below basemat
				Center of common basemat	5 ft below basemat
		90	5,10,15	Bedding (Fleanor-Eidson)	1 Interface
Bedding (Fleanor-Eidson)				1 Interface	
140		5,10,15	Bedding (Fleanor-Eidson)	1 Interface	
	Bedding (Fleanor-Eidson)		1 Interface		

**Notes:**

ft = feet

- (1) Units 1&2 (Site A) or 3&4 (Site B).
- (2) Modeled Site A and Site B cross sections (see *Figure 2-1 through Figure 2-4*).
- (3) Modeled foundation embedment depth (feet below ground surface).
- (4) Modeled cavity diameters.
- (5) Modeled cavity locations.
- (6) Additional detail related to cavity location. For Site A, “1 interface” indicates a single interface element introduced on both sides of the contact between the Benbolt and Rockdell formations. In turn, “2 interfaces” indicates simulation of an interface element on both sides of the Benbolt Formation and Rockdell Formation contact, and simulation of a second interface element located approximately 15 ft above the contact between the Benbolt and Rockdell formations. For Site B, “1 interface” indicates a single interface element introduced on both sides of the contact between the Fleanor and Eidson members of the Lincolnshire Formation.



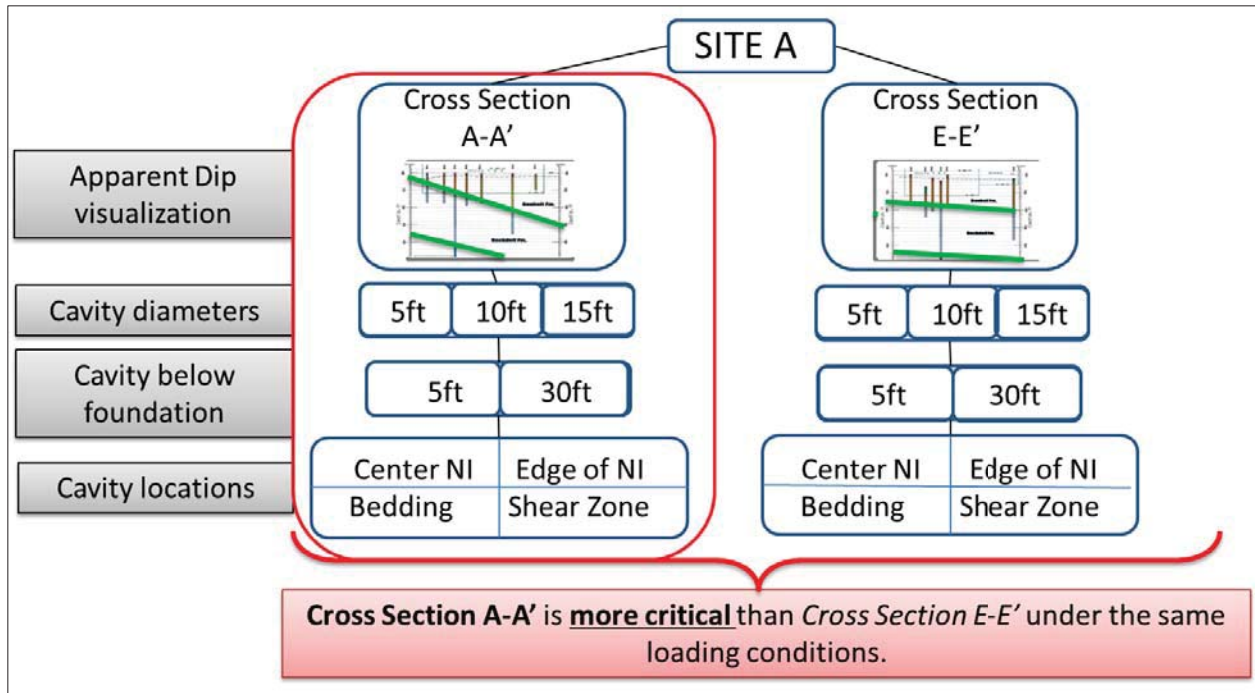


**FIGURE 2-6**  
**FOUNDATION EVALUATION CASES CONSIDERED FOR SITE A**

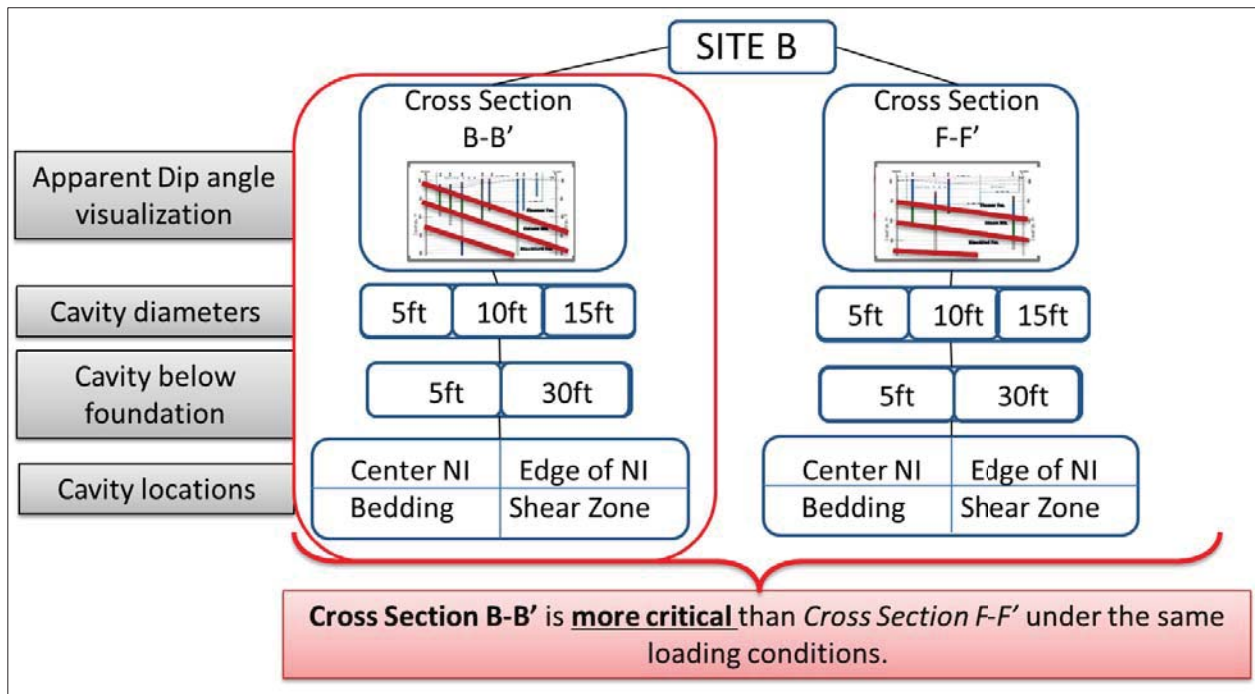


**FIGURE 2-7**  
**FOUNDATION EVALUATION CASES CONSIDERED FOR SITE B**



## 2.1.2 Stress Conditions

Regional folding and faulting suggest a rotation of principal stresses such that horizontal stresses represent the major stress component at Sites A and B. An assumption of principal stress in the vertical direction is nonetheless considered more conservative for the evaluation of bedding plane stresses, given inferred bedding inclinations. Accordingly, a gravitational stress field with  $\sigma_1$  in the vertical direction was used in the PLAXIS 2D simulations, with horizontal stresses as given in *Equation 2-1*:

$$\sigma'_3 = \sigma'_1(1 - \sin \phi) \quad \text{Equation 2-1}$$

The impact of this vertical  $\sigma_1$  assumption was checked in a sensitivity analysis wherein horizontal stress was assumed to be much larger (at least four times) than vertical stress.

## 2.1.3 2-D PLAXIS Models for Site A and Site B

Foundation and bedding plane stress conditions related to dewatering and excavation and structural loads were specifically evaluated for Sites A and B using the PLAXIS 2D models detailed in *Section 2.1.3.1 through Section 2.1.3.6*, below.

Results from the modeling are described in *Section 3.0*.

### 2.1.3.1 Material Constitutive Model

Geologic parameters from field and the laboratory measurements were taken into account in classifying rock masses for inclusion in the Site A and Site B Models, and are reported and considered as a range of GSI values, rather than single values, as presented in *Appendix B* and the CRN Site ESP Application (i.e., the SSAR).

GSI, in addition to unconfined compressive strength (UCS), is used directly in the empirical calculations of deformation moduli ( $E_{rm}$ ) and shear strength parameters ( $\phi'$  and  $c'$ ) for settlement analysis.

Mohr-Coulomb failure parameters  $\phi'$  and  $c'$  (i.e., shear strength parameters) are calculated using UCS laboratory test results, overburden stress characterization information, and material



parameter data. This is typically achieved using the Generalized Hoek-Brown Criterion as expressed by **Equation 2-2**:

$$\sigma'_1 = \sigma'_3 + \sigma_{ci} \left( m_b \frac{\sigma'_3}{\sigma_{ci}} + s \right)^a \quad \text{Equation 2-2}$$

where,

$\sigma'_1$  and  $\sigma'_3$  are major and minor effective principal stresses, respectively, and  $\sigma_{ci}$  is the uniaxial compressive strength, reported from UCS testing.

In **Equation 2-2**,  $m_b$ ,  $s$  and  $a$  represent material properties given by the following additional equations:

$$m_b = m_i \exp\left(\frac{GSI-100}{28-14D}\right) \quad \text{Equation 2-3}$$

$$s = \exp\left(\frac{GSI-100}{9-3D}\right) \quad \text{Equation 2-4}$$

$$a = \frac{1}{2} + \frac{1}{6} \left( \exp\frac{-GSI}{15} - \exp\frac{-20}{3} \right) \quad \text{Equation 2-5}$$

Where,

$m_i$  is a material property for intact rock,  
 $GSI$  is the geologic strength index, and  
 $D$  is a disturbance factor related to the method of excavation or other potential disturbances.

The Mohr-Coulomb failure parameters  $\varphi'$  and  $c'$  are subsequently found using the following equations:

$$\varphi' = \arcsin\left(\frac{6am_b(s+m_b\sigma'_{3n})^{a-1}}{2(1+a)(2+a)+6am_b(s+m_b\sigma'_{3n})^{a-1}}\right) \quad \text{Equation 2-6}$$

$$c' = \frac{\sigma_{ci}[(1+2a)s+(1-a)m_b\sigma'_{3n}](s+m_b\sigma'_{3n})^{a-1}}{(1+a)(2+a)\sqrt{1+(6am_b(s+m_b\sigma'_{3n})^{a-1})/((1+a)(2+a))}} \quad \text{Equation 2-7}$$



where,

$a$ ,  $s$ ,  $m_b$ , and  $\sigma_{ci}$  are material properties defined previously, and  $\sigma'_{3n}$  is given by:

$$\sigma'_{3n} = \sigma'_{3max} / \sigma_{ci} \quad \text{Equation 2-8}$$

The upper limit of confining stress ( $\sigma'_{3max}$ ), for which the Hoek-Brown criterion is calculated, is determined according to the geotechnical application. For the disturbed zone around a cavity, material properties are typically per Hoek-Brown failure criterion (Hoek-Brown, 2002) determined by assuming shallow tunnel conditions (such that the depth below the surface is less than 3 tunnel [cavity] diameters). This is a different assumption than the general stress condition assumption made in the CRN Site ESP Application, and it is only for the zone around the cavity.

Global rock mass strength, as estimated by Mohr-Coulomb relationships, is denoted as  $\sigma'_{cm}$ . For the case of tunnel design these two parameters are defined as follows:

$$\frac{\sigma'_{3max}}{\sigma'_{cm}} = 0.47 \left( \frac{\sigma'_{cm}}{\sigma_0} \right)^{-0.94} \quad \text{Equation 2-9}$$

$$\sigma'_{cm} = \sigma_{ci} \frac{[m_b + 4s - a(m_b - 8s)](m_b/4 + s)^{a-1}}{2(1+a)(2+a)} \quad \text{Equation 2-10}$$

where,

$a$ ,  $s$ ,  $m_b$ , and  $\sigma_{ci}$  are material properties defined previously, and  $\sigma_0$  is the vertical stress from overburden, including effects of ground water.

All three derived material properties ( $a$ ,  $s$ ,  $m_b$ ) depend on GSI values for calculation. In defining the material properties, both qualitative and quantitative methodologies are implemented.

In turn, rock mass modulus ( $E_{rm}$ ) can be calculated from GSI values using the methodology of Hoek and Diederichs (2006):

$$E_{rm} = E_i \left( 0.02 + \frac{1-D/2}{1+e^{\left(\frac{60+15D-GSI}{11}\right)}} \right) \quad \text{Equation 2-11}$$



where,

$E_{rm}$  is the rock mass modulus,

$E_i$  is the intact rock elastic modulus calculated as the product of a UCS value and the modulus ratio MR,

D is the disturbance factor as used in calculation of  $\phi'$  and  $c'$ , and

GSI is the geologic strength index.

For Sites A and B, rock masses were modeled using an elasto-plastic Mohr-Coulomb model, since the strain levels are expected to be low and within the elastic range prior to cavity collapse. The use of Mohr-Coulomb model also dictates the use of a constant stiffness in all layers.

GSI values for the CRN Site are provided in SSAR Section 2.5.1.2.6 as a range of values for each stratigraphic unit. The lower range rock mass properties from the CRN Site ESP Application (SSAR Section 2.5.1.2.6) were used in the FE models, as shown in **Table 2-2**.

Disturbed rock mass properties calculated using **Equation 2-6 and Equation 2-7** above, assuming a disturbance factor (D) of 0.7, are presented in **Table 2-3**.

### **2.1.3.2 Material Geometry and Boundary Conditions**

Settlement was obtained from the 2D finite element method (FEM) in PLAXIS 2D version 9.02 (PLAXIS 2D).

The foundation in the model is considered as a plate element representing a basemat thickness of 6 ft. The plate element has no self-weight, as the applied loads are assumed to be inclusive of the foundation weight. The structural stiffness is limited to the basemat without the inclusion of any other superstructure elements. This is a conservative assumption since superstructural elements would likely increase rigidity and reduce angular distortion or differential settlement.

A finished plant grade elevation of 821 ft NAVD88 was assumed for the power block area. The plan dimensions considered for the models are 1,200 ft (horizontal) by 1,200 ft (vertical). Stress increments at the model boundaries are less than 10% of the initial stress, confirming an adequate model extent. Boundary conditions for the sides of the model were set to allow for



vertical displacement, but the bottom of the model was restrained in both vertical and horizontal directions.

As shown on **Figure 2-8**, 15-node triangle elements were used in the analysis, with a total of approximately 3,000 elements for the design mesh model. The size of the triangular FE is about 2 ft in finely meshed areas around modeled cavities, and 80 ft in the coarsely meshed areas outside of the excavation zone. In the vertical plane, the element length varies between approximately 2 ft and 80 ft.

**TABLE 2-2  
ROCK MASS PROPERTIES FOR SITES A AND B USED IN FE MODELING**

SITE (1)	LAYER (2)	ROCK MASS PROPERTIES (3)						
		UNIT WEIGHT	COHESION		FRICTION ANGLE	POISSON'S RATIO	ELASTIC MODULUS	
		(pcf)	(psf)	(psi)			(ksf)	(ksi)
A	Granular Fill	135	0	0	36	0.35	16,000	111
	Existing Fill	120	150	1	20	0.40	3,750	26
	Benbolt	168	59,760	415	33	0.32	643,680	4,470
	Rockdell	168	56,592	393	31	0.31	452,736	3,144
	Fleanor	168	42,912	298	32	0.34	454,896	3,159
B	Granular Fill	135	0	0	36	0.35	16,000	111
	Existing Fill	120	150	1	20	0.40	3,750	26
	Rockdell	168	56,592	393	31	0.31	452,736	3,144
	Fleanor	168	42,912	298	32	0.34	454,896	3,159
	Eidson	168	48,672	338	30	0.31	340,560	2,365
	Blackford	168	34,848	242	30	0.31	479,232	3,328
	Newala	175	201,024	1,396	35	0.29	1,202,976	8,354

**Notes:**

pcf = pounds per cubic foot

psf = pounds per square foot

psi = pounds per square inch

ksf = kips per square foot

ksi = kips per square inch

(1) Units 1&2 (Site A) or Units 3&4 (Site B).

(2) Geologic layer or material expected to be exposed in the given Site A or Site B location. Units 1&2 in Site A are expected to be founded on Benbolt Formation rock. Units 3&4 in Site B are expected to be founded on rock ascribed to the Fleanor Member of the Lincolnshire Formation.

(3) Rock mass properties from SSAR Section 2.5.4 Table 2.5.4-21, and Table 2.5.4-22.



**TABLE 2-3  
DISTURBED ROCK MASS PROPERTIES (D=0.7)**

LAYER <sup>(1)</sup>	ROCK MASS PROPERTIES <sup>(2)</sup>						
	UNIT WEIGHT (pcf)	COHESION		FRICTION ANGLE	POISSON'S RATIO	ELASTIC MODULUS	
		(psf)	(psi)			(ksf)	(ksi)
Benbolt	168	16,704	116	55	0.32	296,496	2,059
Rockdell	168	5,328	37	61	0.31	163,728	1,137
Fleanor	168	8,928	62	56	0.34	191,088	1,327
Eidson	168	3,312	23	61	0.31	118,958	826
Blackford	168	5,328	37	56	0.31	184,896	1,284

**Notes:**

pcf = pounds per cubic foot

psf = pounds per square foot

psi = pounds per square inch

ksf = kips per square foot

ksi = kips per square inch

<sup>(1)</sup> Geologic layer or material expected to be exposed in the given Site A or Site B location. Units 1&2 in Site A are expected to be founded on Benbolt Formation rock. Units 3&4 in Site B are expected to be founded on rock ascribed to the Fleanor Member of the Lincolnshire Formation.

<sup>(2)</sup> Rock mass properties calculated from *Table 2-3* data, using disturbed rock mass properties from SSAR Section 2.5.4 Table 2.5.4-23 using *Equation 2-6 and Equation 2-7*.

**2.1.3.3 Interface Elements**

It is noted that the use of GSI and Hoek-Brown failure criteria (as described in *Section 2.1.3.1*) assume a homogeneous and isotropic rock mass behavior. However, rock mass discontinuities and fracture zones located along stratigraphic boundaries (such as the contact between the Benbolt and Rockdell formations and the contact between the Eidson and Fleanor members of the Lincolnshire Formation at the CRN Site) can influence or change the failure direction pattern of a rock mass.

Conservatively, interface elements (as introduced in *Section 2.1.1*) were thus included in the PLAXIS 2D models for Sites A and B to represent potential planes of weakness resulting from rock mass discontinuities or bedding plane shear zones at foundation elevations.

In the model, a “virtual thickness” dimension was assigned to each interface to define the material properties of the interface, calculated as the product of a virtual thickness factor and the average element size defined by the mesh generation. A default value of 0.1 was used for the virtual



thickness factor in each of the PLAXIS 2D models with interfaces. Higher virtual thickness factor values resulted in more elastic deformations.

A typical interface element implemented in a CRN Site PLAXIS 2D model is shown on **Figure 2-9** as a dashed line paralleling layer geometries.

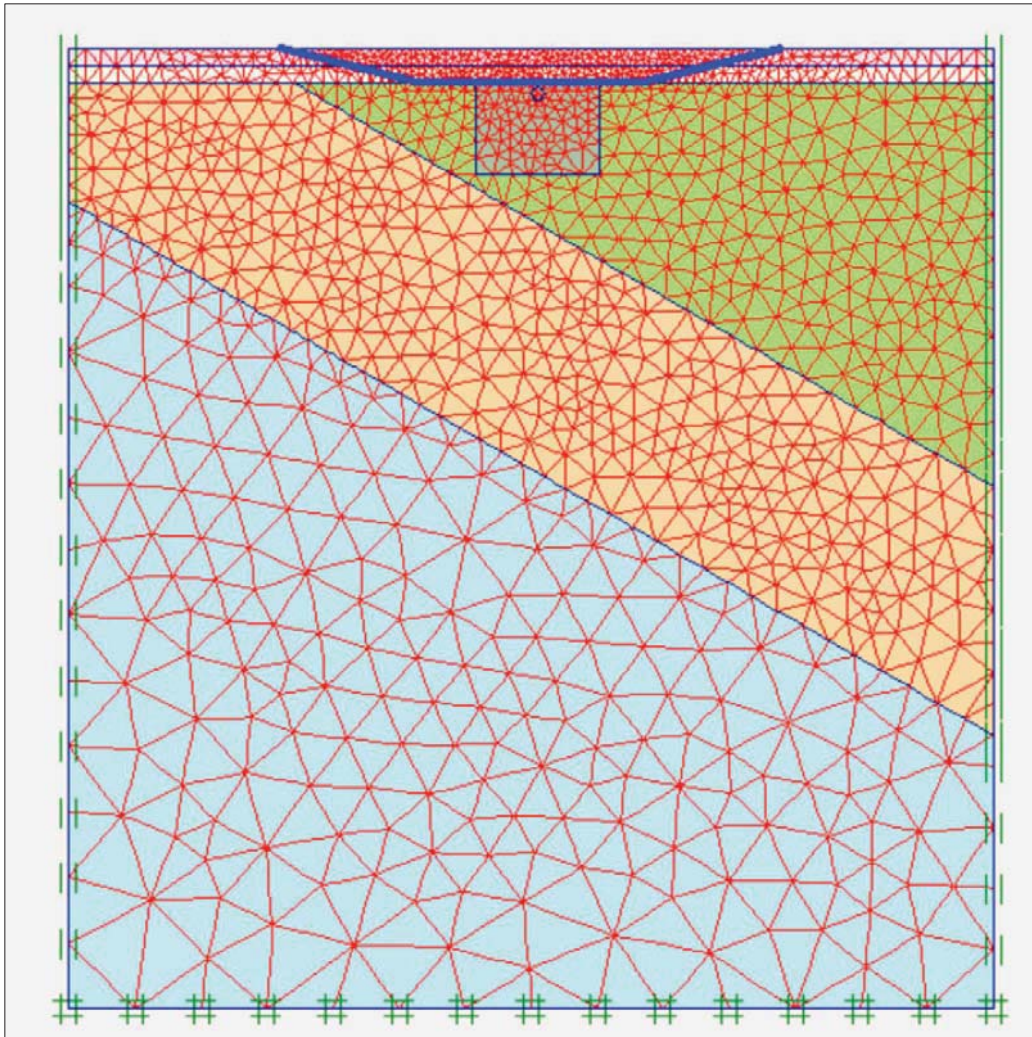


**FIGURE 2-8  
A TYPICAL MODEL WITH REFINED MESH**

In the model, interfaces were placed on both sides of the bedding planes for Site A and Site B. It is important to note that placing interfaces on both sides of the bedding planes enables full interaction between the interface and the surrounding rock. Two possible interfaces are



distinguished by a plus-sign (+) and/or a minus-sign (-). The signs are just for identification purposes for both sides of the interface element and they do not have any influence on the results.

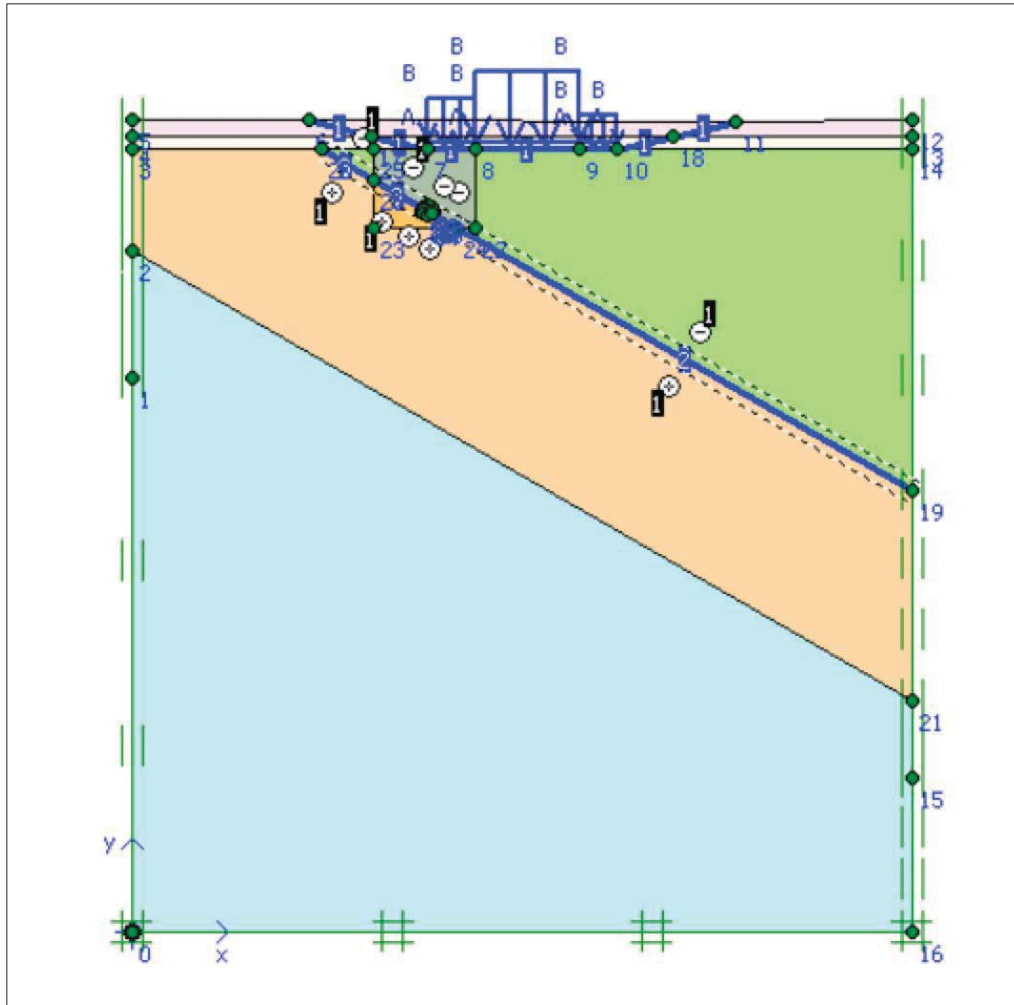


**FIGURE 2-9  
TYPICAL MODEL INTERFACE ELEMENT LOCATED ALONG A BEDDING PLANE**

The primary interface parameter is the interface strength,  $R_{inter}$ . The strength properties of interfaces are directly linked to the strength properties of the adjacent stratigraphic layers via an assigned reduction factor as follows:

$$c' = R_{inter}c'_{rock} \quad \text{Equation 2-12}$$

$$\tan\phi' = R_{inter} \tan\phi'_{rock} \quad \text{Equation 2-13}$$



Interface elements located along (or just above) the contact between the Benbolt and Rockdell formations in Site A were specifically assigned an interface strength factor of 50 percent. Shear fracture zones modeled on the contact between the Fleanor and Eidson members of the Lincolnshire Formation in Site B in turn were assigned an interface strength factor of 30 percent. These calculated parameters using interface strength factors are considered to represent the properties of bedding plane discontinuities (e.g., weathered bedding plane joint zones) and shear fracture zones along stratigraphic contacts for both Site A and Site B.

#### **2.1.3.4 Finite Element Model Characteristics**

PLAXIS 2D simulates dewatering, excavation, and other construction steps as individual phases. Accordingly, differential settlement can be visually examined using contour plots provided for discrete construction steps. Alternatively, numerical values along any given axis can be extracted using calculated nodal displacements.

The PLAXIS 2D models for Site A and Site B specifically included the following simulation phases:

- **Initial Conditions:** Initial effective stresses for the Site are obtained. Cavities are imposed after gravity loading, to simulate development within the rock mass before the initiation of construction activities such as dewatering or excavation.
- **Dewatering:** The water level, initially assumed to be at the top of existing fill for all models, is lowered to the level of embedment depth considered for the analysis.
- **Excavation:** Upon dewatering down to embedment depth, the material between ground surface (EL 821 ft) and embedment depth elevation is removed.
- **Loading:** Average loads on the footprints of support building 1, reactor building, and support building 2 equal to 7.7 ksf, 11.8 ksf, and 5.1 ksf, respectively, are applied. It is important to note that the loads on the footprint of the common basemat are applied while the pore pressure is assumed to be zero at the bottom of the foundation. This condition is kept for conservative purposes.



### 2.1.3.5 PLAXIS 2D Models for Site A

Site A PLAXIS 2D models included two different cross sections, A-A', and E-E', as described in *Section 2.1*. The dip of the stratigraphic layers varies for these sections slightly, as illustrated on *Figure 2-1 and Figure 2-2*. In the model, a disturbed zone was introduced around the simulated cavity with material properties (cohesion and friction angle) calculated using the equations presented in *Section 2.1.3.1* and assuming a disturbance factor of 0.7. Similarly, a bedding plane discontinuity (a weathered, jointed zone) was established along the contact between the Benbolt and Rockdell formations using interface elements (as explained in *Section 2.1.3.3*).

*Figure 2-10 through Figure 2-20* present the individual PLAXIS 2D models evaluated for Site A.

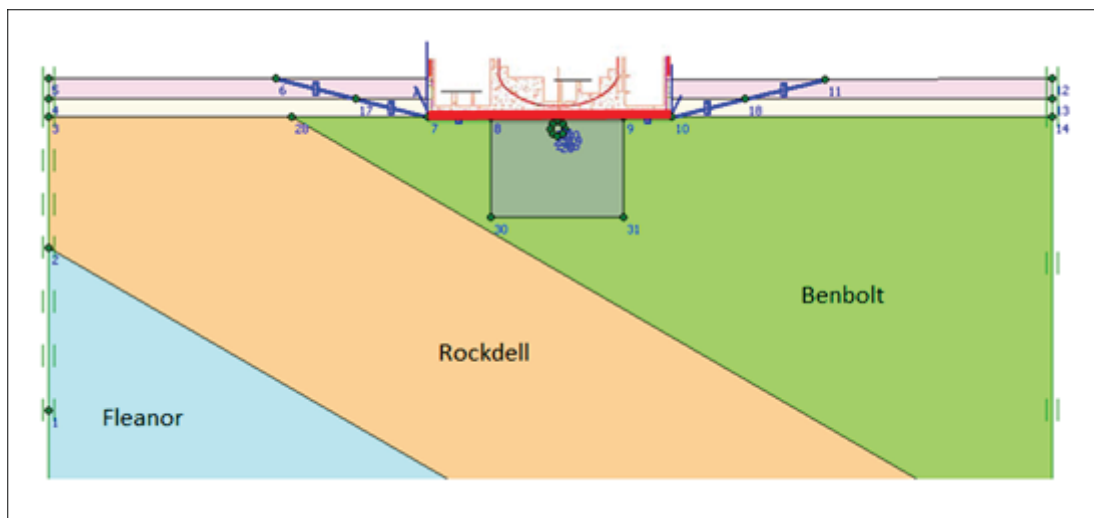


**FIGURE 2-10**  
**SITE A, CROSS SECTION: A-A', CAVITY DIAMETER: 15FT, EMBEDMENT DEPTH:**  
**40FT, CAVITY DEPTH: 5FT BELOW FOUNDATION,**  
**CAVITY LOCATION: CENTER OF NI**



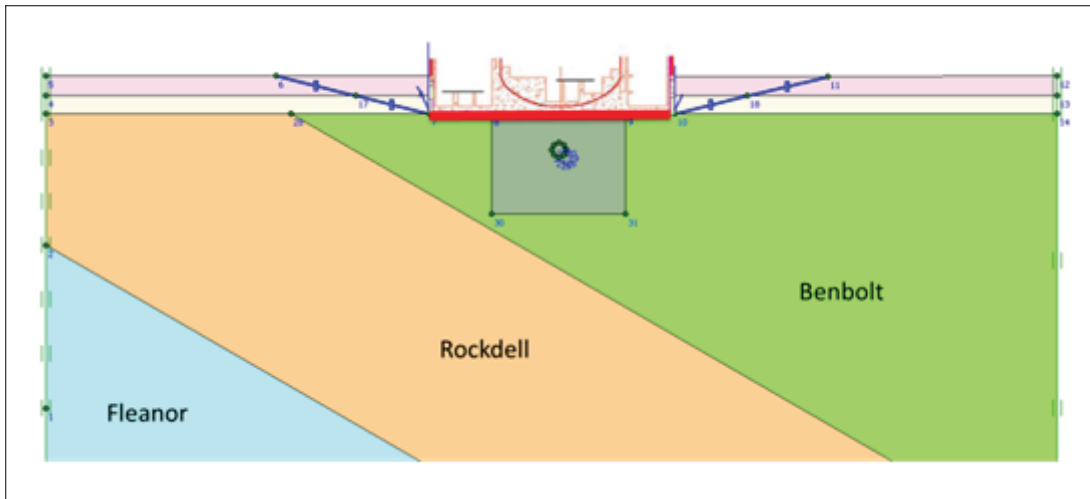


**FIGURE 2-11**  
**SITE A, CROSS SECTION: A-A', CAVITY DIAMETER: 15FT, EMBEDMENT DEPTH:**  
**40FT, CAVITY DEPTH: 30FT BELOW FOUNDATION, CAVITY LOCATION:**  
**CENTER OF COMMON BASEMAT**

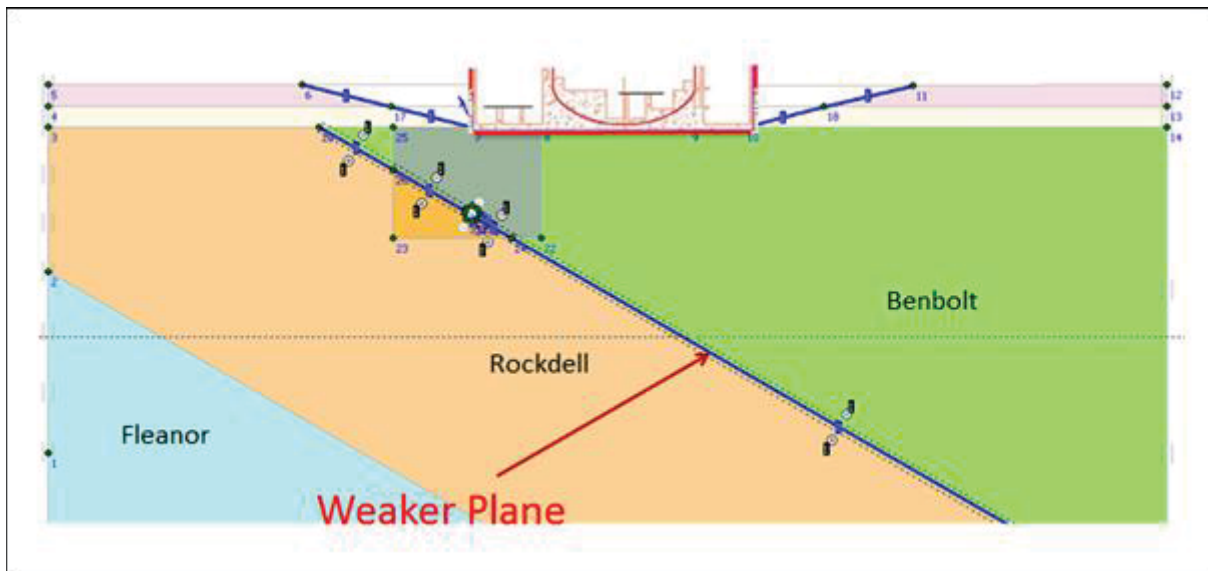


**FIGURE 2-12**  
**SITE A, CROSS SECTION A-A'**  
**SITE A, CROSS SECTION: A-A', CAVITY DIAMETER: 15FT, EMBEDMENT DEPTH:**  
**40FT, CAVITY DEPTH: 30FT BELOW FOUNDATION, CAVITY LOCATION: EDGE**  
**OF COMMON BASEMAT, ON BEDDING PLANE**



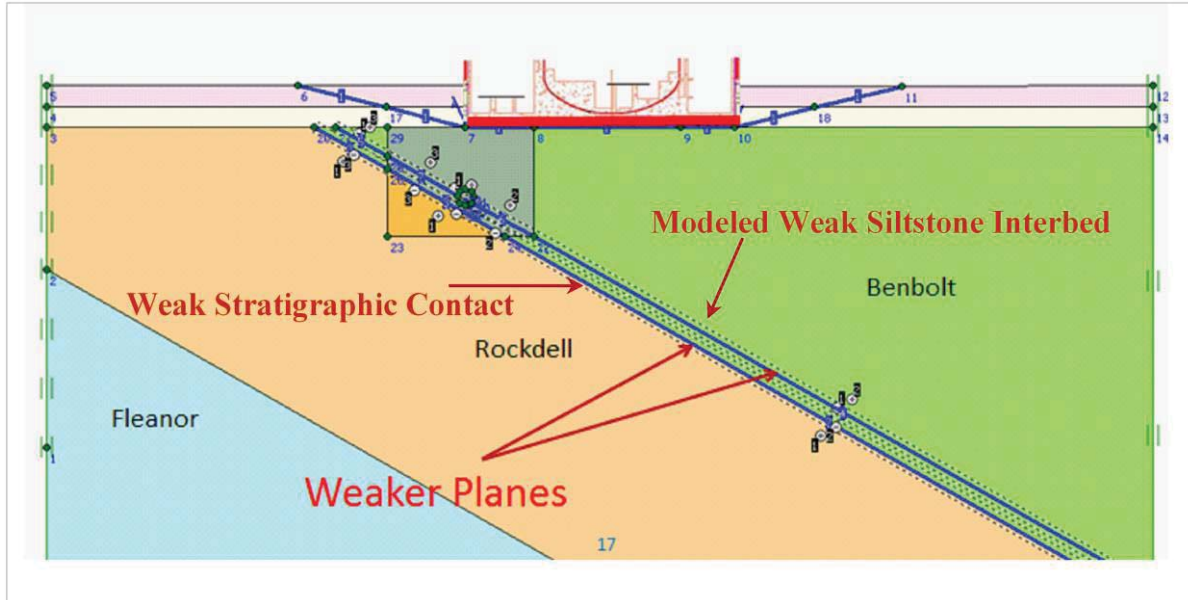


**FIGURE 2-13**  
**SITE A, CROSS SECTION: A-A', CAVITY DIAMETER: 15FT, EMBEDMENT DEPTH:**  
**40FT, CAVITY DEPTH: 30FT BELOW FOUNDATION CAVITY LOCATION: EDGE**  
**OF COMMON BASEMAT, ON BEDDING PLANE, TWO SHEAR JOINT INTERFACES**  
**BASED ON BORING LOGS AND WEAK SILTSTONE REPRESENTATION**

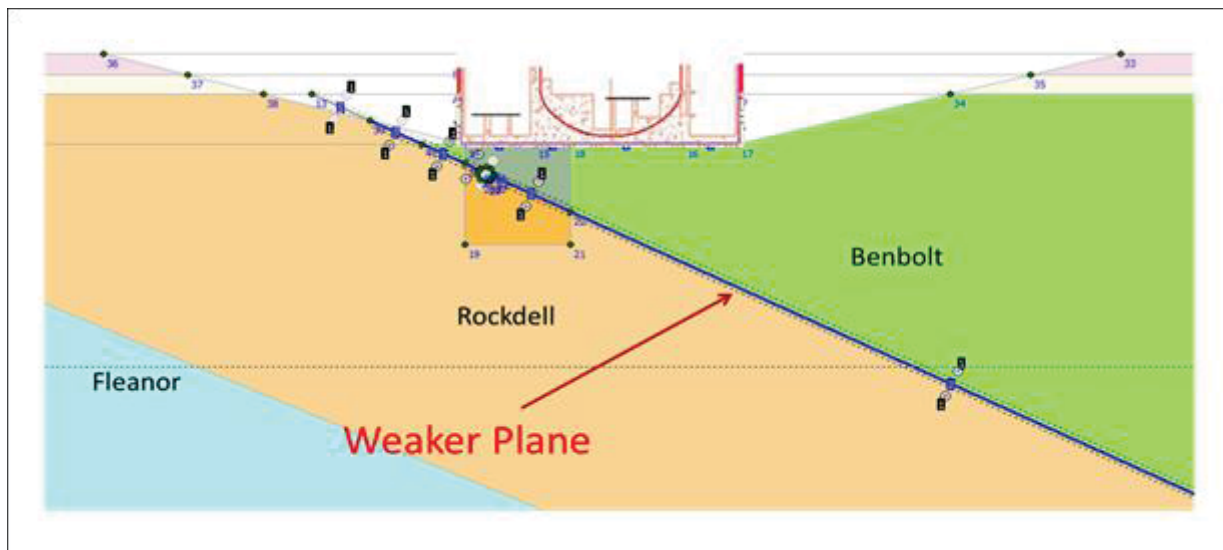


**FIGURE 2-14**  
**SITE A, CROSS SECTION: A-A', CAVITY DIAMETER: 15FT, EMBEDMENT DEPTH:**  
**90FT, CAVITY LOCATION: 30FT BELOW EDGE OF COMMON BASEMAT,**  
**BEDDING PLANE, SHEAR JOINT INTERFACE**



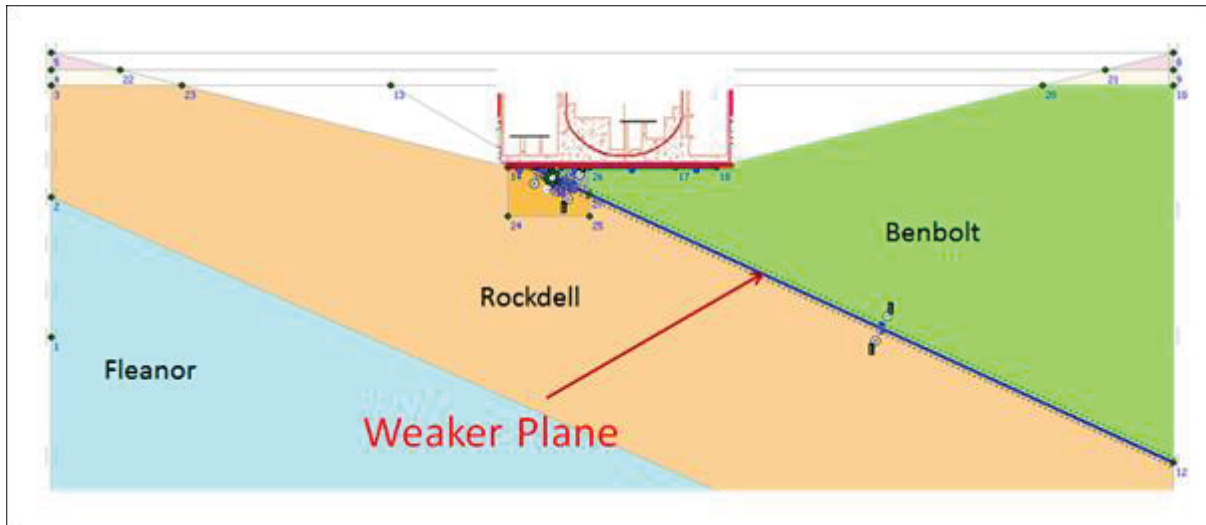


**FIGURE 2-15**  
**SITE A, CROSS SECTION: A-A', CAVITY DIAMETER: 15FT, EMBEDMENT DEPTH:**  
**140FT, CAVITY DEPTH: 5FT BELOW FOUNDATION,**  
**CAVITY LOCATION: EDGE OF COMMON BASEMAT, ON BEDDING PLANE,**  
**SHEAR JOINT INTERFACE**

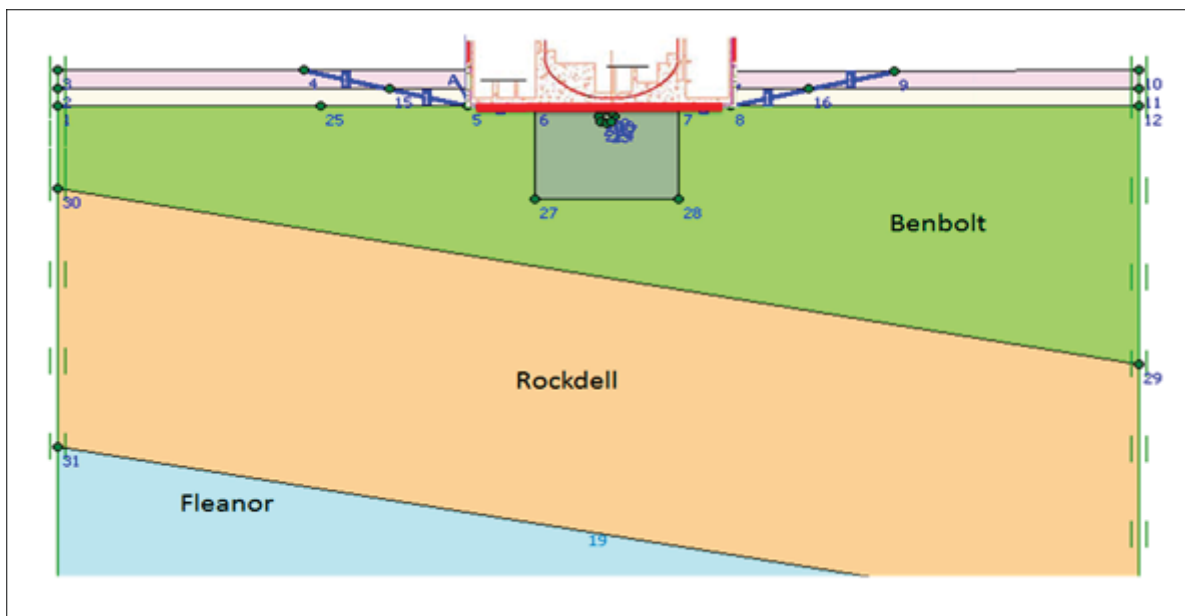


**FIGURE 2-16**  
**SITE A, CROSS SECTION: E-E', CAVITY DIAMETER: 15FT, EMBEDMENT DEPTH:**  
**40FT, CAVITY DEPTH: 5FT BELOW FOUNDATION,**  
**CAVITY LOCATION: CENTER OF COMMON BASEMAT**



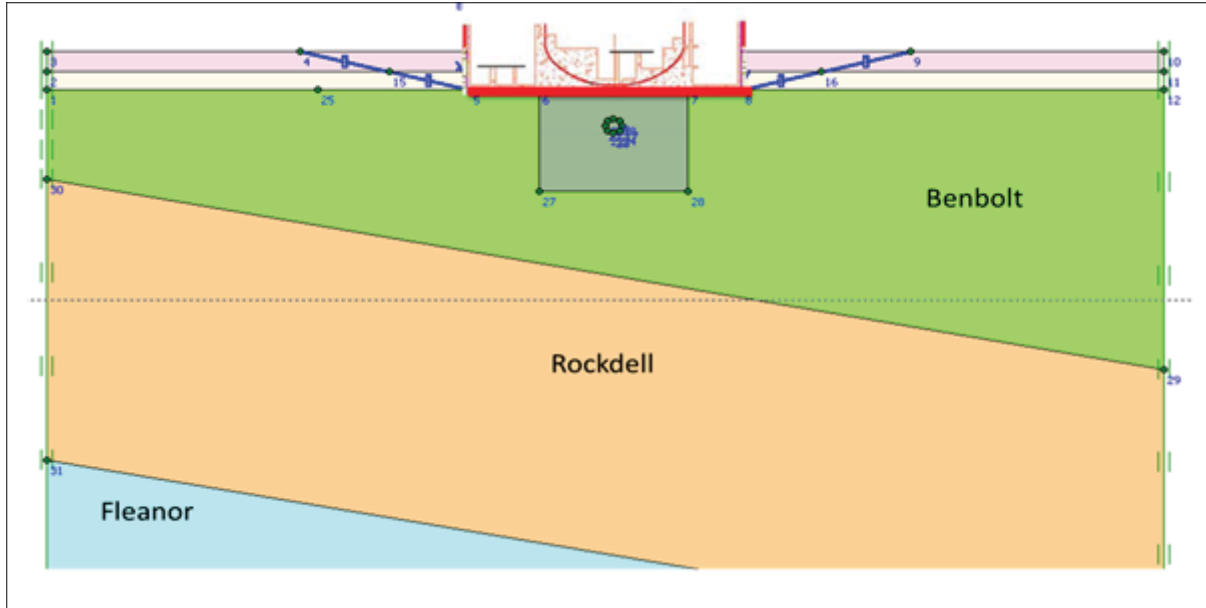


**FIGURE 2-17**  
**SITE A, CROSS SECTION: E-E', CAVITY DIAMETER: 15FT, EMBEDMENT DEPTH:**  
**40FT, CAVITY DEPTH: 30FT BELOW FOUNDATION,**  
**CAVITY LOCATION: CENTER OF COMMON BASEMAT**

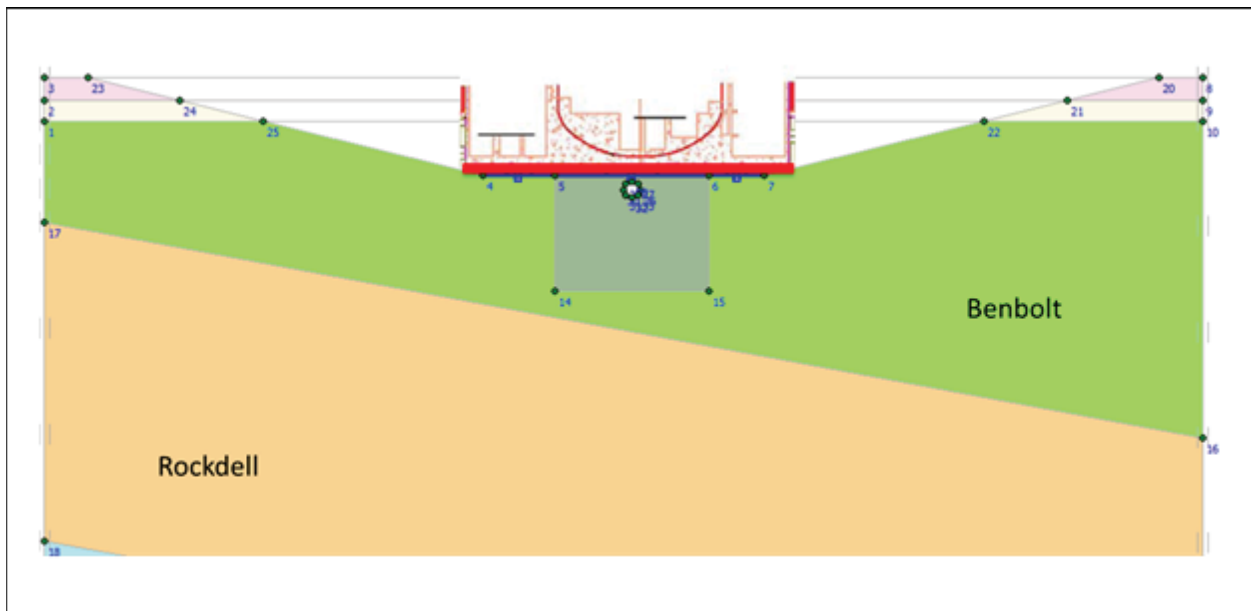


**FIGURE 2-18**  
**SITE A, CROSS SECTION: E-E', CAVITY DIAMETER: 15FT, EMBEDMENT DEPTH:**  
**90FT, CAVITY DEPTH: 5FT BELOW FOUNDATION,**  
**CAVITY LOCATION: CENTER OF COMMON BASEMAT**



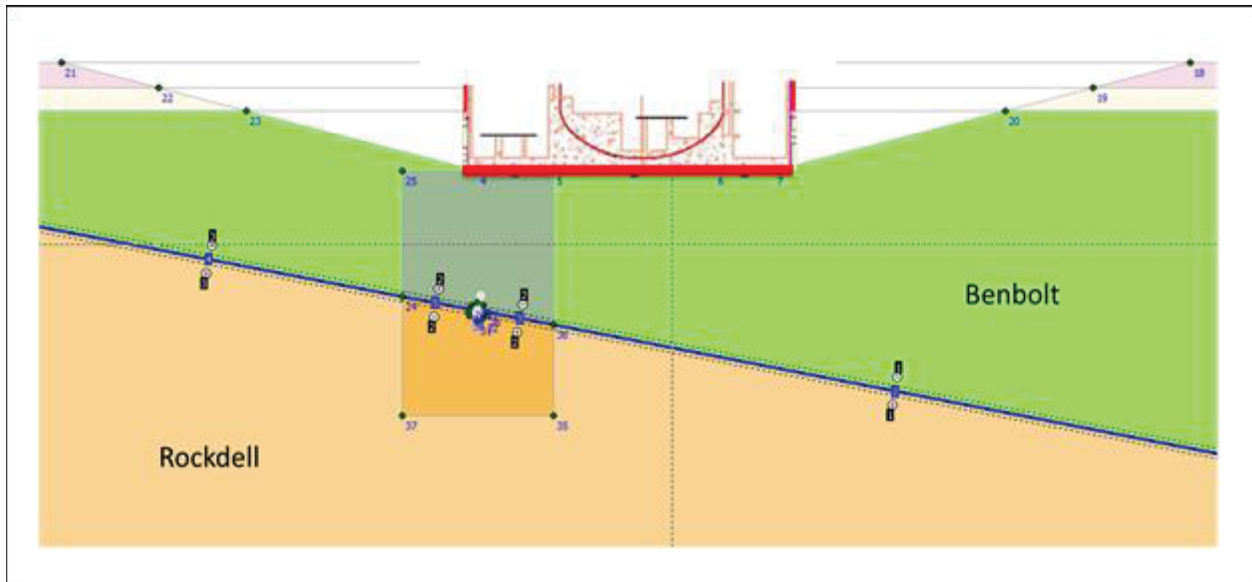


**FIGURE 2-19**  
**SITE A, CROSS SECTION: E-E', CAVITY DIAMETER: 15FT, EMBEDMENT DEPTH:**  
**90FT, CAVITY DEPTH: >30FT BELOW FOUNDATION,**  
**CAVITY LOCATION: EDGE OF COMMON BASEMAT, ON THE BEDDING PLANE**

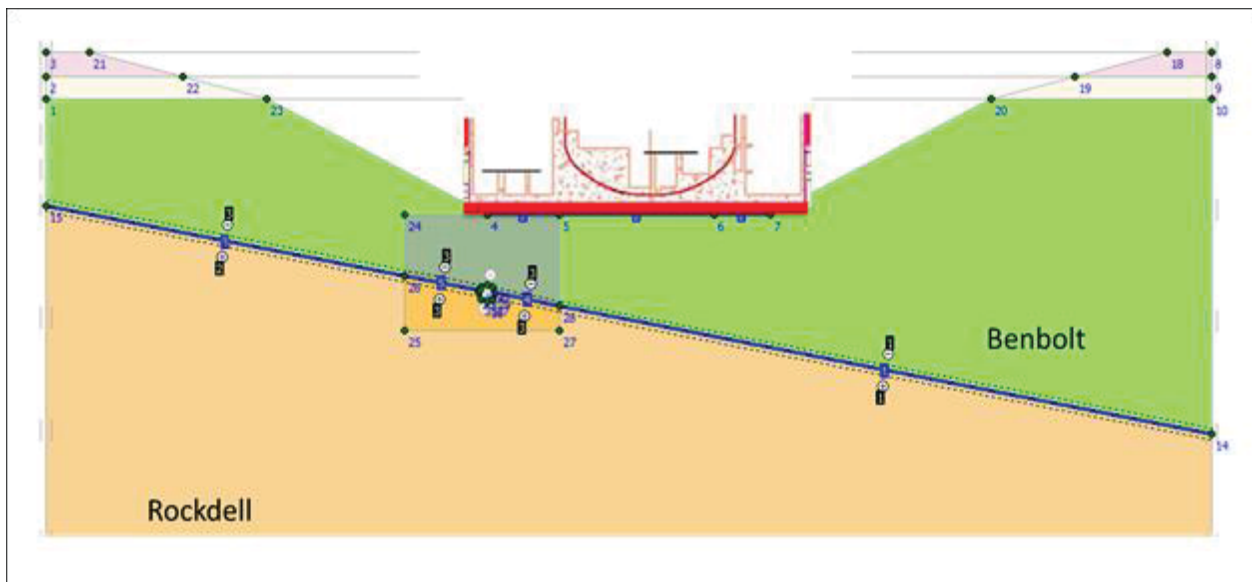


**FIGURE 2-20**  
**SITE A, CROSS SECTION: E-E', CAVITY DIAMETER: 15FT, EMBEDMENT DEPTH:**  
**140FT, CAVITY DEPTH: 30FT BELOW FOUNDATION,**  
**CAVITY LOCATION: EDGE OF COMMON BASEMAT**



### 2.1.3.6 PLAXIS 2D Models for Site B

PLAXIS 2D models were created for Site B based on cross sections B-B' and F-F', as shown on *Figure 2-3 and Figure 2-4* (and as described in Section 2.1). Similar to Site A, a zone of disturbed material properties was introduced around simulated cavities assuming a disturbance factor equal to 0.7, using the Mohr-Coulomb parameter equations previously described in *Section 2.1.3.1*.

PLAXIS 2D interface elements (discontinuities and shear fracture zones) and cavity diameter and location scenarios for Site B are depicted on *Figure 2-21 through Figure 2-31*.

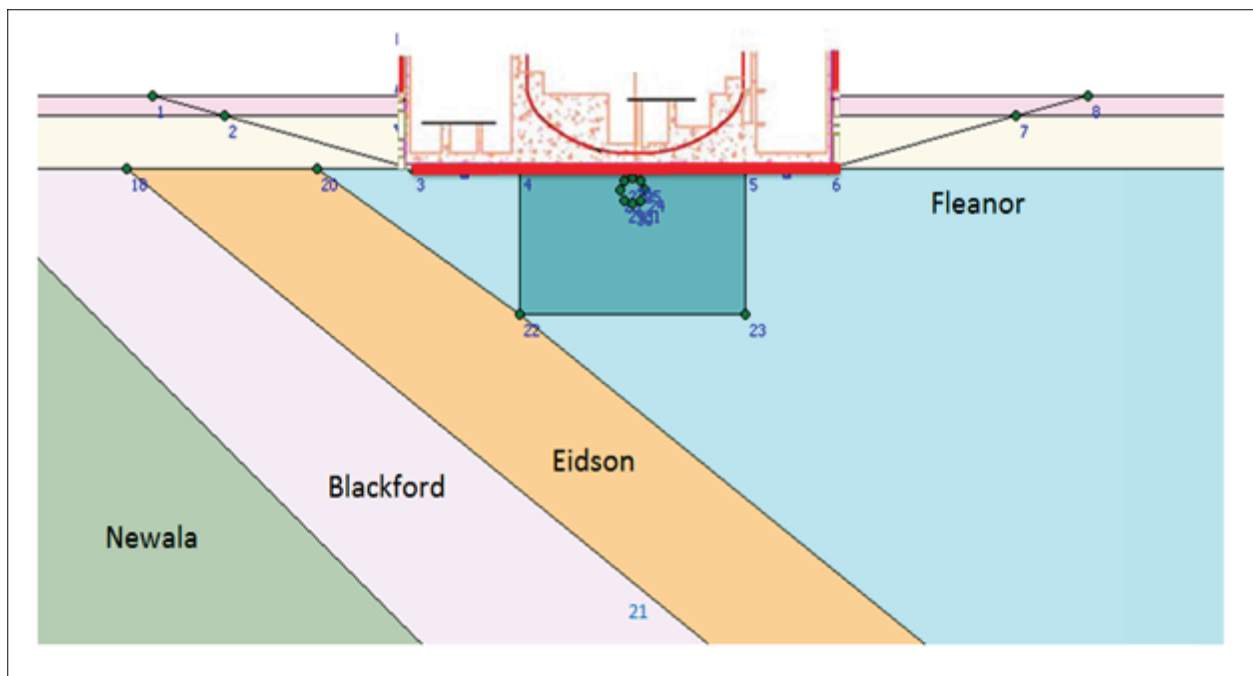


**FIGURE 2-21**  
**SITE B, CROSS SECTION: B-B', CAVITY DIAMETER: 15FT, EMBEDMENT DEPTH:**  
**40FT, CAVITY DEPTH: 5FT BELOW FOUNDATION,**  
**CAVITY LOCATION: CENTER OF COMMON BASEMAT**



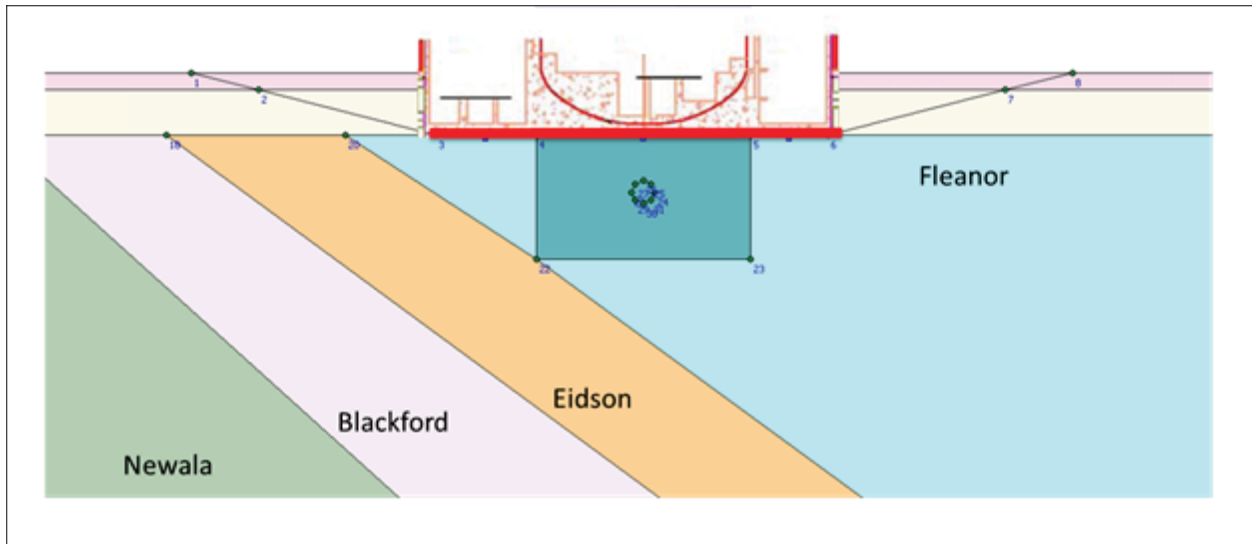


**FIGURE 2-22**  
**SITE B, CROSS SECTION: B-B', CAVITY DIAMETER: 15FT, EMBEDMENT DEPTH:**  
**40FT, CAVITY DEPTH: 30FT BELOW FOUNDATION, CAVITY LOCATION:**  
**CENTER OF COMMON BASEMAT**

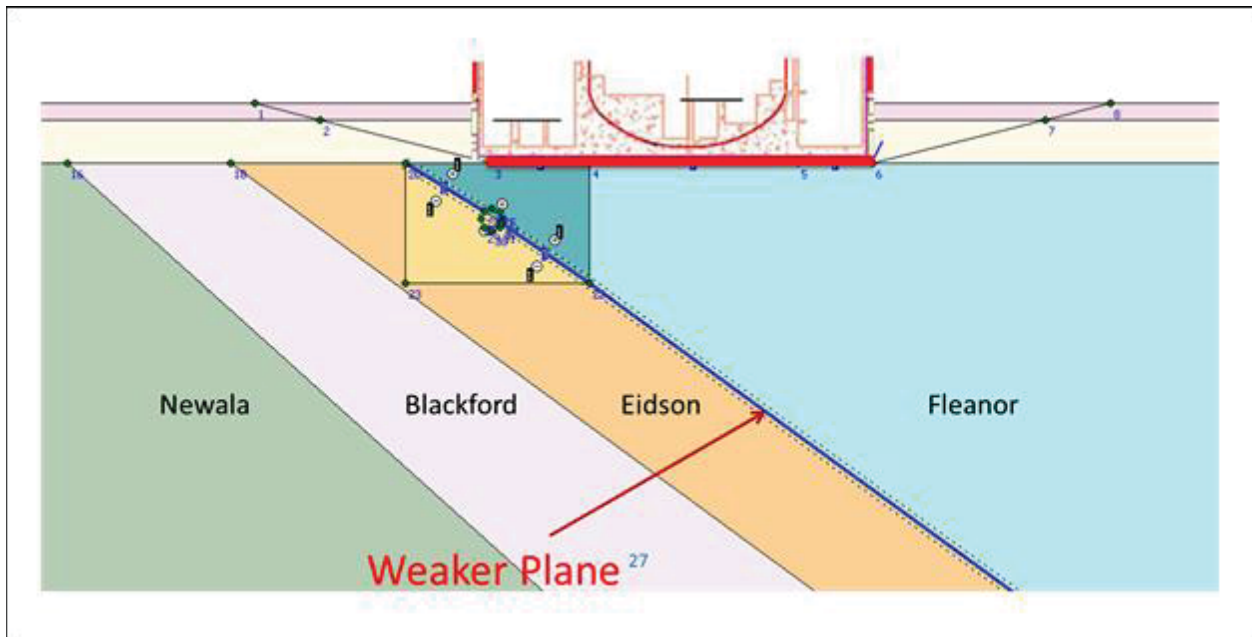


**FIGURE 2-23**  
**SITE B, CROSS SECTION: B-B', CAVITY DIAMETER: 15FT, EMBEDMENT DEPTH:**  
**40FT, CAVITY DEPTH: 30FT BELOW FOUNDATION, CAVITY LOCATION:**  
**EDGE OF COMMON BASEMAT WITH SHEAR FRACTURE ZONE INTERFACE**



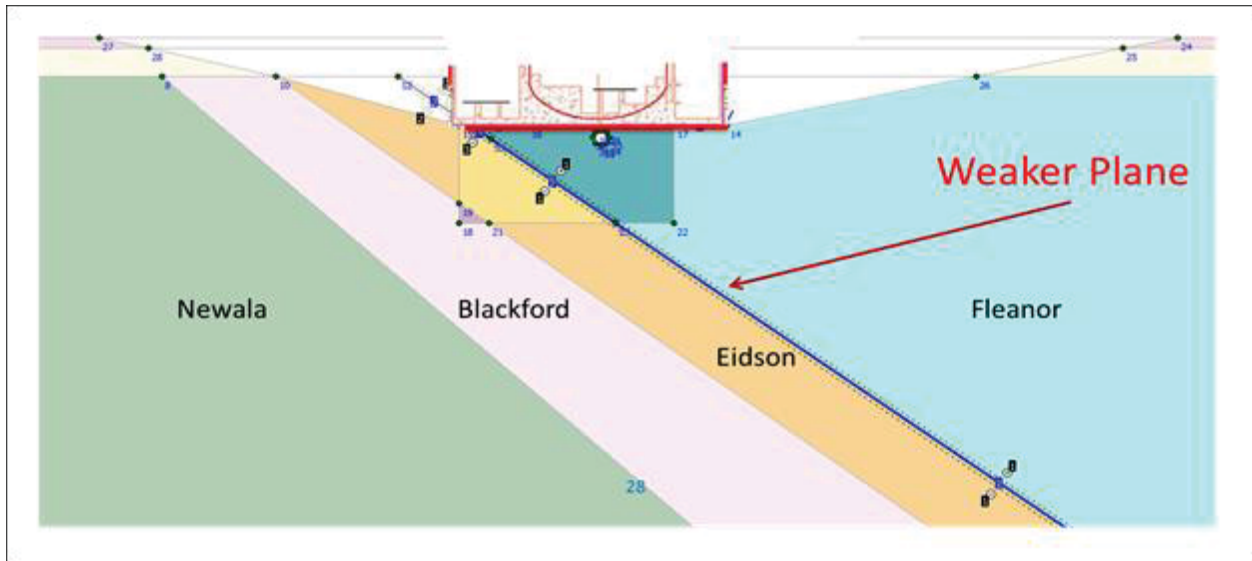


**FIGURE 2-24**  
**SITE B, CROSS SECTION: B-B', CAVITY DIAMETER: 15FT, EMBEDMENT DEPTH: 90FT, CAVITY DEPTH: 5FT BELOW FOUNDATION, CAVITY LOCATION: CENTER OF COMMON BASEMAT WITH SHEAR FRACTURE ZONE INTERFACE**

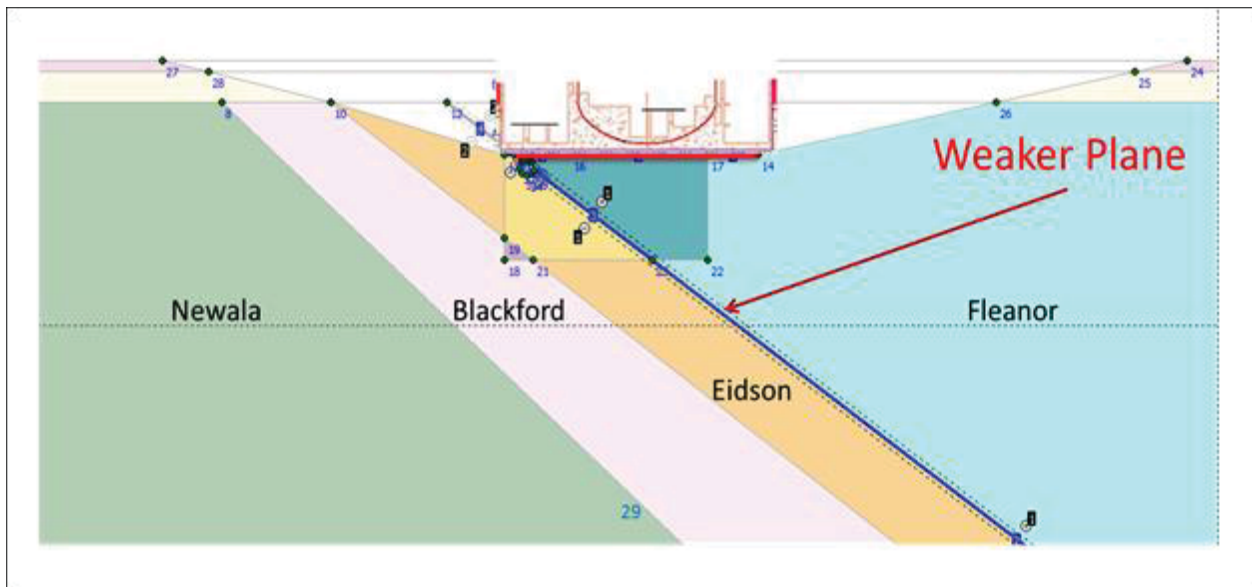


**FIGURE 2-25**  
**SITE B, CROSS SECTION: B-B', CAVITY DIAMETER: 15FT, EMBEDMENT DEPTH: 90FT, CAVITY DEPTH: 5FT BELOW FOUNDATION, CAVITY LOCATION: EDGE OF COMMON BASEMAT WITH SHEAR FRACTURE ZONE INTERFACE**



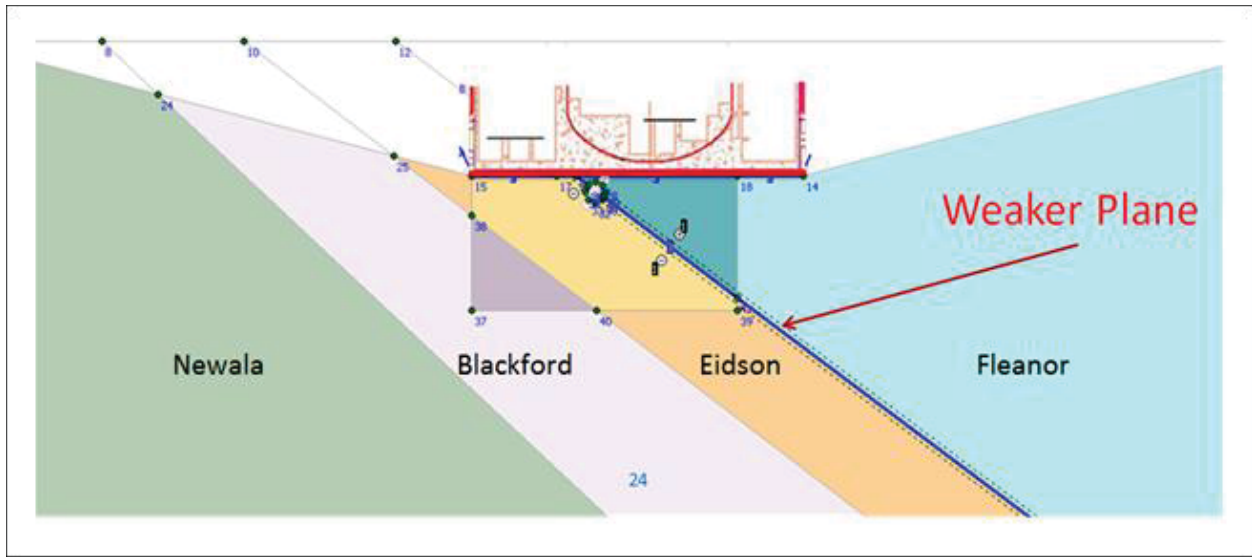


**FIGURE 2-26**  
**SITE B, CROSS SECTION: B-B', CAVITY DIAMETER: 15FT, EMBEDMENT DEPTH:**  
**140FT, CAVITY DEPTH: 5FT BELOW FOUNDATION, CAVITY LOCATION: ON**  
**BEDDING PLANE WITH SHEAR FRACTURE ZONE INTERFACE**

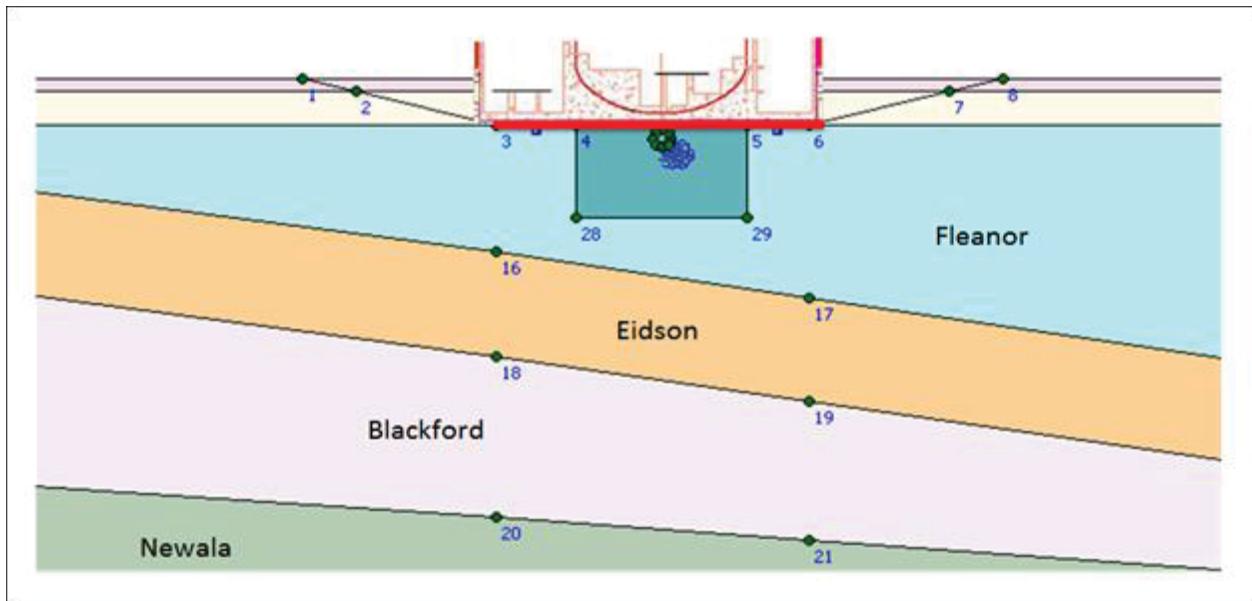


**FIGURE 2-27**  
**SITE B, CROSS SECTION: F-F', CAVITY DIAMETER: 15FT, EMBEDMENT DEPTH:**  
**40FT, CAVITY DEPTH: 5FT BELOW FOUNDATION CAVITY LOCATION: CENTER**  
**OF COMMON BASEMAT**



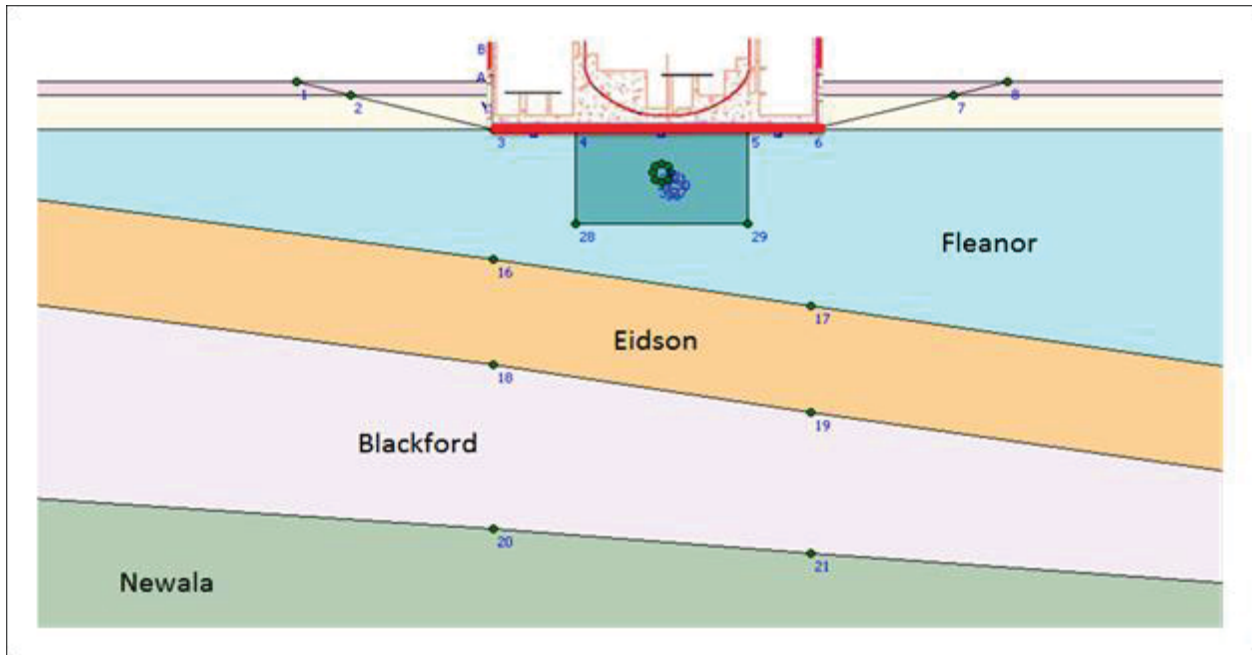


**FIGURE 2-28**  
**SITE B, CROSS SECTION: F-F', CAVITY DIAMETER: 15FT, EMBEDMENT DEPTH:**  
**40FT, CAVITY DEPTH: 30FT BELOW FOUNDATION, CAVITY LOCATION:**  
**CENTER OF COMMON BASEMAT**

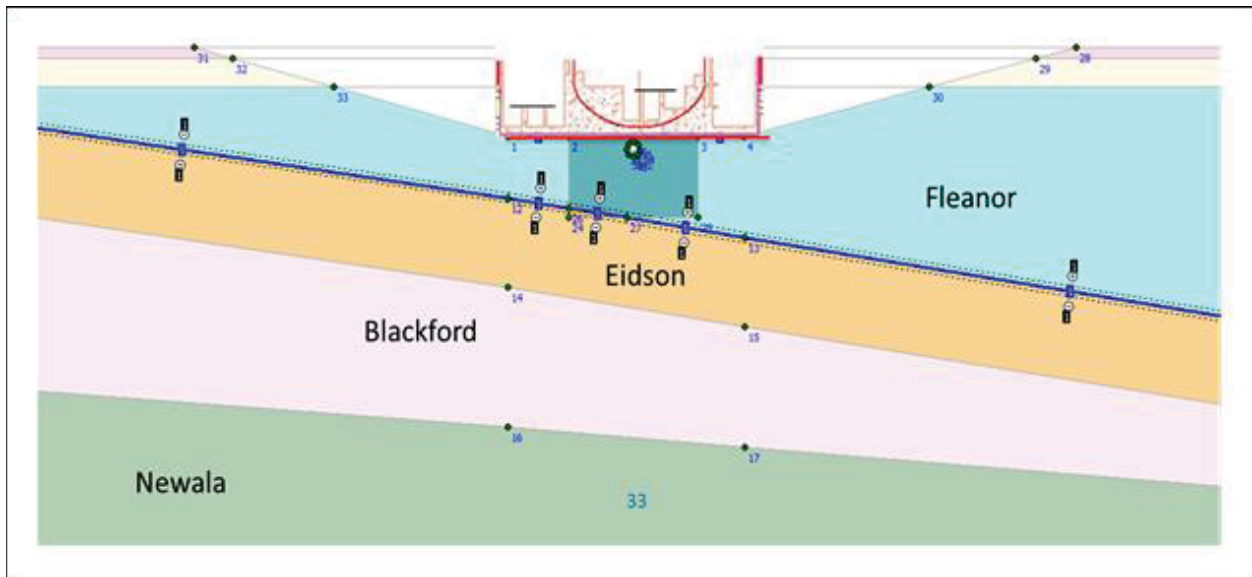


**FIGURE 2-29**  
**SITE B, CROSS SECTION: F-F', CAVITY DIAMETER: 15FT, EMBEDMENT DEPTH:**  
**90FT, CAVITY DEPTH: 5FT BELOW FOUNDATION, CAVITY LOCATION: CENTER**  
**OF COMMON BASEMAT WITH SHEAR FRACTURE ZONE INTERFACE**



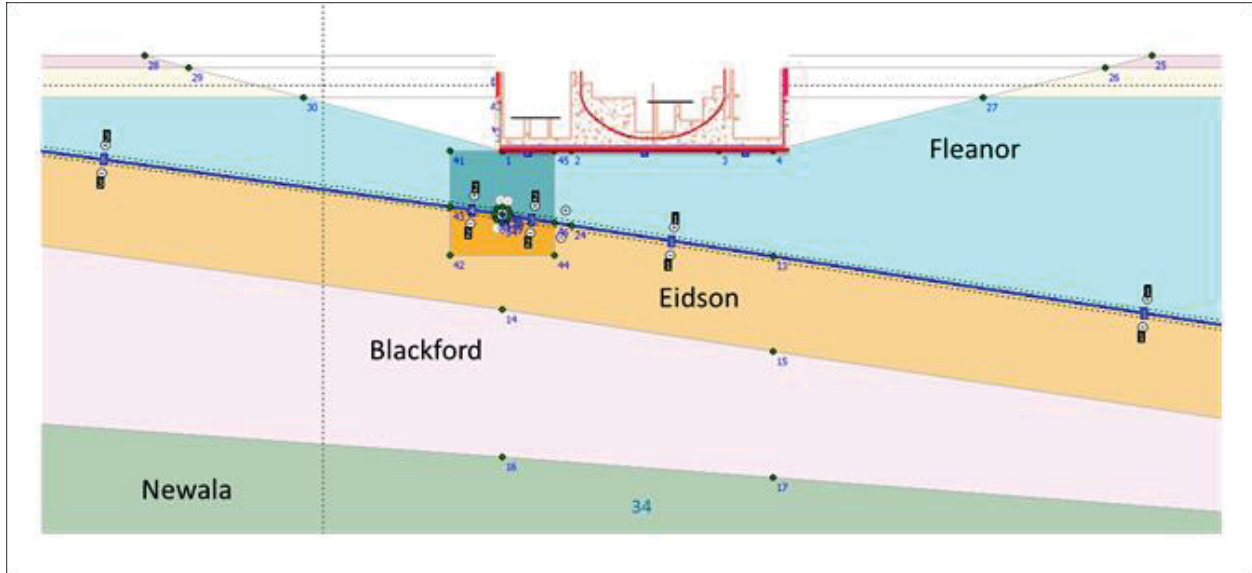


**FIGURE 2-30**  
**SITE B, CROSS SECTION: F-F', CAVITY DIAMETER: 15FT, EMBEDMENT DEPTH:**  
**90FT, CAVITY DEPTH: 30FT BELOW FOUNDATION, CAVITY LOCATION: EDGE**  
**OF COMMON BASEMAT ON THE BEDDING PLANE WITH SHEAR FRACTURE**  
**ZONE INTERFACE**

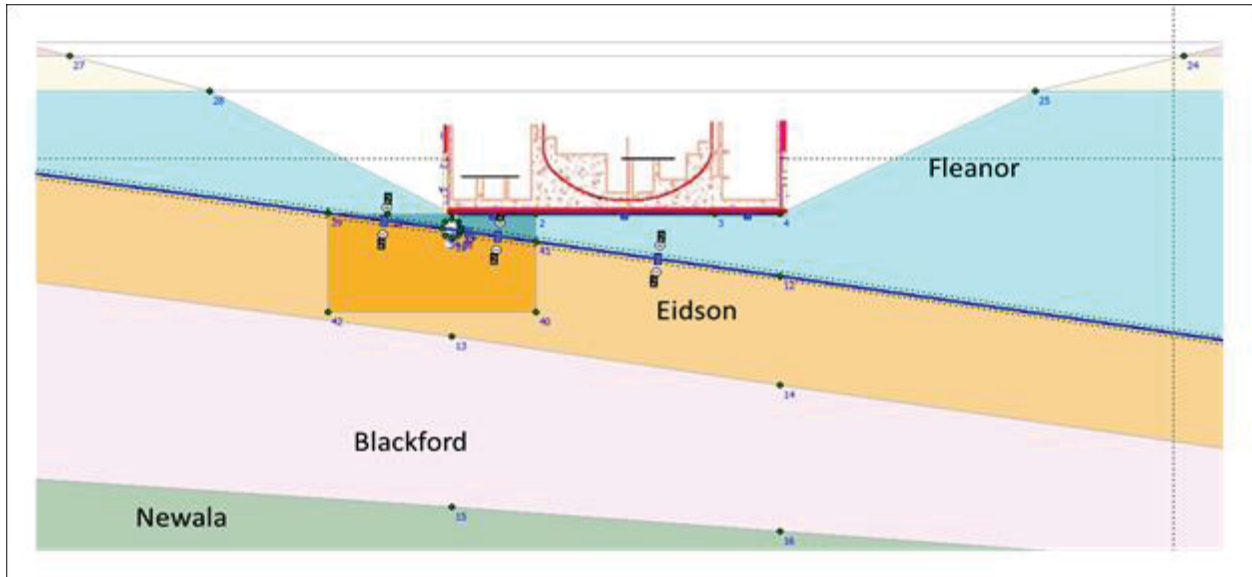


**FIGURE 2-31**  
**SITE B, CROSS SECTION: F-F', CAVITY DIAMETER: 15FT, EMBEDMENT DEPTH:**  
**140FT, CAVITY DEPTH: 5FT BELOW FOUNDATION, CAVITY LOCATION: ON THE**  
**BEDDING PLANE WITH SHEAR FRACTURE ZONE INTERFACE**



## 3.0 RESULTS

The results of the FE models were evaluated with one primary goal: to identify a cavity size that may potentially collapse under static excavation, dewatering, and structural loads.

Anticipated foundation host rocks, namely the Fleanor Member of the Lincolnshire Formation and the Benbolt and Rockdell formations, are all relatively stiff/competent rocks. Excluding potential cavity collapses, these rock formations are not expected to undergo large strains or deformation under excavation, dewatering, or structural static loads (i.e., foundation deformations are expected to be negligible). As such, the foundations should be safe provided that potential cavities do not collapse.

Here, the collapse potential of cavities is evaluated in terms of relative shear. Relative shear is the ratio of induced shear stress (due to static loads) to shear strength. As/if this ratio reaches 100 percent, a plastic zone (Mohr-Coulomb failure) starts to develop around a cavity, and collapse is initiated. For Site A and Site B modeling purposes, a critical relative shear ratio value of 0.85 (85 percent) was conservatively selected to provide a margin of safety of 15 percent:

All model results after loading phase were specifically evaluated in terms of relative shear and vertical deformation, with consideration for cavity diameters, depths, and locations, and foundation embedment depths.

### 3.1 CAVITY DIAMETERS

For model scenarios featuring 15 ft cavity diameters, relative shear values are about 10 percent higher relative to models utilizing 5 ft cavity diameter, as shown on *Figure 3-1*. Vertical deformation resulting from a 15 ft cavity diameter is also about 2 percent higher than the vertical deformations resulting from a 5 ft diameter cavity (*Figure 3-2*).



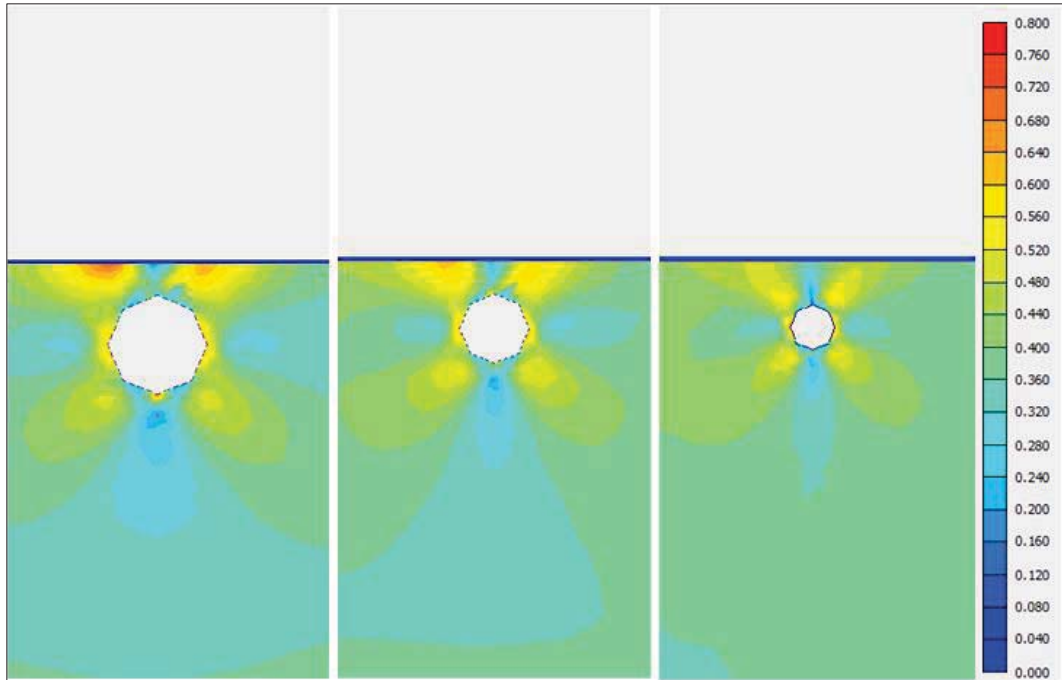


**FIGURE 3-1  
EXAMPLE RELATIVE SHEAR VALUE RESULTS FOR  
15 FT (LEFT), 10 FT (CENTER), AND 5 FT (RIGHT) CAVITY HEIGHTS**

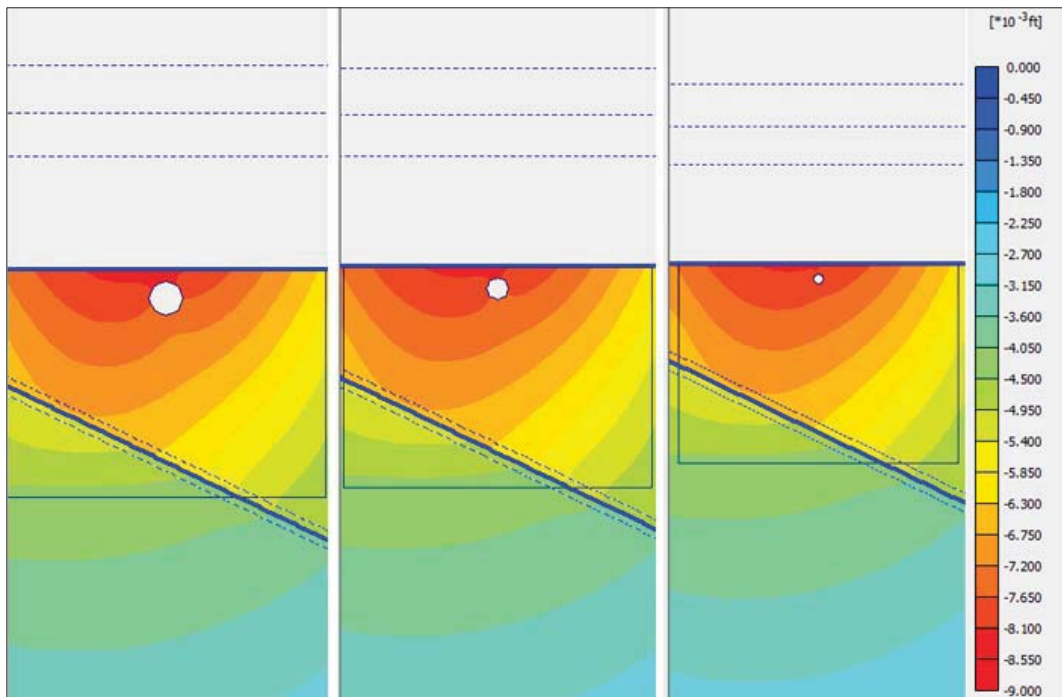


**FIGURE 3-2  
EXAMPLE VERTICAL DEFORMATION VALUE RESULTS FOR  
15 FT (LEFT), 10 FT (CENTER), AND 5 FT (RIGHT) CAVITY HEIGHTS**



The computational results suggest that models of 15 ft cavity diameters represent the most critical case of failure, relative to models of 10 ft and 5 ft cavity diameters. However, the effect of cavity size on deformation is negligible given that calculated critical ratios indicate that collapse is not initiated, and is only near the critical limit for the 15 ft cavity size.

### 3.2 CAVITY DEPTHS

Relative shear values are about 10 percent higher for PLAXIS 2D models of cavities located 30 ft below foundation basemat, relative to models featuring cavity depths 5 ft below the basemat (*Figure 3-3*). However, vertical deformations resulting from cavities located 5 ft below the foundation basemat are approximately 6% higher than vertical deformations resulting from cavities located 30 ft below the foundation basemat (*Figure 3-4*).

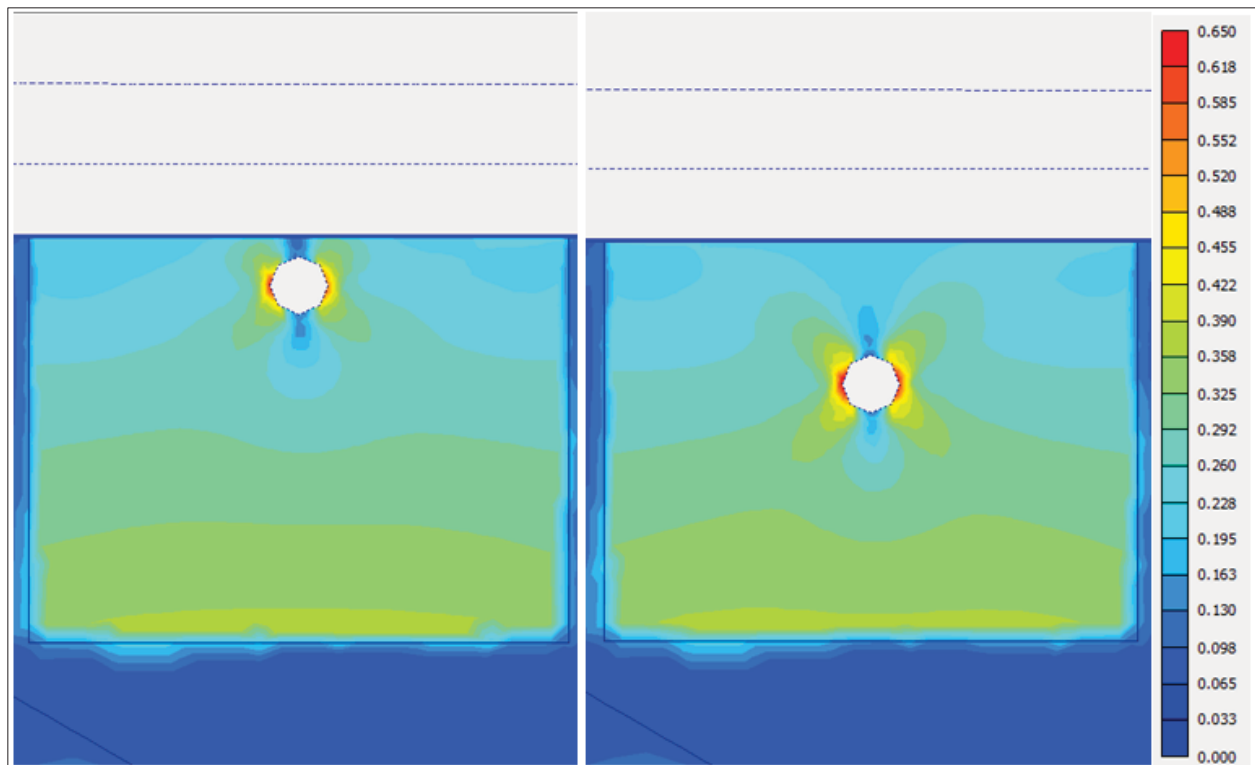


**FIGURE 3-3**  
**EXAMPLE RELATIVE SHEAR VALUE RESULTS FOR CAVITY DEPTHS OF 5 FT (LEFT) AND 30 FT (RIGHT) BELOW FOUNDATION BASEMAT**



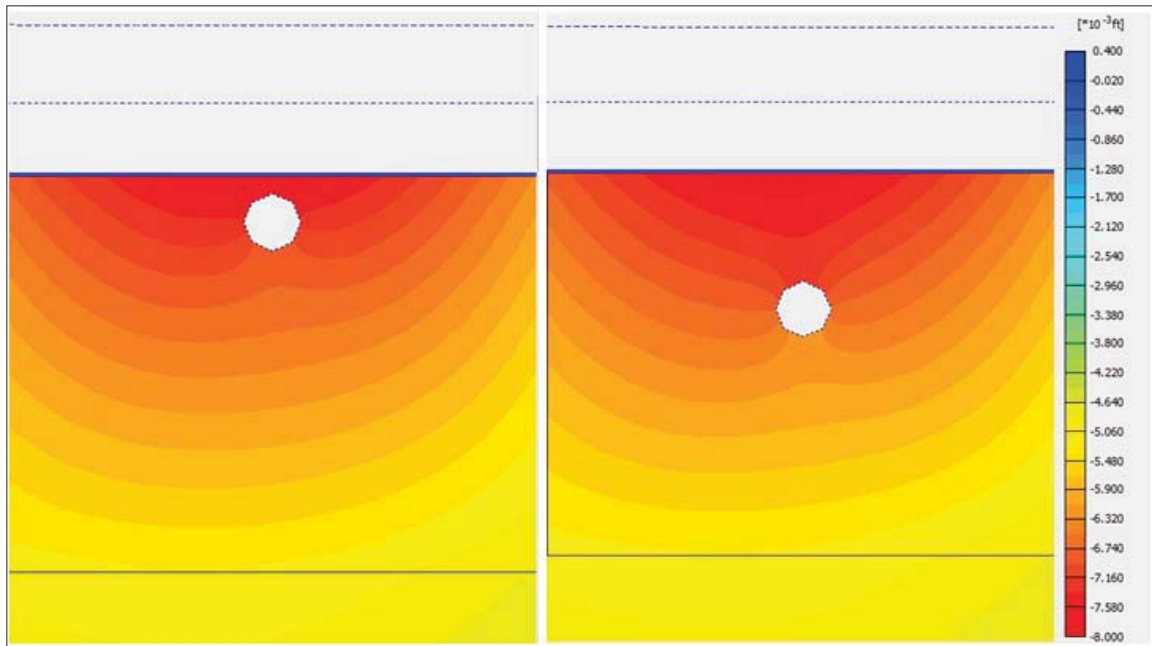


**FIGURE 3-4**  
**EXAMPLE VERTICAL DEFORMATION RESULTS FOR CAVITY DEPTHS OF 5 FT**  
**(LEFT) AND 30 FT (RIGHT) BELOW FOUNDATION BASEMAT**

### 3.3 CAVITY LOCATIONS

Models of cavities located below the center of the common basemat or below the edge of common basemat exhibit nearly comparable relative shear values. In contrast, models featuring cavities positioned on a stratigraphic contact (i.e., a bedding plane) demonstrate relative shear values about 40% higher (*Figure 3-5*).

As regards vertical deformations, models of cavity location 5 ft below foundation basemat levels exhibit deformations roughly 50% higher than models of cavities located on bedding plane discontinuities (*Figure 3-6*).



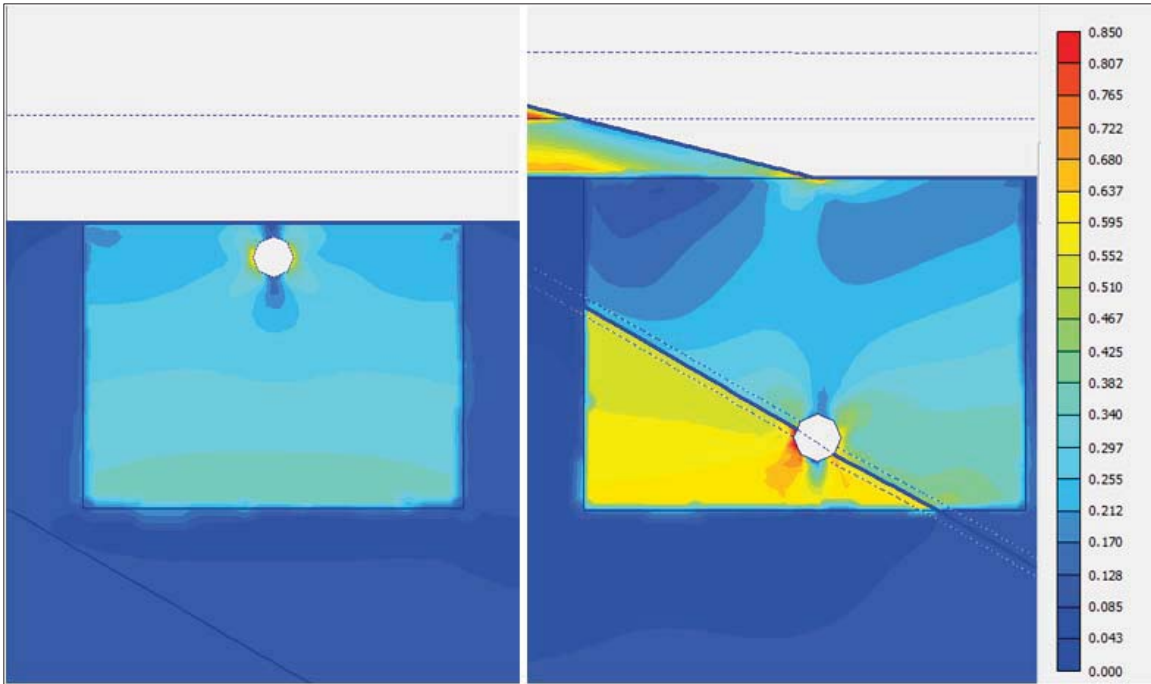


**FIGURE 3-5  
EXAMPLE RELATIVE SHEAR VALUE RESULTS FOR CAVITY LOCATIONS 5 FT  
BELOW FOUNDATION BASEMAT (LEFT) AND ON A BEDDING PLANE  
DISCONTINUITY (RIGHT)**

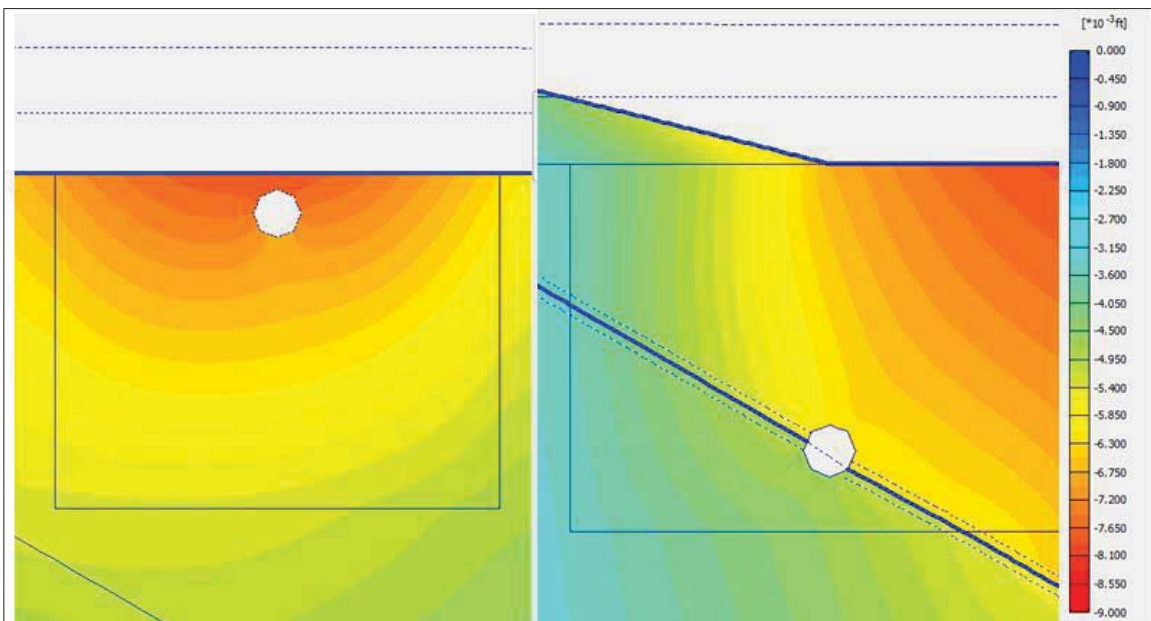


**FIGURE 3-6  
EXAMPLE VERTICAL DEFORMATION RESULTS FOR CAVITY LOCATIONS 5 FT  
BELOW FOUNDATION BASEMAT (LEFT) AND ON A BEDDING PLANE  
DISCONTINUITY (RIGHT)**



### 3.4 EMBEDMENT DEPTHS

For the foundation embedment depths of 40 ft, 90 ft, and 140 ft, consideration was provided for the most critical cavity diameter (15 ft) and cavity location (bedding planes). Vertical deformation and relative shear values were compared under static loading.

For all embedment depths, relative shear values are about the same (*Figure 3-7*). Vertical deformations, in contrast, appear to increase with decreasing depth of bedding planes, relative to excavation surfaces (*Figure 3-8*).

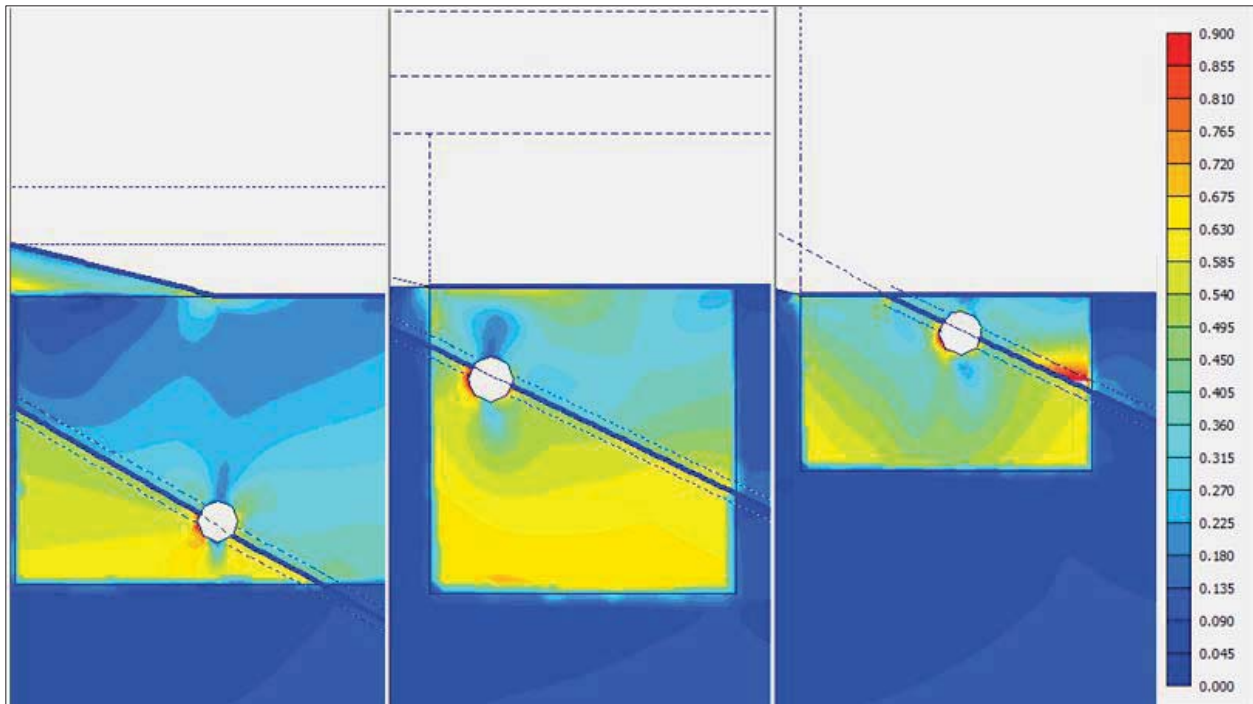


**FIGURE 3-7**  
**EXAMPLE RELATIVE SHEAR VALUE RESULTS FOR FOUNDATION**  
**EMBEDMENT DEPTHS OF 40 FT (LEFT), 90 FT (CENTER), AND 140 FT (RIGHT)**



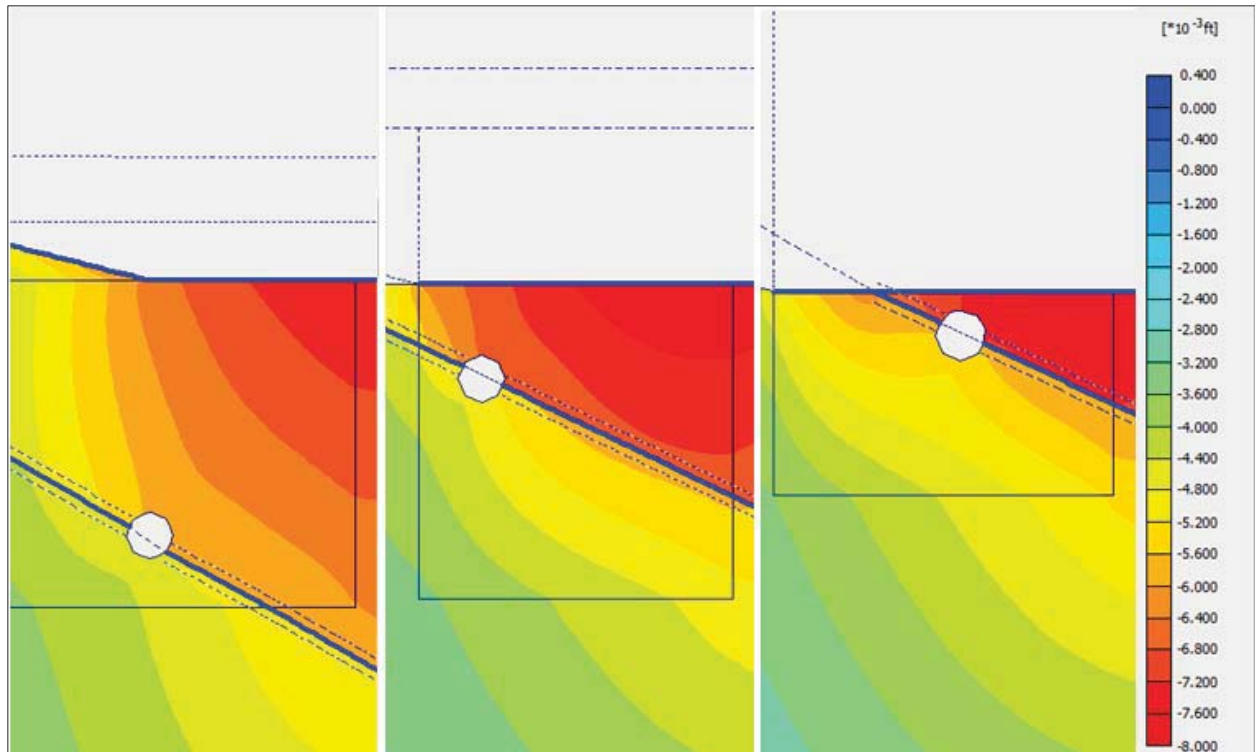


**FIGURE 3-8**  
**EXAMPLE RESULTS FOR VERTICAL DEFORMATIONS FOR FOUNDATION**  
**EMBEDMENT DEPTHS OF 40 FT (LEFT), 90 FT (CENTER), AND 140 FT (RIGHT)**

### 3.5 OVERALL MODEL LOADING RESULTS

*Table 3-1* presents the most critical cases in terms of relative shear and vertical deformation for Site A and Site B respectively. From the static analysis, the maximum relative shear observed for Sites A and B is 0.90 and 0.92, respectively.

Relative shear results from the PLAXIS 2D models are shown on *Figure 3-9 through Figure 3-14* for both Site A and Site B. Model results suggest that relative shear is highest at the edges of the simulated cavities, as expected.

Interface element sensitivity analyses in turn are presented on *Figure 3-15 and Figure 3-16*, and demonstrate clearly the increase in vertical deformation associated with bedding plane discontinuities and shear fracture zones. Specifically, *Figure 3-15* shows model results with an interface element located on a bedding plane, whereas *Figure 3-16* shows the same model considered on *Figure 3-15* without the interface element.



Maximum estimated vertical deformation shown on **Figure 3-15** is  $-9.34\text{E-}3$  ft. Maximum vertical displacement shown on **Figure 3-16** is nearly 50 percent lower ( $-6.27\text{E-}3$  ft).



**TABLE 3-1  
MODEL RESULTS IN LOADING PHASES FOR SITES A AND B**

SITE <sup>(1)</sup>	SECTION <sup>(2)</sup>	FOUNDATION DEPTH <sup>(3)</sup> (ft)	CAVITY SIZE <sup>(4)</sup> (ft)	CRITICAL CAVITY LOCATION <sup>(5)</sup>	REMARKS <sup>(6)</sup>	RELATIVE SHEAR <sup>(7)</sup>	DEFORMATION <sup>(8)</sup> (ft)
Site A	A-A'	40	15	Center of common basemat Bedding (Benbolt-Rockdell)	5 ft below basemat 1 Interface	0.60	0.008
		90	15	Center of common basemat Bedding (Benbolt-Rockdell)	5 ft below basemat 1 Interface	0.70	0.008
		140	15	Center of common basemat Bedding (Benbolt-Rockdell)	5 ft below basemat 1 Interface	0.90	0.007
Site A	E-E'	40	15	Center of common basemat	5 ft below basemat	0.60	0.008
		90	15	Center of common basemat Bedding (Benbolt-Rockdell)	5 ft below basemat 1 Interface	0.60	0.008
		140	15	Center of common basemat Bedding (Benbolt-Rockdell)	5 ft below basemat 1 Interface	0.90	0.005
Site B	B-B'	40	15	Center of common basemat Bedding (Benbolt-Rockdell)	5 ft below basemat 1 Interface	0.80	0.008
		90	15	Center of common basemat Bedding (Benbolt-Rockdell)	5 ft below basemat 1 Interface	0.95	0.009
		140	15	Center of common basemat Bedding (Benbolt-Rockdell)	5 ft below basemat 1 Interface	0.75	0.011
Site B	F-F'	40	15	Center of common basemat	5 ft below basemat	0.90	0.007
		90	15	Center of common basemat Bedding (Benbolt-Rockdell)	5 ft below basemat 1 Interface	0.92	0.011
		140	15	Center of common basemat Bedding (Benbolt-Rockdell)	5 ft below basemat 1 Interface	0.75	0.007

**Notes:**

ft = feet

- (1) Units 1&2 (Site A) or 3&4 (Site B).
- (2) Modeled Site A and Site B cross sections (see *Figure 2-1 through Figure 2-4*).
- (3) Modeled foundation embedment depth (feet below ground surface).
- (4) Critical cavity diameter.
- (5) Critical cavity locations.
- (6) Additional detail related to cavity location. For Site A, "1 interface" indicates a single interface element introduced on both sides of the contact between the Benbolt and Rockdell formations. For Site B, "1 interface" indicates a single interface element introduced on both sides of the contact between the Fleonor and Eidson members of the Lincolnshire Formation.
- (7) Calculated relative shear.
- (8) Calculated vertical deformation.



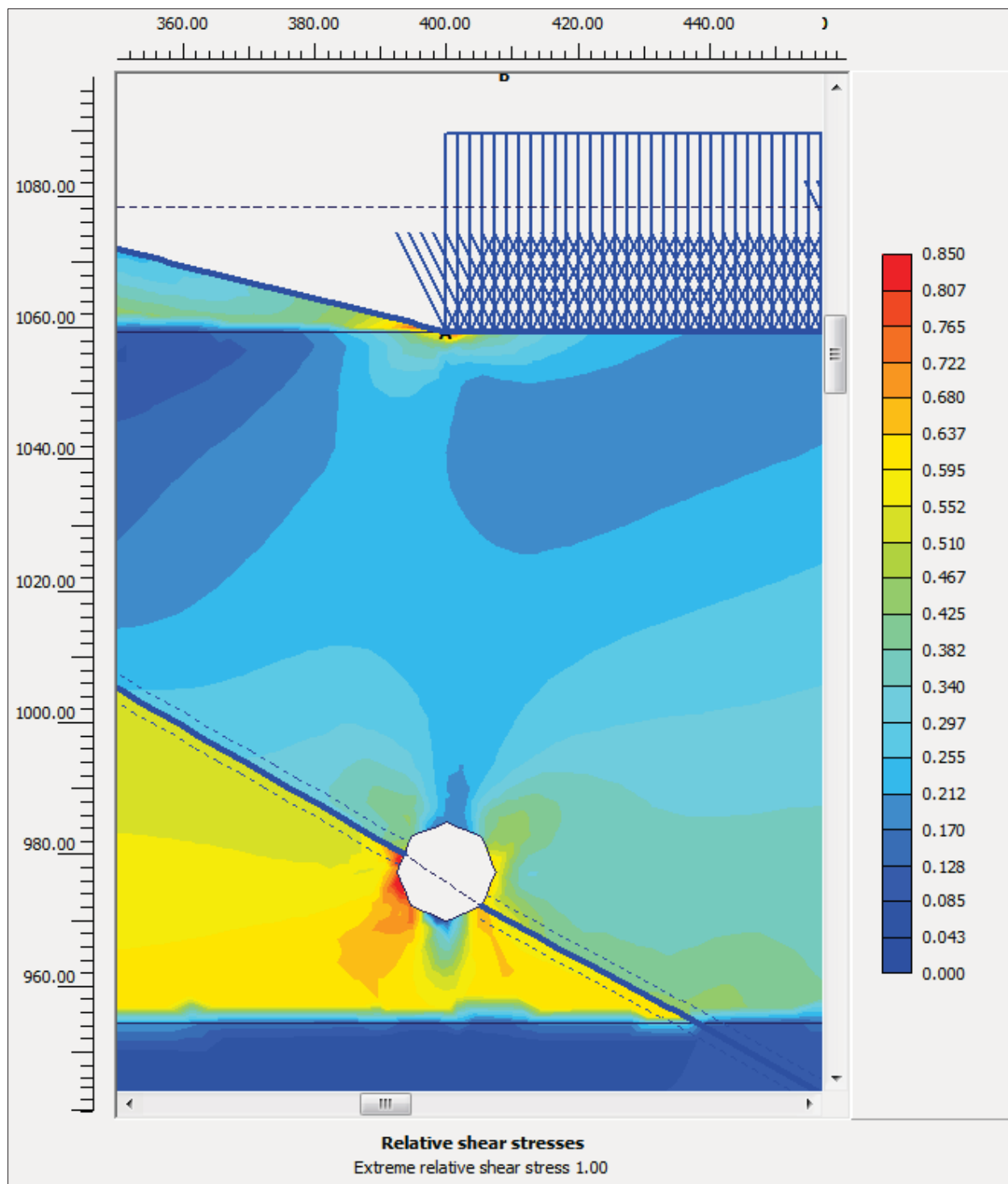


**FIGURE 3-9**  
**SITE A CROSS SECTION A-A'**  
**FOUNDATION DEPTH 40 FT**  
**CAVITY (15 FT) ON THE BEDDING PLANE INTERFACE**  
**RELATIVE SHEAR=0.85**



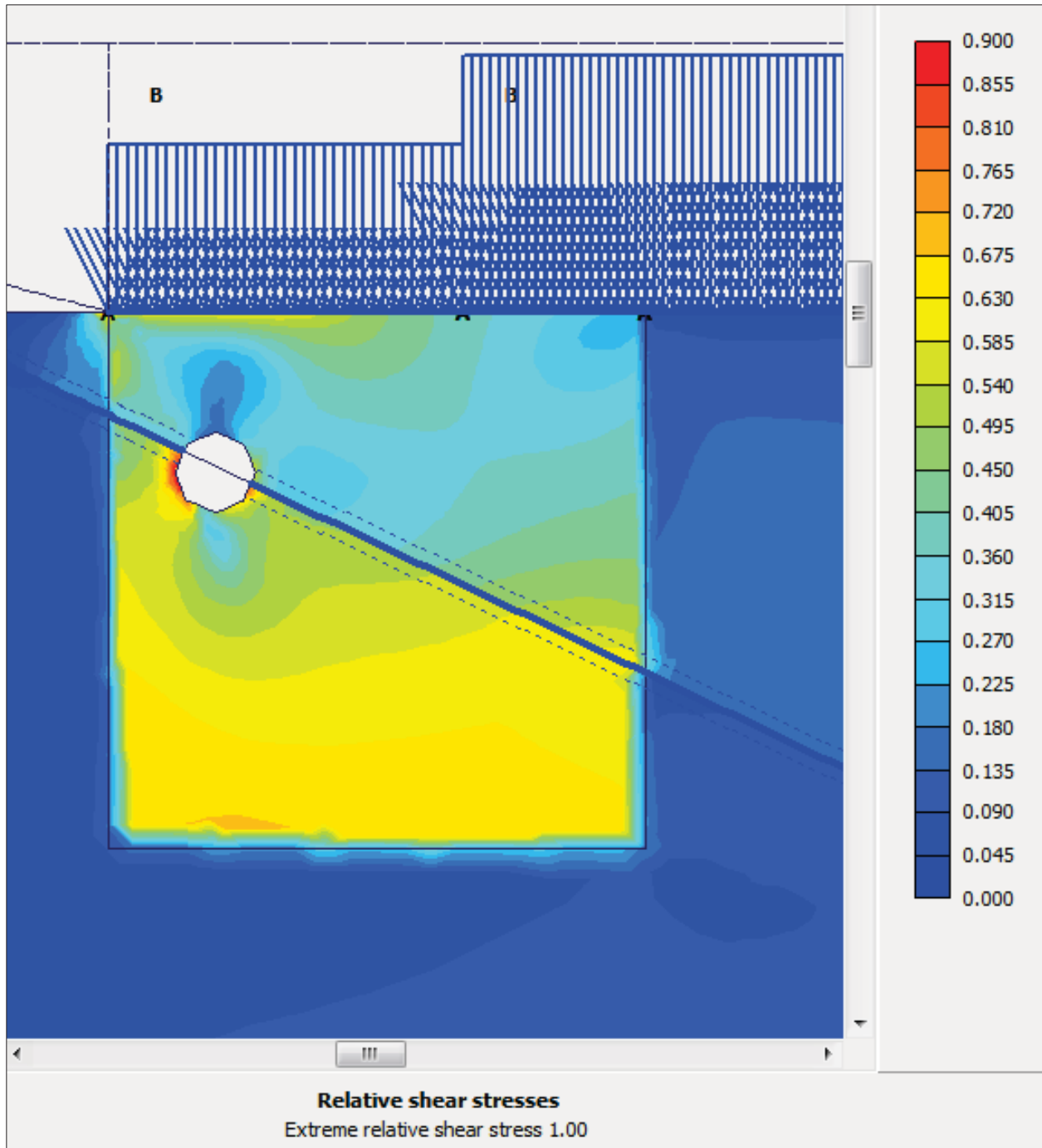


**FIGURE 3-10**  
**SITE A CROSS SECTION A-A'**  
**FOUNDATION DEPTH 90 FT**  
**CAVITY (15 FT) ON THE BEDDING PLANE INTERFACE**  
**RELATIVE SHEAR=0.90**



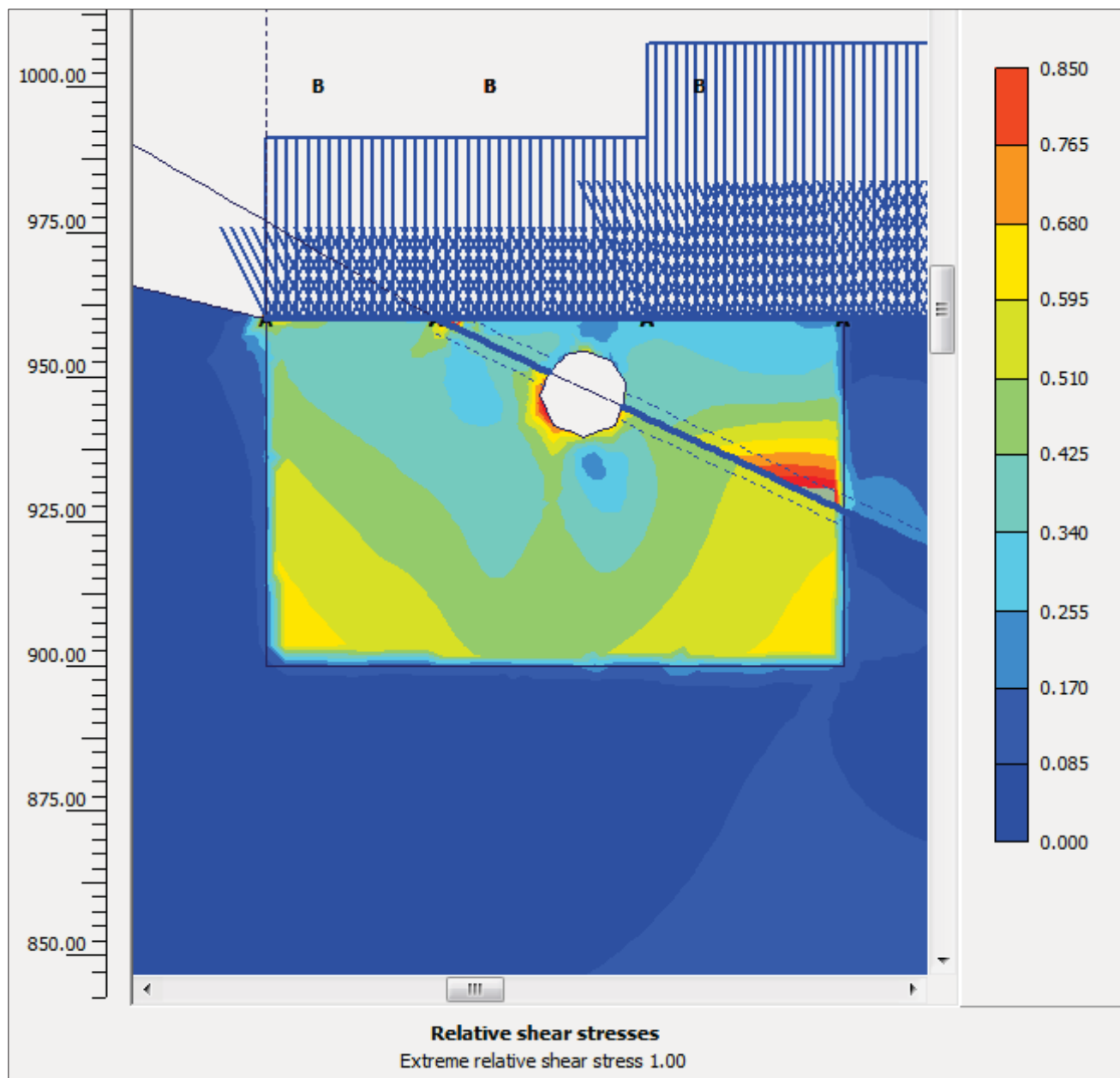


**FIGURE 3-11**  
**SITE A CROSS SECTION A-A'**  
**FOUNDATION DEPTH 140 FT**  
**CAVITY (15 FT) ON THE BEDDING PLANE INTERFACE**  
**RELATIVE SHEAR=0.85**



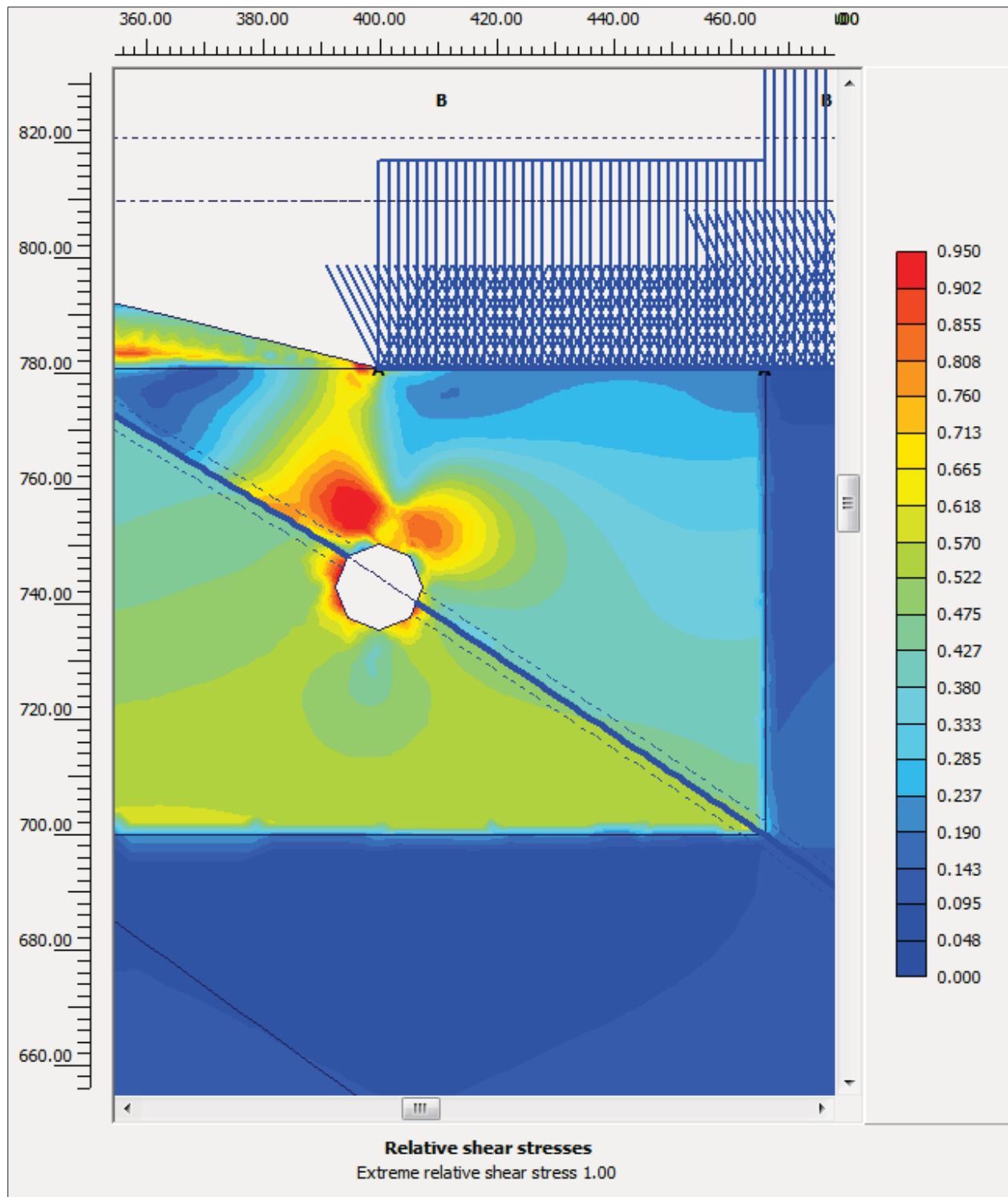


**FIGURE 3-12**  
**SITE B CROSS SECTION B-B'**  
**FOUNDATION DEPTH 40 FT**  
**CAVITY (15 FT) LOCATED 30 FT BELOW EDGE OF COMMON BASEMAT**  
**RELATIVE SHEAR=0.95**



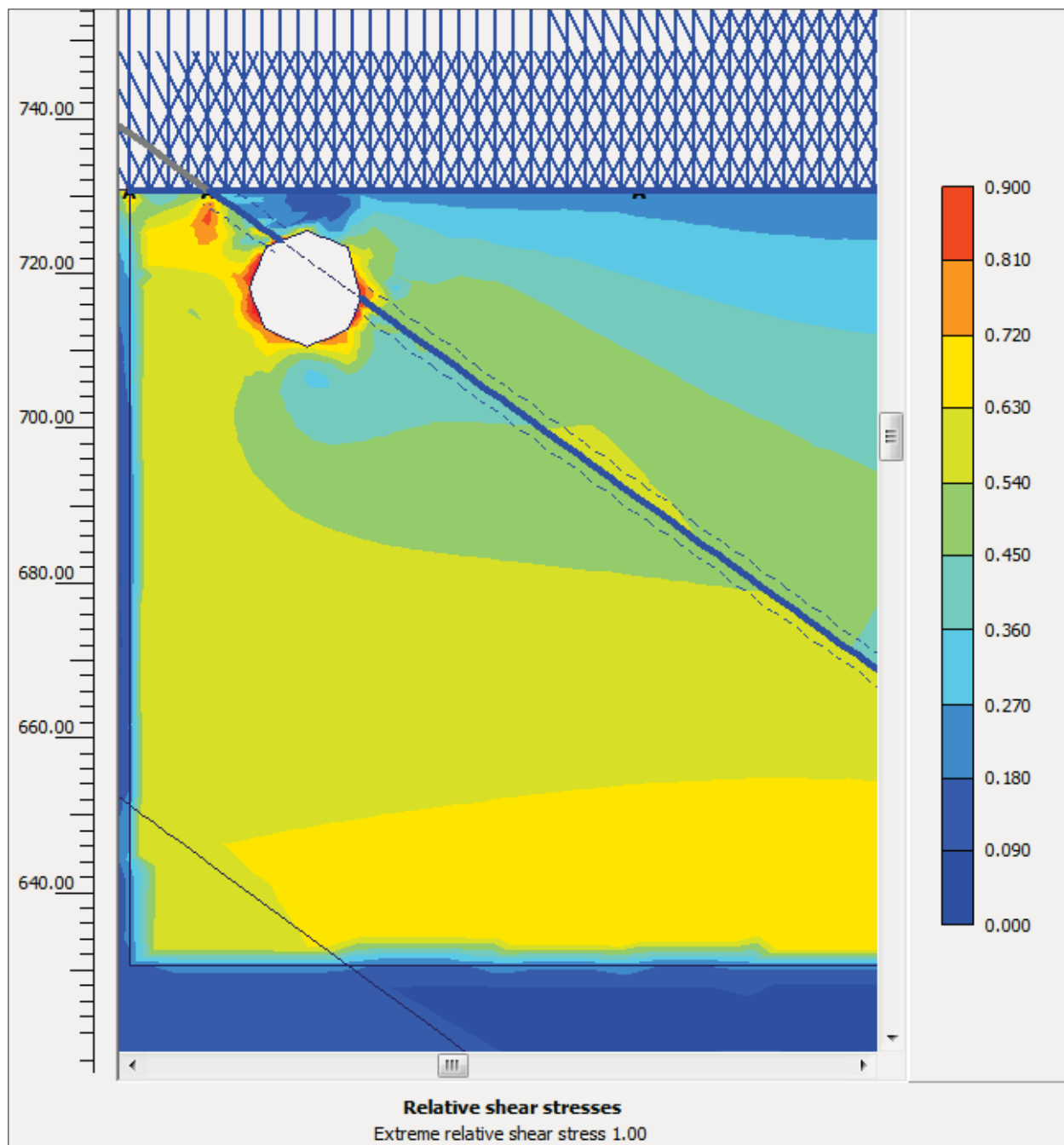


**FIGURE 3-13**  
**SITE B CROSS SECTION B-B'**  
**FOUNDATION DEPTH 90 FT**  
**CAVITY (15 FT) LOCATED 5 FT BELOW EDGE OF COMMON BASEMAT**  
**RELATIVE SHEAR=0.90**



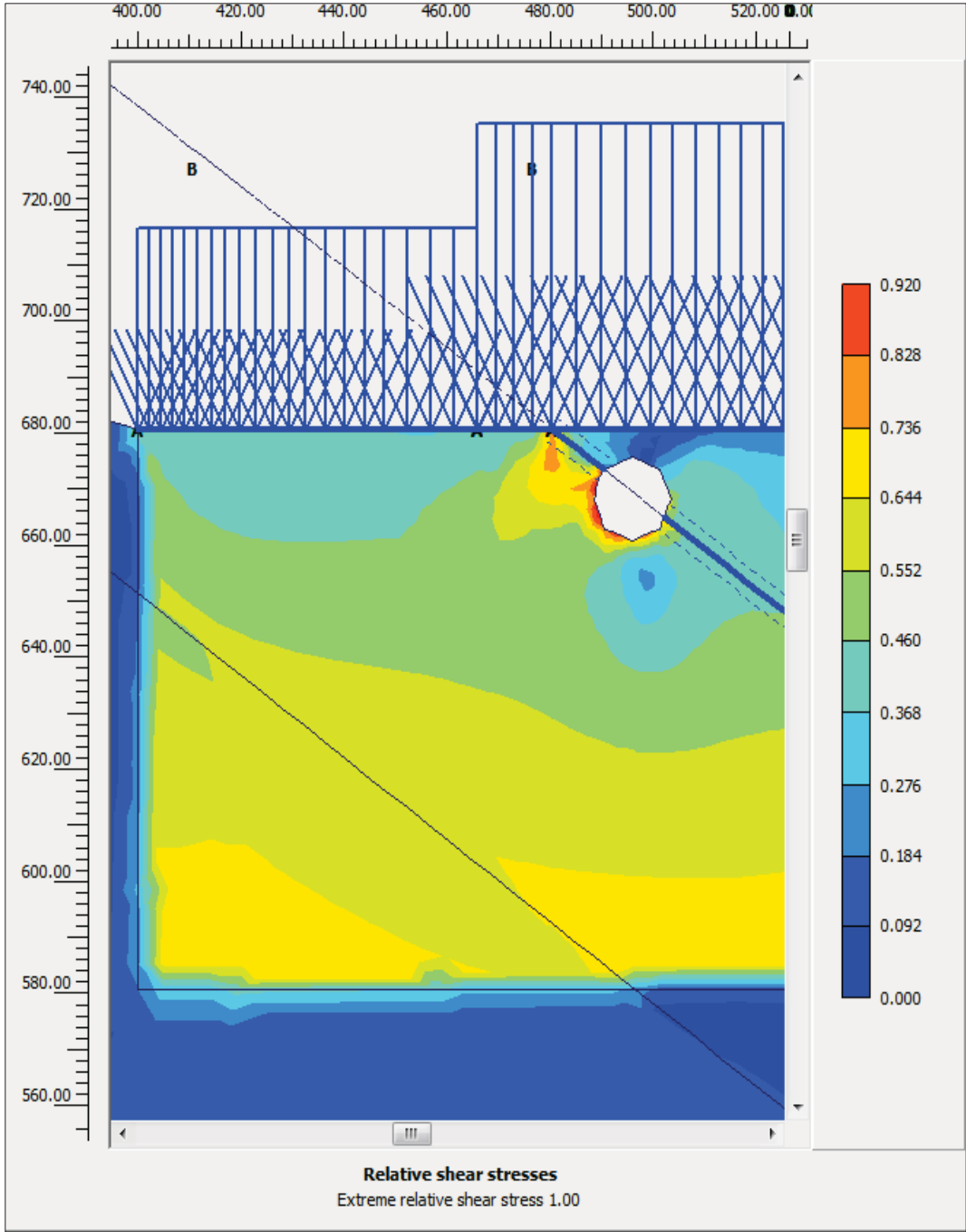


**FIGURE 3-14**  
**SITE B CROSS SECTION B-B'**  
**FOUNDATION DEPTH 140 FT**  
**CAVITY (15 FT) LOCATED 5 FT BELOW CENTER OF COMMON BASEMAT**  
**ON BEDDING PLANE INTERFACE**  
**RELATIVE SHEAR=0.92**



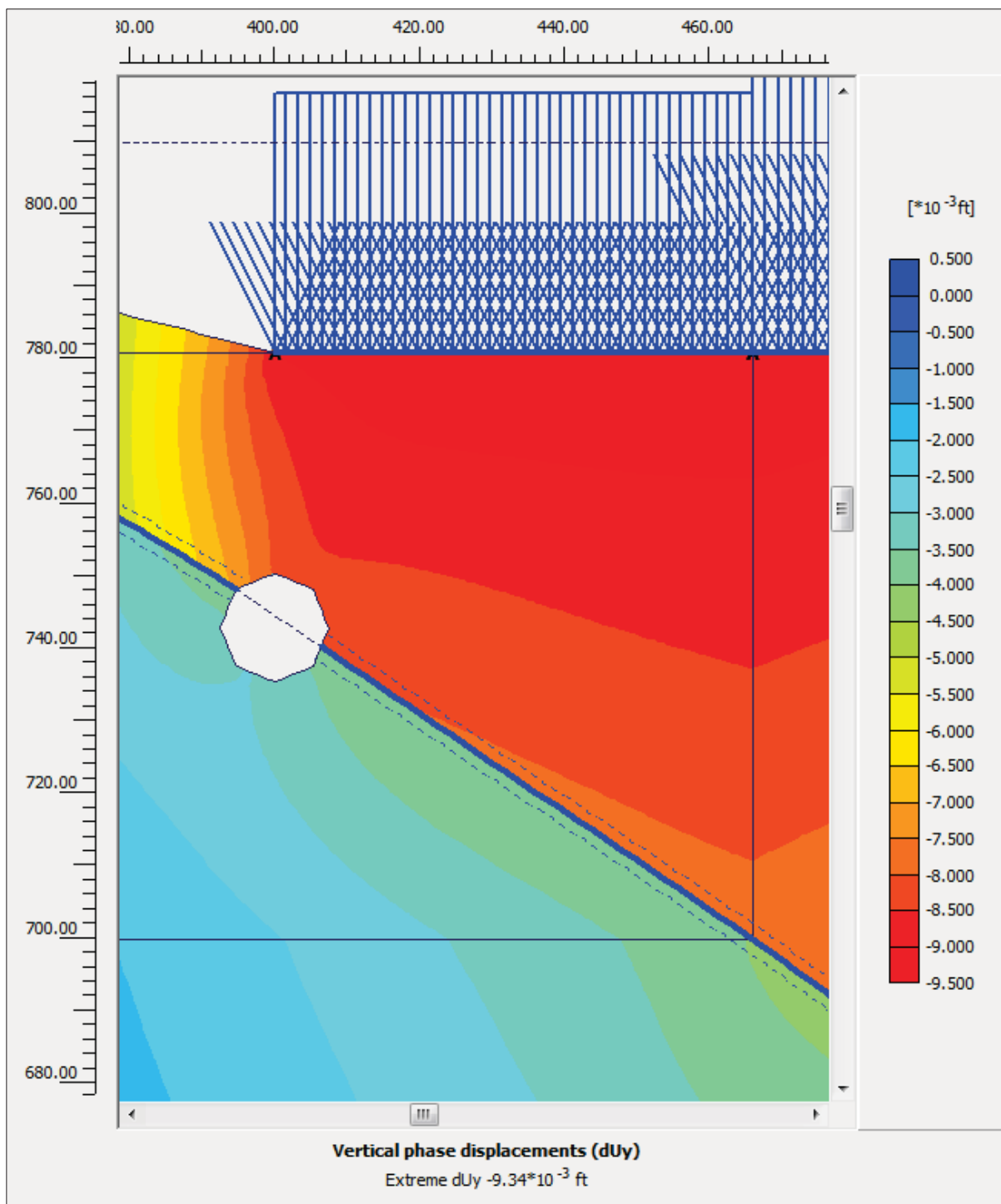


**FIGURE 3-15**  
**EFFECT OF INTERFACE ON SITE B RESPONSE**  
**CROSS SECTION B-B',**  
**CAVITY 30 FT BELOW EDGE OF COMMON BASEMAT, ON SHEAR ZONE**  
**INTERFACE**  
**MAXIMUM VERTICAL DEFORMATION =  $-9.34 \times 10^{-3}$  FT**



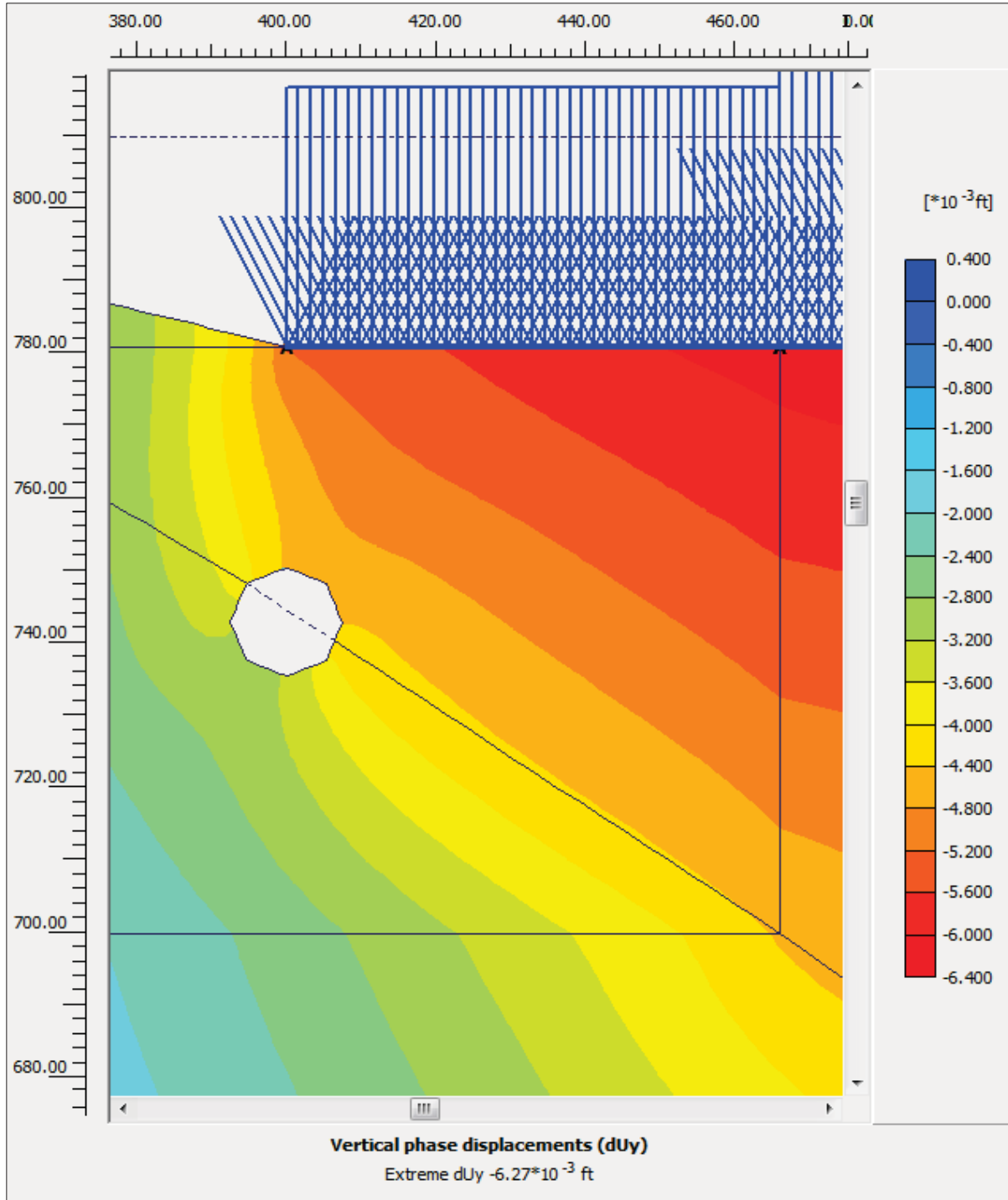


**FIGURE 3-16**  
**EFFECT OF INTERFACE ON SITE B RESPONSE**  
**CROSS SECTION B-B'**  
**CAVITY 30 FT BELOW EDGE OF COMMON BASEMAT, ON SHEAR ZONE**  
**INTERFACE**  
**MAXIMUM VERTICAL DEFORMATION =  $-6.27 \times 10^{-3}$  FT (RIGHT)**



## 4.0 SUMMARY AND RECOMMENDATIONS

Postulated collapse of karstic cavities is a geologic hazard to be addressed for the proposed SMR Units 1&2 and 3&4 at the Clinch River Nuclear Site. Accordingly, the impact of various postulated cavity sizes and locations on SMR foundation performance were evaluated using a PLAXIS 2D model. Specifically, the PLAXIS 2D model developed for Units 1&2 (Site A) and 3&4 (Site B) considered

- cavity diameters equal to 5 ft, 10 ft, and 15 ft (selected based on what size is likely to fail and based on observed cavity sizes),
- cavity depths of 5 ft and 30 ft below foundation embedment depths,
- foundation embedment depths of 40 ft, 90 ft, and 140 ft, and
- cavity locations on the edge of the common basemat, the center of the common basemat, and on or along bedding planes conservatively assumed to feature significant discontinuities or shear fracture zones.

For all cases considered, we draw the following main conclusions:

1. For all model simulations, the largest cavity diameter (15 ft) was determined to be most critical as expected.
2. Deeper cavities produce increased relative shear around the cavity, which is attributed to the larger initial in situ stresses.
3. Relative shears around the cavities are comparable for individual embedment depths. However, vertical deformation increases with decreasing depth of a cavity relative to foundation embedment depths/excavation surfaces.
4. Cavities located on bedding plane discontinuities or in bedding plane shear fracture zones are most critical and result in highest relative shear around the cavity.

Approximately 99 percent of the cavities observed in Site A and Site B borings are less than 11 ft in inferred height. Maximum observed cavity height does not exceed 17 ft. Moreover, cavity development in CRN Site areas is generally limited to the most markedly weathered zone immediately below ground surface, to depths less than 100 ft; 75 percent of reported cavities in CRN Site A and B borings occur at depths less than 55 ft. Consequently, cavity-related failure



has a higher potential to occur at relatively shallow depths, less than about 30 ft. Given that foundation embedment depths are deeper than 30 ft and that the 15 ft critical cavity diameter determined by PLAXIS 2D modeling is significantly larger than the 11 ft height that bounds 99 percent of the cavities observed in CRN Site borings, Sites A and B are generally suitable for SMR foundation.

Nonetheless, foundation performance should be re-evaluated on selection of a final technology, taking into account specific plant design, specific plant loads, and any potential ground improvement or grouting plans. Final foundation locations should also be re-evaluated using specific plant information, with consideration for specific Site stratigraphy, subsurface layering orientation, and specific shear fracture or bedding plane discontinuity zonation.

During the combined operating license application, it is recommended to conduct targeted supplemental field investigations to further define geological discontinuities, including potential shear zones. The following activities are recommended to be conducted during the targeted supplemental field investigation:

- The targeted field investigation should be conducted in areas with less soil cover, and with drill angles that take into account the dip and strike of the considered discontinuity.
- Samples should be obtained with the least disturbance, to retain cavity and/or discontinuity filling materials. Joint fill material and bedding plane material are important to recover for testing, recognizing that will require special sampling techniques.
- Collected samples should be subjected to direct shear tests to obtain additional interface friction parameters to refine model assumptions.
- Field tests may be required to measure in situ stress conditions and define in situ stress fields.
- High resolution (an inch or two-inch resolution) topographic mapping with LiDAR or photogrammetric methods should be conducted to identify potential depression areas.

Finally, the analysis conducted in this Report should be repeated for the Combined Operating License Application (COLA) process, for the selected technology and based on the results obtained from the targeted supplemental field investigation and using existing ESP Application data.



## 5.0 REFERENCES

Bechtel, 2014, Geologic Cross Sections, Calculation No. 25847-000-KOC-0000-00017, Rev. 001, July 2014

Hatcher et al., Status Report on the Geology of the Oak Ridge Reservation, Oak Ridge National Laboratory, Environmental Sciences Division, Publication No. 3860, October 1992.

Hoek, Evert, and Mark S. Diederichs, "Empirical Estimation of Rock Mass Modulus," International Journal of Rock Mechanics and Mining Sciences 43.2 (2006): 203-215.

Hoek, Evert, Carlos Carranza-Torres, and Brent Corkum, "Hoek-Brown Failure Criterion-2002 edition," Proceedings of NARMS-Tac 1 (2002): 267-273.

Kummerle, R.P., and D.A. Benvie, Exploration, Design and Excavation of Clinch River Breeder Reactor Foundations, 28th U.S. Symposium on Rock Mechanics, Tucson, June 1987.

ML16144A059 - Part 02 SSAR (Rev. 0) - Part 2 - SSAR - Chapter 2 - Site Characteristics - Section 2.5.1 Geologic Characterization Information, 2016

ML16144A060 - Part 02 SSAR (Rev. 0) - Part 2 - SSAR - Chapter 2 - Site Characteristics - Section 2.5.1 - Figures 1-35, 2016

ML16144A061 - Part 02 SSAR (Rev. 0) - Part 2 - SSAR - Chapter 2 - Site Characteristics - Section 2.5.1 - Figures 36-63, 2016

ML16144A063 - Part 02 SSAR (Rev. 0) - Part 2 - SSAR - Chapter 2 - Site Characteristics - Section 2.5.2 - Vibratory Ground Motion, 2016

ML16144A065 - Part 02 SSAR (Rev. 0) - Part 2 - SSAR - Chapter 2 - Site Characteristics - Section 2.5.3 - Surface Deformation, 2016

ML16144A067 - Part 02 SSAR (Rev. 0) - Part 2 - SSAR - Chapter 2 - Site Characteristics - Section 2.5.4 - Stability of Subsurface Materials and Foundations, 2016



N. S. Drakulich, Geologic Mapping of the Clinch River Breeder Reactor Plant Excavations, Stone and Webster Engineering Corp, 1984.

Project Management Corporation, Clinch River Breeder Reactor Project Preliminary Safety Analysis Report, Vol. 2, 1982.

Project Management Corporation, Clinch River Breeder Reactor Project Preliminary Safety Analysis Report, Vol. 3, 1982.



## **APPENDIX A**

# **STRATIGRAPHIC UNIT DEPTHS IN INDIVIDUAL CLINCH RIVER NUCLEAR SITE BORINGS**







## **APPENDIX B**

# **BEST ESTIMATE ENGINEERING PROPERTIES VALUES FOR CLINCH RIVER NUCLEAR SITE STRATIGRAPHIC UNITS**



**APPENDIX B**  
**BEST ESTIMATE ENGINEERING PROPERTIES VALUES FOR CLINCH RIVER NUCLEAR SITE AREA STRATIGRAPHIC UNITS**  
**(ADAPTED FROM SSAR TABLE 2.5.4-21)**

PROPERTY <sup>(1)</sup>	UNIT <sup>(2)</sup>	BEST ESTIMATE ENGINEERING PROPERTY VALUE PER STRATIGRAPHIC UNIT <sup>(3)</sup>									
		EXISTING FILL/SOIL	GRANULAR FILL	WEATHERED ROCK	BENBOLT FM.	ROCKDELL FM.	FLEANOR MB.	EDISON MB.	BLACKFORD FM.	NEWALA FM.	
Total Unit Weight	pcf	120	135	140	168	168	168	168	168	175	
Specific Gravity	-	2.75	2.70	-	2.70	2.69	2.70	2.68	2.68	2.80	
Natural Water Content	percent	30	-	-	1	1	1	1	1	1	
Fines Content	percent	80	5(a)	-	-	-	-	-	-	-	
Liquid Limit	percent	67	-	-	-	-	-	-	-	-	
Plastic Limit	percent	27	-	-	-	-	-	-	-	-	
Plasticity Index	percent	40	-	-	-	-	-	-	-	-	
SPT N <sub>60</sub>	blows/ft	15	50	Refusal	-	-	-	-	-	-	
Undrained Shear Strength	psf	1,300	-	-	-	-	-	-	-	-	
Effective Cohesion	psf	150	-	-	-	-	-	-	-	-	
Effective Friction Angle	degrees	20	36	-	-	-	-	-	-	-	
Rock Core Recovery	percent	-	-	-	98	98	98	95	96	99	
RQD	percent	-	-	<2.5	88	88	89	80	81	93	
U	psi	-	-	-	6,200	7,500	5,000	7,000	4,500	20,000	
V <sub>s</sub>	fps	600	1,200	1,870	8,000	9,000	7,200	9,000	8,200	10,800	
V <sub>p</sub>	fps	3,020	2,500	5,740	15,400	17,100	14,500	17,000	15,700	19,900	
Poisson's Ratio	-	0.40	0.35	0.40	0.32	0.31	0.34	0.31	0.31	0.29	
G <sub>u</sub>	ksi	9	42	-	2,300	2,900	1,900	2,900	2,400	4,400	
G <sub>h</sub>	ksi	2	5	-	2,300	2,900	1,900	2,900	2,400	4,400	
E <sub>u</sub>	ksi	26	111	-	6,100	7,700	5,000	7,700	6,400	11,400	
E <sub>h</sub>	ksi	5	13	-	6,100	7,700	5,000	7,700	6,400	11,400	
Dry Density	pcf	116	125	-	-	-	-	-	-	-	
Moisture Content	percent	12	8	-	-	-	-	-	-	-	
Coefficient of Sliding	-	-	0.5	-	0.7	0.7	0.7	0.7	0.7	0.7	
Carbonate Content	percent	-	-	-	27	58	34	53	39	84	
Slake Durability Index	-	-	-	-	97	99	98	NA	94	NA	

**Notes:**

- SPT N<sub>60</sub> = standardized SPT blow count
- RQD = rock quality designation
- U = unconfined compressive strength
- V<sub>s</sub> = shear wave velocity
- V<sub>p</sub> = compression wave velocity
- G<sub>u</sub>, G<sub>h</sub> = low and high strain shear modulus, respectively
- E<sub>u</sub>, E<sub>h</sub> = low and high elastic strain modulus, respectively
- pcf = pounds per cubic foot
- psf = pounds per square foot
- fps = feet per second
- ksi = kips per square inch

<sup>(1)</sup> Select soil or rock physical properties, per SSAR Table 2.5.4-21  
<sup>(2)</sup> Measurement unit for a given rock physical property. Note that shear modulus and elastic strain modulus values for existing fill and proposed granular backfill materials were originally reported (in SSAR Table 2.5.4-21) in units of kips per square foot (ksf).  
<sup>(3)</sup> Best estimate engineering property value for discrete stratigraphic units in the CRN Site area, per SSAR Table 2.5.4-21.

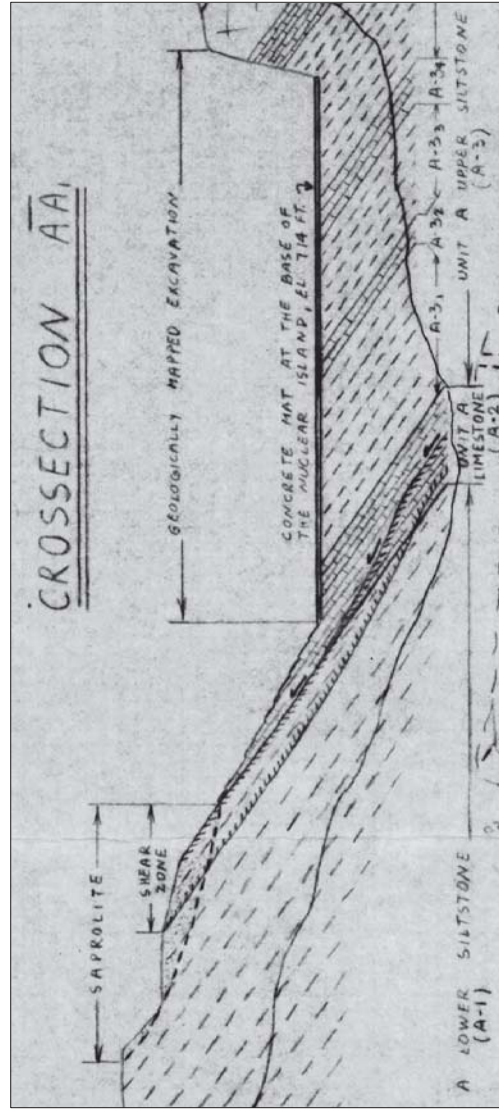
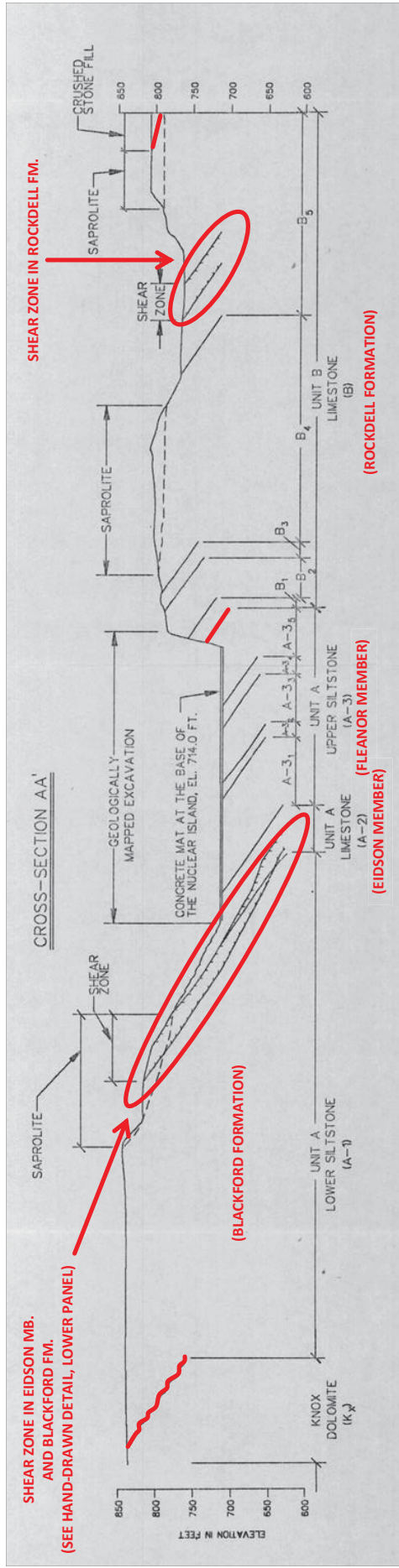


## **APPENDIX C**

# **GEOLOGIC CROSS SECTIONS OF THE CRBRP EXCAVATION AND SLOPES**



**APPENDIX C**  
**GEOLOGIC CROSS-SECTIONS OF THE CRBP EXCAVATION AND SLOPES**  
 (ADAPTED FROM DRAKULICH, 1984)



## **APPENDIX D**

# **CAVITIES IN INDIVIDUAL CLINCH RIVER NUCLEAR SITE BORINGS**



**APPENDIX D  
CAVITIES IN INDIVIDUAL CLINCH RIVER NUCLEAR SITE BORINGS  
(ADAPTED FROM SSAR TABLE 2.5.1-11)**

BOREHOLE <sup>(1)</sup>	UNIT <sup>(2)</sup>	CAVITY LOCATION <sup>(3)</sup>							CAVITY HEIGHT <sup>(4)</sup>		CAVITY COUNT <sup>(5)</sup> (number)
		TOP DEPTH (ft bgs)	BOTTOM DEPTH (ft bgs)	MEDIAN DEPTH (ft bgs)	TOP ELEVATION (ft)	BOTTOM ELEVATION (ft)	MEDIAN ELEVATION (ft)	(ft)	(ft)		
19	Benbolt	19.7	20.1	19.9	777.4	777.0	777.2	0.4			
19	Benbolt	25.0	25.1	25.1	772.1	772.0	772.1	0.1			
19	Benbolt	30.7	32.7	31.7	766.4	764.4	765.4	2.0			
23	Benbolt	8.7	9.6	9.2	770.3	769.4	769.9	0.9			
24	Benbolt	3.6	6.3	5.0	776.0	773.3	774.7	2.7			
24	Benbolt	7.1	7.4	7.3	772.5	772.2	772.4	0.3			
24	Benbolt	10.6	10.7	10.7	769.0	768.9	769.0	0.1			
58	Benbolt?	14.3	14.7	14.5	751.8	751.4	751.6	0.4			
MP-102	Benbolt	7.8	8.0	7.9	788.1	787.9	788.0	0.2			
MP-102	Benbolt	9.8	10.0	9.9	790.1	789.9	790.0	0.2			
MP-102	Benbolt	12.8	14.3	13.6	785.1	783.6	784.4	1.5			
MP-104	Benbolt	28.0	28.6	28.3	769.7	769.1	769.4	0.6			
12	Rockdell?	5.6	6.0	5.8	846.4	846.0	846.2	0.4			
12	Rockdell?	6.4	7.0	6.7	845.6	845.0	845.3	0.6			
12	Rockdell?	7.4	8.0	7.7	844.6	844.0	844.3	0.6			
12	Rockdell?	8.5	10.0	9.3	843.5	842.0	842.8	1.5			
12	Rockdell?	11.1	12.0	11.6	840.9	840.0	840.5	0.9			
13	Rockdell	38.3	38.5	38.4	816.4	816.2	816.3	0.2			
13	Rockdell	40.3	40.7	40.5	803.5	803.1	803.3	0.4			
13	Rockdell	41.2	41.7	41.5	813.5	813.0	813.3	0.5			
13	Rockdell	44.2	47.1	45.7	810.5	807.6	809.1	2.9			
13	Rockdell	48.1	48.5	48.3	814.4	814.0	814.2	0.4			
13	Rockdell	48.7	50.5	49.6	806.0	804.2	805.1	1.8			
13	Rockdell	51.2	51.6	51.4	806.6	806.2	806.4	0.4			
13	Rockdell	52.1	52.6	52.4	802.6	802.1	802.4	0.5			
13	Rockdell	54.2	58.5	56.4	800.5	796.2	798.4	4.3			
16	Rockdell	18.9	19.9	19.4	812.0	811.0	811.5	1.0			
16	Rockdell	25.1	25.4	25.3	805.8	805.5	805.7	0.3			
16	Rockdell	29.9	32.8	31.4	801.0	798.1	799.6	2.9			
16	Rockdell	33.1	33.9	33.5	797.8	797.0	797.4	0.8			
17	Rockdell	33.9	47.9	40.9	824.2	810.2	817.2	14.0			
17	Rockdell	53.7	53.8	53.8	804.4	804.3	804.4	0.1			

106



**APPENDIX D  
CAVITIES IN INDIVIDUAL CLINCH RIVER NUCLEAR SITE BORINGS  
(ADAPTED FROM SSAR TABLE 2.5.1-11)  
(CONTINUED)**

BOREHOLE <sup>(1)</sup>	UNIT <sup>(2)</sup>	CAVITY LOCATION <sup>(3)</sup>										CAVITY HEIGHT <sup>(4)</sup> (ft)	CAVITY COUNT <sup>(5)</sup> (number)
		TOP DEPTH	BOTTOM DEPTH	MEDIAN DEPTH	TOP ELEVATION	BOTTOM ELEVATION	MEDIAN ELEVATION						
		(ft bgs)	(ft bgs)	(ft bgs)	(ft)	(ft)	(ft)	(ft)	(ft)	(ft)	(ft)		
18	Rockdell	16.4	19.7	18.1	818.7	815.4	817.1	815.4	817.1	817.1	817.1	3.3	
18	Rockdell	20.1	20.9	20.5	815.0	814.2	814.6	814.2	814.6	814.6	814.6	0.8	
18	Rockdell	21.1	21.6	21.4	814.0	813.5	813.8	814.0	813.5	813.8	813.8	0.5	
18	Rockdell	22.5	22.8	22.7	812.6	812.3	812.5	812.6	812.3	812.5	812.5	0.3	
18	Rockdell	23.7	25.1	24.4	811.4	810.0	810.7	811.4	810.0	810.7	810.7	1.4	
18	Rockdell	25.3	28.1	26.7	809.8	807.0	808.4	809.8	807.0	808.4	808.4	2.8	
18	Rockdell	28.6	29.3	29.0	806.5	805.8	806.2	806.5	805.8	806.2	806.2	0.7	
18	Rockdell	29.8	30.1	30.0	805.3	805.0	805.2	805.3	805.0	805.2	805.2	0.3	
18	Rockdell	30.9	31.1	31.0	804.2	804.0	804.1	804.2	804.0	804.1	804.1	0.2	
18	Rockdell	31.5	32.1	31.8	803.6	803.0	803.3	803.6	803.0	803.3	803.3	0.6	
18	Rockdell	32.3	32.7	32.5	802.8	802.4	802.6	802.8	802.4	802.6	802.6	0.4	
18	Rockdell	32.8	33.4	33.1	802.3	801.7	802.0	802.3	801.7	802.0	802.0	0.6	
18	Rockdell	33.5	33.7	33.6	801.6	801.4	801.5	801.6	801.4	801.5	801.5	0.2	
18	Rockdell	34.7	35.6	35.2	800.4	799.5	800.0	800.4	799.5	800.0	800.0	0.9	
18	Rockdell	37.1	37.9	37.5	798.0	797.2	797.6	798.0	797.2	797.6	797.6	0.8	
18	Rockdell	38.8	39.4	39.1	796.3	795.7	796.0	796.3	795.7	796.0	796.0	0.6	
18	Rockdell	39.9	40.2	40.1	795.2	794.9	795.1	795.2	794.9	795.1	795.1	0.3	
18	Rockdell	41.3	42.0	41.7	793.8	793.1	793.5	793.8	793.1	793.5	793.5	0.7	
18	Rockdell	44.0	44.8	44.4	791.1	790.3	790.7	791.1	790.3	790.7	790.7	0.8	
18	Rockdell	51.1	53.7	52.4	784.0	781.4	782.7	784.0	781.4	782.7	782.7	2.6	
20	Rockdell	29.6	34.3	32.0	771.5	766.8	769.2	771.5	766.8	769.2	769.2	4.7	
20	Rockdell	37.5	41.1	39.3	763.6	760.0	761.8	763.6	760.0	761.8	761.8	3.6	
20	Rockdell	80.3	80.7	80.5	720.8	720.4	720.6	720.8	720.4	720.6	720.6	0.4	
20	Rockdell	87.3	90.1	88.7	713.8	711.0	712.4	713.8	711.0	712.4	712.4	2.8	
20	Rockdell	93.1	96.1	94.6	708.0	705.0	706.5	708.0	705.0	706.5	706.5	3.0	
20	Rockdell	101.1	101.8	101.5	700.0	699.3	699.7	700.0	699.3	699.7	699.7	0.7	
21	Rockdell	19.1	19.9	19.5	782.8	782.0	782.4	782.8	782.0	782.4	782.4	0.8	
21	Rockdell	40.2	40.4	40.3	761.7	761.5	761.6	761.7	761.5	761.6	761.6	0.2	
22	Rockdell	39.3	39.5	39.4	758.0	757.8	757.9	758.0	757.8	757.9	757.9	0.2	
22	Rockdell	40.3	41.5	40.9	757.0	755.8	756.4	757.0	755.8	756.4	756.4	1.2	
22	Rockdell	41.7	43.5	42.6	753.6	753.8	754.7	753.6	753.8	754.7	754.7	1.8	
22	Rockdell	44.3	49.3	46.8	753.0	748.0	750.5	753.0	748.0	750.5	750.5	5.0	



**APPENDIX D  
CAVITIES IN INDIVIDUAL CLINCH RIVER NUCLEAR SITE BORINGS  
(ADAPTED FROM SSAR TABLE 2.5.1-11)  
(CONTINUED)**

BOREHOLE <sup>(1)</sup>	UNIT <sup>(2)</sup>	CAVITY LOCATION <sup>(3)</sup>							CAVITY HEIGHT <sup>(4)</sup>		CAVITY COUNT <sup>(5)</sup> (number)
		TOP DEPTH (ft bgs)	BOTTOM DEPTH (ft bgs)	MEDIAN DEPTH (ft bgs)	TOP ELEVATION (ft)	BOTTOM ELEVATION (ft)	MEDIAN ELEVATION (ft)	CAVITY HEIGHT (ft)	CAVITY COUNT (number)		
22	Rockdell	49.5	51.7	50.6	747.8	745.6	746.7	2.2			
22	Rockdell	51.9	52.2	52.1	711.3	711.0	711.2	0.3			
22	Rockdell	52.3	53.4	52.9	745.0	743.9	744.5	1.1			
22	Rockdell	54.0	54.3	54.2	745.4	745.1	745.3	0.3			
22	Rockdell	55.6	56.3	56.0	741.7	741.0	741.4	0.7			
22	Rockdell	57.0	57.3	57.2	743.3	743.0	743.2	0.3			
22	Rockdell	58.8	59.3	59.1	738.5	738.0	738.3	0.5			
22	Rockdell	59.6	60.3	60.0	737.7	737.0	737.4	0.7			
22	Rockdell	60.8	60.9	60.9	736.5	736.4	736.5	0.1			
22	Rockdell	61.3	61.5	61.4	736.0	735.8	735.9	0.2			
22	Rockdell	63.1	63.5	63.3	734.2	733.8	734.0	0.4			
22	Rockdell	64.3	64.8	64.6	733.0	732.5	732.8	0.5			
22	Rockdell	67.7	75.3	71.5	729.6	722.0	725.8	7.6			
22	Rockdell	86.0	86.3	86.2	740.3	740.0	740.2	0.3			
25	Rockdell	14.0	14.4	14.2	840.4	840.0	840.2	0.4			
38	Rockdell	47.4	48.3	47.9	833.6	832.7	833.2	0.9			
41	Rockdell	53.8	54.0	53.9	767.3	767.1	767.2	0.2			
48	Rockdell	26.7	29.4	28.1	797.1	794.4	795.8	2.7			
49	Rockdell	54.6	55.9	55.3	777.3	776.0	776.7	1.3			
50	Rockdell	33.9	39.6	36.8	773.6	767.9	770.8	5.7			
50	Rockdell	40.7	47.3	44.0	766.8	760.2	763.5	6.6			
50	Rockdell	47.5	50.0	48.8	760.0	757.5	758.8	2.5			
50	Rockdell	52.0	58.0	55.0	755.5	749.5	752.5	6.0			
50	Rockdell	58.8	61.1	60.0	748.7	746.4	747.6	2.3			
50	Rockdell	62.0	70.5	66.3	745.5	737.0	741.3	8.5			
80	Rockdell	26.7	27.7	27.2	800.0	799.5	799.5	1.0			
100	Rockdell	46.3	49.0	47.7	807.3	804.6	806.0	2.7			
100	Rockdell	50.9	51.6	51.3	802.7	802.0	802.4	0.7			
103	Rockdell	25.3	26.1	25.7	847.2	846.4	846.8	0.8			
127	Rockdell	14.6	16.6	15.6	826.3	824.3	825.3	2.0			
128	Rockdell	42.7	45.2	44.0	799.1	796.6	797.9	2.5			

106



**APPENDIX D  
CAVITIES IN INDIVIDUAL CLINCH RIVER NUCLEAR SITE BORINGS  
(ADAPTED FROM SSAR TABLE 2.5.1-11)  
(CONTINUED)**

BORRHOLE <sup>(1)</sup>	UNIT <sup>(2)</sup>	CAVITY LOCATION <sup>(3)</sup>										CAVITY HEIGHT <sup>(4)</sup> (ft)	CAVITY COUNT <sup>(6)</sup> (number)	
		TOP DEPTH (ft bgs)	BOTTOM DEPTH (ft bgs)	MEDIAN DEPTH (ft bgs)	TOP ELEVATION (ft)	BOTTOM ELEVATION (ft)	MEDIAN ELEVATION (ft)							
129	Rockdell	40.7	46.7	43.7	804.5	798.5	801.5	6.0						
130	Rockdell	15.0	16.0	15.5	831.0	830.5	830.5	1.0						
130	Rockdell	38.8	39.8	39.3	807.2	806.2	806.7	1.0						
131	Rockdell	64.7	65.7	65.2	776.3	775.3	775.8	1.0						
133	Rockdell	35.3	36.3	35.8	810.0	809.0	809.5	1.0						
140	Rockdell	43.3	59.8	51.6	797.2	780.7	789.0	16.5						
140	Rockdell	142.4	143.4	142.9	698.1	697.1	697.6	1.0						
142	Rockdell	43.5	49.7	46.6	799.0	792.8	795.9	6.2						
142	Rockdell	123.4	123.5	123.5	719.1	719.0	719.1	0.1						
143	Rockdell	48.5	49.0	48.8	790.5	790.0	790.3	0.5						
144	Rockdell	60.6	60.7	60.7	782.7	782.6	782.7	0.1						
144	Rockdell	61.5	61.6	61.6	781.8	781.7	781.8	0.1						106
144	Rockdell	62.4	63.2	62.8	780.9	780.1	780.5	0.8						
145	Rockdell	62.3	63.6	63.0	781.8	780.5	781.2	1.3						
147	Rockdell	14.5	14.6	14.5	850.1	850.0	850.1	0.1						
147	Rockdell	31.9	32.0	32.0	832.7	832.6	832.7	0.1						
147	Rockdell	52.8	52.9	52.9	811.8	811.7	811.8	0.1						
149	Rockdell	29.8	45.1	37.5	819.1	803.8	811.5	15.3						
MP-410	Rockdell	12.2	13.2	12.7	797.2	796.2	796.7	1.0						
MP-410	Rockdell	14.3	16.0	15.2	795.1	793.4	794.3	1.7						
MP-410	Rockdell	16.3	17.7	17.0	793.1	791.7	792.4	1.4						
MP-410	Rockdell	21.2	31.3	26.3	788.2	778.1	783.2	10.1						
MP-428	Rockdell	35.2	39.8	37.5	768.6	764.0	766.3	4.6						
8	Fleanor?	3.6	3.7	3.7	827.6	827.5	827.6	0.1						
8	Fleanor	6.7	7.2	7.0	824.5	824.0	824.3	0.5						
11	Fleanor	10.3	11.2	10.8	771.1	770.2	770.7	0.9						
11	Fleanor	12.0	13.4	12.7	769.4	768.0	768.7	1.4						
11	Fleanor	15.5	16.0	15.8	765.9	765.4	765.7	0.5						19
11	Fleanor	18.6	19.5	19.1	762.8	761.9	762.4	0.9						
12	Fleanor?	16.3	17.0	16.7	835.7	835.0	835.4	0.7						
12	Fleanor?	24.2	24.5	24.4	827.8	827.5	827.7	0.3						
15	Fleanor	11.7	12.5	12.1	755.8	755.0	755.4	0.8						



**APPENDIX D  
CAVITIES IN INDIVIDUAL CLINCH RIVER NUCLEAR SITE BORINGS  
(ADAPTED FROM SSAR TABLE 2.5.1-11)  
(CONTINUED)**

BORRHOLE <sup>(1)</sup>	UNIT <sup>(2)</sup>	CAVITY LOCATION <sup>(3)</sup>								CAVITY HEIGHT <sup>(4)</sup> (ft)	CAVITY COUNT <sup>(5)</sup> (number)
		TOP DEPTH (ft bgs)	BOTTOM DEPTH (ft bgs)	MEDIAN DEPTH (ft bgs)	TOP ELEVATION (ft)	BOTTOM ELEVATION (ft)	MEDIAN ELEVATION (ft)				
15	Fleanor	13.3	14.5	13.9	754.2	753.0	753.6	1.2			
15	Fleanor	15.0	15.5	15.3	752.5	752.3	752.3	0.5			
15	Fleanor	21.5	21.8	21.7	746.0	745.7	745.9	0.3			
26	Fleanor	20.6	21.7	21.2	786.4	785.3	785.9	1.1			
30	Fleanor	89.1	89.6	89.4	720.0	719.5	719.8	0.5			
40	Fleanor	76.8	77.1	77.0	761.3	761.0	761.2	0.3	19		
54	Fleanor	37.3	37.7	37.5	728.2	727.8	728.0	0.4			
54	Fleanor	68.2	68.6	68.4	759.1	758.7	758.9	0.4			
102	Fleanor	21.1	21.4	21.3	772.7	772.4	772.6	0.3			
102	Fleanor	29.3	29.6	29.5	764.5	764.2	764.4	0.3			
3	Eidson	15.5	15.6	15.6	861.8	861.7	861.8	0.1			
3	Eidson	17.8	18.2	18.0	859.5	859.1	859.3	0.4			
3	Eidson	22.3	22.8	22.6	855.0	854.5	854.8	0.5			
3	Eidson	23.3	25.1	24.2	854.0	852.2	853.1	1.8			
3	Eidson	25.5	26.3	25.9	851.8	851.0	851.4	0.8			
3	Eidson	26.8	30.3	28.6	850.5	847.0	848.8	3.5			
3	Eidson	39.3	39.9	39.6	857.4	856.8	857.1	0.6			
3	Eidson	85.3	85.5	85.4	860.5	860.3	860.4	0.2			
4	Eidson	62.6	63.3	63.0	730.0	729.3	729.7	0.7			
6	Eidson	32.6	34.5	33.6	824.0	822.1	823.1	1.9			
6	Eidson	35.3	36.1	35.7	821.3	820.5	820.9	0.8			
6	Eidson	40.5	40.9	40.7	816.1	815.7	815.9	0.4			
6	Eidson	60.3	60.6	60.5	820.0	819.7	819.9	0.3			
7	Eidson	15.1	16.0	15.6	778.5	777.6	778.1	0.9			
7	Eidson	16.4	16.6	16.5	771.4	771.2	771.3	0.2			
7	Eidson	16.9	17.6	17.3	776.7	776.0	776.4	0.7			
7	Eidson	18.4	19.4	18.9	775.2	774.2	774.7	1.0			
7	Eidson	19.6	21.1	20.4	774.0	772.5	773.3	1.5			
7	Eidson	22.2	22.4	22.3	777.2	777.0	777.1	0.2			
7	Eidson	22.6	26.0	24.3	771.0	767.6	769.3	3.4			
7	Eidson	27.5	29.1	28.3	766.1	764.5	765.3	1.6			
7	Eidson	45.2	45.6	45.4	748.4	748.0	748.2	0.4			



**APPENDIX D  
CAVITIES IN INDIVIDUAL CLINCH RIVER NUCLEAR SITE BORINGS  
(ADAPTED FROM SSAR TABLE 2.5.1-11)  
(CONTINUED)**

BORRHOLE <sup>(1)</sup>	UNIT <sup>(2)</sup>	CAVITY LOCATION <sup>(3)</sup>										CAVITY HEIGHT <sup>(4)</sup> (ft)	CAVITY COUNT <sup>(6)</sup> (number)	
		TOP DEPTH (ft bgs)	BOTTOM DEPTH (ft bgs)	MEDIAN DEPTH (ft bgs)	TOP ELEVATION (ft)	BOTTOM ELEVATION (ft)	MEDIAN ELEVATION (ft)	MEDIAN ELEVATION (ft)	TOP ELEVATION (ft)	BOTTOM ELEVATION (ft)	MEDIAN ELEVATION (ft)			
9	Eidson	61.2	64.1	62.7	787.2	784.3	785.8	785.8	787.2	784.3	785.8	785.8	2.9	
10	Eidson	21.3	22.0	21.7	791.2	790.5	790.9	790.9	791.2	790.5	790.9	790.9	0.7	
10	Eidson	26.3	26.9	26.6	786.2	785.6	785.9	785.9	786.2	785.6	785.9	785.9	0.6	
10	Eidson	36.1	37.5	36.8	776.4	775.0	775.7	775.7	776.4	775.0	775.7	775.7	1.4	
10	Eidson	37.7	39.5	38.6	774.8	773.0	773.9	773.9	774.8	773.0	773.9	773.9	1.8	
10	Eidson	40.9	41.5	41.2	771.6	771.0	771.3	771.3	771.6	771.0	771.3	771.3	0.6	
10	Eidson	43.8	46.5	45.2	768.7	766.0	767.4	767.4	768.7	766.0	767.4	767.4	2.7	
10	Eidson	48.5	53.4	51.0	764.0	759.1	761.6	761.6	764.0	759.1	761.6	761.6	4.9	
11	Eidson	33.4	34.2	33.8	748.0	747.2	747.6	747.6	748.0	747.2	747.6	747.6	0.8	
31	Eidson	52.8	53.3	53.1	750.0	749.5	749.8	749.8	750.0	749.5	749.8	749.8	0.5	
31	Eidson	92.3	92.8	92.6	710.5	710.0	710.3	710.3	710.5	710.0	710.3	710.3	0.5	
34	Eidson	33.1	37.6	35.4	760.0	755.5	757.8	757.8	760.0	755.5	757.8	757.8	4.5	
34	Eidson	39.2	40.1	39.7	753.9	753.0	753.5	753.5	753.9	753.0	753.5	753.5	0.9	
34	Eidson	63.1	64.0	63.6	730.0	729.1	729.6	729.6	730.0	729.1	729.6	729.6	0.9	
34	Eidson	79.5	81.3	80.4	713.6	711.8	712.7	712.7	713.6	711.8	712.7	712.7	1.8	
35	Eidson	24.7	25.2	25.0	789.1	788.6	788.9	788.9	789.1	788.6	788.9	788.9	0.5	
35	Eidson	25.6	26.1	26.1	788.2	787.3	787.8	787.8	788.2	787.3	787.8	787.8	0.9	
35	Eidson	29.2	29.7	29.5	784.6	784.1	784.4	784.4	784.6	784.1	784.4	784.4	0.5	
35	Eidson	37.9	40.8	39.4	775.9	773.0	774.5	774.5	775.9	773.0	774.5	774.5	2.9	
51	Eidson	71.4	77.0	74.2	733.6	728.0	730.8	730.8	733.6	728.0	730.8	730.8	5.6	
56	Eidson	49.2	49.6	49.4	723.6	723.2	723.4	723.4	723.6	723.2	723.4	723.4	0.4	
56	Eidson	81.2	81.6	81.4	755.6	755.2	755.4	755.4	755.6	755.2	755.4	755.4	0.4	
56	Eidson	82.1	88.9	85.5	722.7	715.9	719.3	719.3	722.7	715.9	719.3	719.3	6.8	
70	Eidson	51.8	52.1	51.9	757.3	757.1	757.2	757.2	757.3	757.1	757.2	757.2	0.3	
70	Eidson	52.7	53.2	53.0	755.9	755.9	756.2	756.2	755.9	755.9	756.2	756.2	0.5	
70	Eidson	55.4	55.9	55.7	753.7	753.2	753.5	753.5	753.7	753.2	753.5	753.5	0.5	
70	Eidson	57.8	59.1	58.5	751.3	750.0	750.7	750.7	751.3	750.0	750.7	750.7	1.3	
94	Eidson	51.4	51.7	51.6	735.5	735.2	735.4	735.4	735.5	735.2	735.4	735.4	0.3	
MP-418	Eidson	49.4	60.2	54.8	762.2	751.4	756.8	756.8	762.2	751.4	756.8	756.8	10.8	
MP-418	Eidson	61.4	63.5	62.5	750.2	748.1	749.2	749.2	750.2	748.1	749.2	749.2	2.1	
MP-418	Eidson	65.2	67.7	66.5	746.4	743.9	745.2	745.2	746.4	743.9	745.2	745.2	2.5	
MP-418	Eidson	69.7	70.5	70.1	741.9	741.1	741.5	741.5	741.9	741.1	741.5	741.5	0.8	



**APPENDIX D  
CAVITIES IN INDIVIDUAL CLINCH RIVER NUCLEAR SITE BORINGS  
(ADAPTED FROM SSAR TABLE 2.5.1-11)  
(CONTINUED)**

BORRHOLE <sup>(1)</sup>	UNIT <sup>(2)</sup>	CAVITY LOCATION <sup>(3)</sup>								CAVITY HEIGHT <sup>(4)</sup> (ft)	CAVITY COUNT <sup>(5)</sup> (number)
		TOP DEPTH (ft bgs)	BOTTOM DEPTH (ft bgs)	MEDIAN DEPTH (ft bgs)	TOP ELEVATION (ft)	BOTTOM ELEVATION (ft)	MEDIAN ELEVATION (ft)				
MP-418	Eidson	71.5	81.0	76.3	740.1	730.6	735.4	9.5			
MP-423	Eidson	43.0	44.8	43.9	756.0	754.2	755.1	1.8			
2	Blackford	13.9	14.2	14.1	838.3	838.0	838.2	0.3			
2	Blackford	15.0	15.2	15.1	837.2	837.0	837.1	0.2			
2	Blackford	19.2	20.7	20.0	833.0	831.5	832.3	1.5			
3	Blackford	16.8	17.0	16.9	827.9	827.7	827.8	0.2			
3	Blackford	19.9	20.5	20.2	838.0	837.4	837.7	0.6			
3	Blackford	37.1	37.3	37.2	840.2	840.0	840.1	0.2			
3	Blackford	42.1	42.3	42.2	835.2	835.0	835.1	0.2			
3	Blackford	47.6	47.9	47.8	829.7	829.4	829.6	0.3			
3	Blackford	48.6	49.3	49.0	828.7	828.0	828.4	0.7			
3	Blackford	49.4	49.6	49.5	792.0	791.8	791.9	0.2			
3	Blackford	81.2	81.3	81.3	796.1	796.0	796.1	0.1			
5	Blackford	21.4	22.2	21.8	868.0	867.2	867.6	0.8			
5	Blackford	25.9	28.4	27.2	863.5	861.0	862.3	2.5			
5	Blackford	34.1	34.4	34.3	855.3	855.0	855.2	0.3			
5	Blackford	34.9	35.9	35.4	854.5	853.5	854.0	1.0			
5	Blackford	41.4	41.7	41.6	848.0	847.7	847.9	0.3			
5	Blackford	45.8	47.2	46.5	843.6	842.2	842.9	1.4			
5	Blackford	74.4	75.6	75.0	815.0	813.8	814.4	1.2			
6	Blackford	36.6	36.9	36.8	796.3	796.0	796.2	0.3			
6	Blackford	50.6	50.8	50.7	806.0	805.8	805.9	0.2			
6	Blackford	51.5	52.9	52.2	805.1	803.7	804.4	1.4			
9	Blackford	82.3	82.6	82.5	766.1	765.8	766.0	0.3			
9	Blackford	88.4	89.5	89.0	760.0	758.9	759.5	1.1			
9	Blackford	90.2	91.2	90.7	758.2	757.2	757.7	1.0			
9	Blackford	91.7	92.6	92.2	756.7	755.8	756.3	0.9			
35	Blackford	83.8	85.6	84.7	730.0	728.2	729.1	1.8			
52	Blackford	73.4	73.6	73.5	767.8	767.6	767.7	0.2			
52	Blackford	104.8	105.9	105.4	736.4	735.3	735.9	1.1			
MP-406	Blackford	54.3	55.4	54.9	800.8	799.7	800.3	1.1			
MP-412	Blackford	15.6	16.3	16.0	808.1	807.4	807.8	0.7			

30



**APPENDIX D  
CAVITIES IN INDIVIDUAL CLINCH RIVER NUCLEAR SITE BORINGS  
(ADAPTED FROM SSAR TABLE 2.5.1-11)  
(CONTINUED)**

BOREHOLE <sup>(1)</sup>	UNIT <sup>(2)</sup>	CAVITY LOCATION <sup>(3)</sup>								CAVITY HEIGHT <sup>(4)</sup> (ft)	CAVITY COUNT <sup>(5)</sup> (number)
		TOP DEPTH (ft bgs)	BOTTOM DEPTH (ft bgs)	MEDIAN DEPTH (ft bgs)	TOP ELEVATION (ft)	BOTTOM ELEVATION (ft)	MEDIAN ELEVATION (ft)				
61	Ok/Oma	102.3	103.1	102.7	749.0	748.2	748.6	0.8			
61	Ok/Oma	107.7	109.3	108.5	743.6	742.0	742.8	1.6			
65	Ok/Oma	5.9	6.5	6.2	870.0	869.4	869.7	0.6			
66	Ok/Oma	8.6	12.7	10.7	841.8	837.7	839.8	4.1			
66	Ok/Oma	24.0	25.0	24.5	826.4	825.4	825.9	1.0			
66	Ok/Oma	26.8	27.3	27.1	823.6	823.1	823.4	0.5	10		
66	Ok/Oma	28.6	31.1	29.9	821.8	819.3	820.6	2.5			
66	Ok/Oma	33.1	33.4	33.3	817.3	817.0	817.2	0.3			
66	Ok/Oma	74.1	74.3	74.2	776.3	776.1	776.2	0.2			
MP-420	Ok/Oma	40.6	46.9	43.8	762.5	756.2	759.4	6.3			
	Minimum	3.6	3.7	3.7	698.1	697.1	697.6	0.1			
	Quartile 1	22.3	22.8	22.7	757.0	755.8	756.4	0.4			
	Quartile 2	38.3	39.9	39.3	785.1	782.6	784.4	0.8			
	Quartile 3	53.8	55.9	54.8	812.6	811.0	811.8	1.6			
	Interquartile Range	31.5	33.1	32.2	55.6	55.2	55.4	1.2			
	Extreme Value Lower Limit	101.1	105.6	103.0	896.0	893.8	894.8	3.4			

**Notes:**

ft bgs = feet below ground surface  
ft = feet

- (1) Borehole number designation, from SSAR Table 2.5.1-11. Boring MP-424 is not included owing to depth and elevation disparities in existing data (presumably due to boring inclination and depth to elevation corrections).
- (2) Assigned stratigraphic unit, per SSAR Table 2.5.1-11.
- (3) Cavity top, bottom, and calculated median depth and elevation, adapted from SSAR Table 2.5.1-11.
- (4) Cavity height inferred from CRN Site borings.
- (5) Total number of cavities per stratigraphic unit.



**Attachment 2**  
**Addendum to Non-Proprietary Report**  
**Foundation Assessment**  
**Clinch River Nuclear Site, Revision 0**

**ADDENDUM TO NON-PROPRIETARY REPORT  
FOUNDATION ASSESSMENT  
CLINCH RIVER NUCLEAR SITE**

**PROJECT No. 16-5737  
REVISION 0  
JUNE 15, 2017**

**RIZZO ASSOCIATES  
PENN CENTER EAST, 500 PENN CENTER BLVD.  
BUILDING 5, SUITE 100  
PITTSBURGH, PENNSYLVANIA 15235  
TELEPHONE: (412) 856-9700  
TELEFAX: (412) 856-9749  
WWW.RIZZOASSOC.COM**





## CHANGE MANAGEMENT RECORD

**Project No.:** 16-5737

**Report Name:** Addendum to Non-Proprietary Report  
Foundation Assessment  
Clinch River Nuclear Site

<b>REVISION NO.</b>	<b>DATE</b>	<b>DESCRIPTIONS OF CHANGES/AFFECTED PAGES</b>
0	June 15, 2017	Initial Submittal



# TABLE OF CONTENTS

	<b>PAGE</b>
LIST OF TABLES .....	6
LIST OF FIGURES .....	7
1.0 INTRODUCTION .....	9
2.0 FINITE-ELEMENT MODELING OF BEARING CAPACITY .....	10
2.1 CASES EVALUATED.....	10
2.2 DESCRIPTION OF MODELS .....	10
2.2.1 Material Properties and Geometry.....	11
2.2.2 Finite-Element Mesh .....	15
2.2.3 Loading.....	15
3.0 RESULTS .....	17
4.0 SUMMARY .....	29
5.0 REFERENCES .....	30



## LIST OF TABLES

<b>TABLE NO.</b>	<b>TITLE</b>	<b>PAGE</b>
TABLE 2-1	ROCK MASS PROPERTIES FOR SITES A AND B USED IN FE MODELING.....	12
TABLE 3-1	ULTIMATE BEARING CAPACITY FROM PLAXIS 2D.....	18
TABLE 4-1	COMPARISON OF PLAXIS AND SSAR BEARING CAPACITY.....	29



## LIST OF FIGURES

FIGURE NO.	TITLE	PAGE
FIGURE 2-1	LOCATION OF SECTIONS USED IN SITE A AND SITE B MODELS .....	10
FIGURE 2-2	SITE A, CROSS SECTION: A-A', EMBEDMENT DEPTH: 80 FT.....	13
FIGURE 2-3	SITE A, CROSS SECTION: A-A', EMBEDMENT DEPTH: 138 FT.....	13
FIGURE 2-4	SITE B, CROSS SECTION: B-B', EMBEDMENT DEPTH: 80 FT.....	14
FIGURE 2-5	SITE B, CROSS SECTION: B-B', EMBEDMENT DEPTH: 138 FT.....	14
FIGURE 2-6	A TYPICAL MODEL WITH REFINED MESH .....	15
FIGURE 3-1	TYPICAL BEARING CAPACITY FAILURE WITH PLASTIC ZONES .....	17
FIGURE 3-2	LOAD DEFORMATION CURVE FOR SECTION A-A', 80 FT EMBEDMENT.....	18
FIGURE 3-3	LOAD DEFORMATION CURVE FOR SECTION A-A', 138 FT EMBEDMENT.....	19
FIGURE 3-4	LOAD DEFORMATION CURVE FOR SECTION B-B', 80 FT EMBEDMENT.....	19
FIGURE 3-5	LOAD DEFORMATION CURVE FOR SECTION B-B', 138 FT EMBEDMENT.....	20
FIGURE 3-6	PLASTIC POINTS FOR SECTION A-A', 80 FT EMBEDMENT 100 KSF LOAD (ELASTIC RESPONSE).....	21
FIGURE 3-7	PLASTIC POINTS FOR SECTION A-A', 80 FT EMBEDMENT 500 KSF LOAD (DEFINED ULTIMATE BEARING CAPACITY) .....	21
FIGURE 3-8	PLASTIC POINTS FOR SECTION A-A', 80 FT EMBEDMENT 1500 KSF LOAD (BEYOND ULTIMATE BEARING CAPACITY) .....	22
FIGURE 3-9	PLASTIC POINTS FOR SECTION A-A', 138 FT EMBEDMENT 100 KSF LOAD (ELASTIC RESPONSE).....	23
FIGURE 3-10	PLASTIC POINTS FOR SECTION A-A', 138 FT EMBEDMENT 440 KSF LOAD (DEFINED ULTIMATE BEARING CAPACITY) .....	23



**TABLE OF FIGURES  
(CONTINUED)**

<b>FIGURE NO.</b>	<b>TITLE</b>	<b>PAGE</b>
FIGURE 3-11	PLASTIC POINTS FOR SECTION A-A', 138 FT EMBEDMENT 1200 KSF LOAD (BEYOND ULTIMATE BEARING CAPACITY) .....	24
FIGURE 3-12	PLASTIC POINTS FOR SECTION B-B', 80 FT EMBEDMENT 100 KSF LOAD (ELASTIC RESPONSE).....	25
FIGURE 3-13	PLASTIC POINTS FOR SECTION B-B', 80 FT EMBEDMENT 520 KSF LOAD (DEFINED ULTIMATE BEARING CAPACITY) .....	25
FIGURE 3-14	PLASTIC POINTS FOR SECTION B-B', 80 FT EMBEDMENT 620 KSF LOAD (BEYOND ULTIMATE BEARING CAPACITY) .....	26
FIGURE 3-15	PLASTIC POINTS FOR SECTION B-B', 138 FT EMBEDMENT 100 KSF LOAD (ELASTIC RESPONSE).....	27
FIGURE 3-16	PLASTIC POINTS FOR SECTION B-B', 138 FT EMBEDMENT 320 KSF LOAD (DEFINED ULTIMATE BEARING CAPACITY) .....	27
FIGURE 3-17	PLASTIC POINTS FOR SECTION B-B', 138 FT EMBEDMENT 1500 KSF LOAD (BEYOND ULTIMATE BEARING CAPACITY) .....	28



**ADDENDUM TO NON-PROPRIETARY REPORT  
FOUNDATION ASSESSMENT  
CLINCH RIVER NUCLEAR SITE**

**1.0 INTRODUCTION**

This Addendum discusses a foundation assessment for proposed Small Modular Reactors (SMRs) at the Tennessee Valley Authority (TVA) Clinch River Nuclear (CRN) Site, in support of TVA's Early Site Permit (ESP) Application for the SMRs. This assessment involves finite-element (FE) modeling, using PLAXIS 2D analysis software, to estimate the ultimate bearing capacity at the CRN Site.



## 2.0 FINITE-ELEMENT MODELING OF BEARING CAPACITY

Bearing capacity is evaluated using the 2D finite-element method (FEM) in PLAXIS 2D version 9.02 (PLAXIS 2D). The following subsections provide an overview of the analysis and the FE models.

### 2.1 CASES EVALUATED

Bearing capacity models are developed for Section A-A' from Site A and Section B-B' from Site B, as depicted on *Figure 2-1*. For each Section, two embedment depths are considered: 80 feet (ft) embedment and 138 ft embedment.

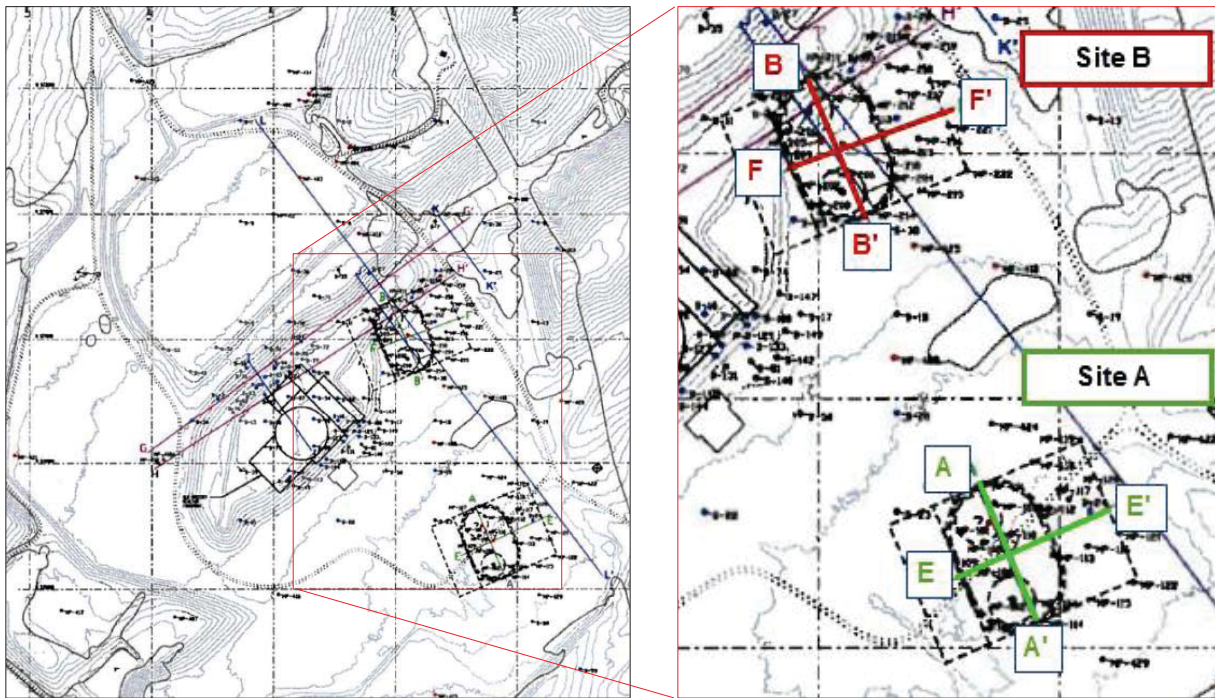


**FIGURE 2-1  
LOCATION OF SECTIONS USED IN SITE A AND SITE B MODELS**

### 2.2 DESCRIPTION OF MODELS

Material constitutive models, geologic layering, and the modeling of shear fracture zones follow the same methodology used in the PLAXIS settlement model described in the Non-Proprietary



Foundation Assessment (RIZZO, 2017). Model scenarios assume plane strain in two-dimensional space and static loading conditions.

### 2.2.1 Material Properties and Geometry

Material properties used for this analysis are presented in *Table 2-1*. Consistent with the settlement and voids analysis, a discrete interface element located along the Rockdell Formation and Benbolt Formation contact is modeled for Site A, and a similar interface element is modeled along the Fleanor and Eidson formation contact for Site B.

It is noted that the material properties in *Table 2-1* correspond to the lower GSI values presented in Site Safety Analysis Report (SSAR) Table 2.5.4-22 and Table 2.5.4-23. Using these lower values provides a conservative estimate of ultimate bearing capacity.

*Figure 2-2 and Figure 2-3* present the individual PLAXIS models considered for Site A. *Figure 2-4 and Figure 2-5* present the individual PLAXIS models considered for Site B. The following changes are implemented to the bearing capacity model compared to the settlement model reported in the non-proprietary Report to make sure the bearing capacity analysis assumes similar conditions to those assumed in the SSAR:

- For excavation into rock, the excavation slope is modeled at 0.5H:1V with a 35 ft setback from the toe of the excavation to the edge of the basemat. For excavation in soil, the excavation slope is modeled as 2H:1V.
- The bearing capacity evaluation does not consider potential subsurface voids. As such, the voids modeled in the settlement analysis have been eliminated.
- The tunnel rock mass properties surrounding the voids have been eliminated, and all material properties correspond to general Hoek-Brown rock mass material.
- The depths of embedment evaluated are 80 ft and 138 ft, compared to the settlement model embedment depths of 90 ft and 140 ft. The 40 ft embedment depth for the settlement model is not evaluated in the bearing capacity model.
- The width of the foundation basemat is 221 ft.



**TABLE 2-1  
ROCK MASS PROPERTIES FOR SITES A AND B USED IN FE MODELING**

SITE (1)	LAYER (2)	ROCK MASS PROPERTIES (3)						
		UNIT WEIGHT	COHESION		FRICTION ANGLE	POISSON'S RATIO	ELASTIC MODULUS	
		(pcf)	(psf)	(psi)			(ksf)	(ksi)
A	Granular Fill	135	0	0	36	0.35	16,000	111
	Existing Fill	120	150	1	20	0.40	3,750	26
	Benbolt	168	59,760	415	33	0.32	643,680	4,470
	Rockdell	168	56,592	393	31	0.31	452,736	3,144
	Fleanor	168	42,912	298	32	0.34	454,896	3,159
B	Granular Fill	135	0	0	36	0.35	16,000	111
	Existing Fill	120	150	1	20	0.40	3,750	26
	Rockdell	168	56,592	393	31	0.31	452,736	3,144
	Fleanor	168	42,912	298	32	0.34	454,896	3,159
	Eidson	168	48,672	338	30	0.31	340,560	2,365
	Blackford	168	34,848	242	30	0.31	479,232	3,328
	Newala	175	201,024	1,396	35	0.29	1,202,976	8,354

**Notes:**

pcf = pounds per cubic foot

psf = pounds per square foot

psi = pounds per square inch

ksf = kips per square foot

ksi = kips per square inch

(1) Units 1&2 (Site A) or Units 3&4 (Site B).

(2) Geologic layer or material expected to be exposed in the given Site A or Site B location. Units 1&2 in Site A are expected to be founded on Benbolt Formation rock. Units 3&4 in Site B are expected to be founded on rock ascribed to the Fleanor Member of the Lincolnshire Formation.

(3) Rock mass properties from SSAR Section 2.5.4 Table 2.5.4-21, and Table 2.5.4-22.



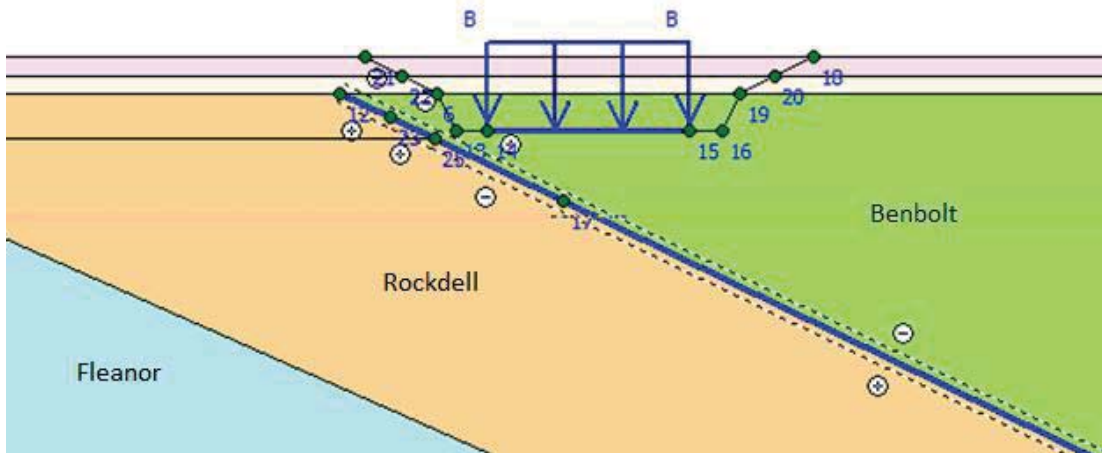


**FIGURE 2-2**  
**SITE A, CROSS SECTION: A-A', EMBEDMENT DEPTH: 80 FT**

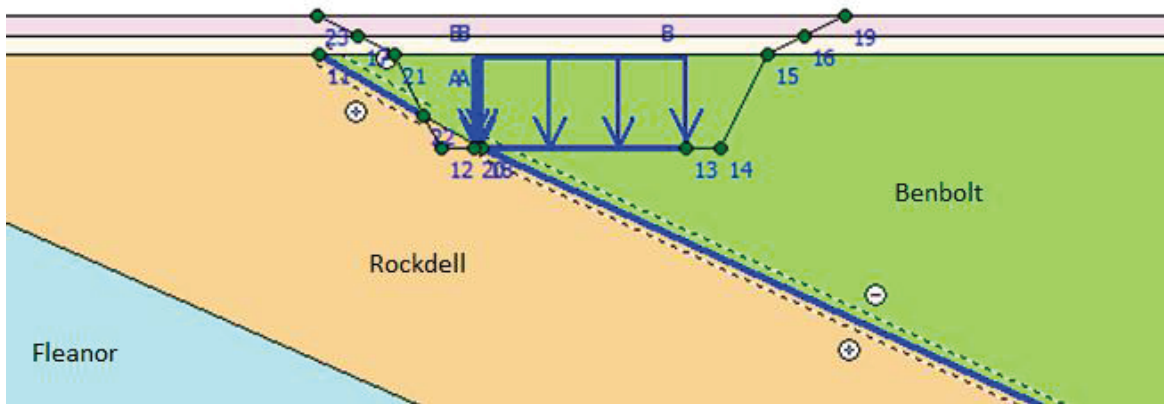


**FIGURE 2-3**  
**SITE A, CROSS SECTION: A-A', EMBEDMENT DEPTH: 138 FT**



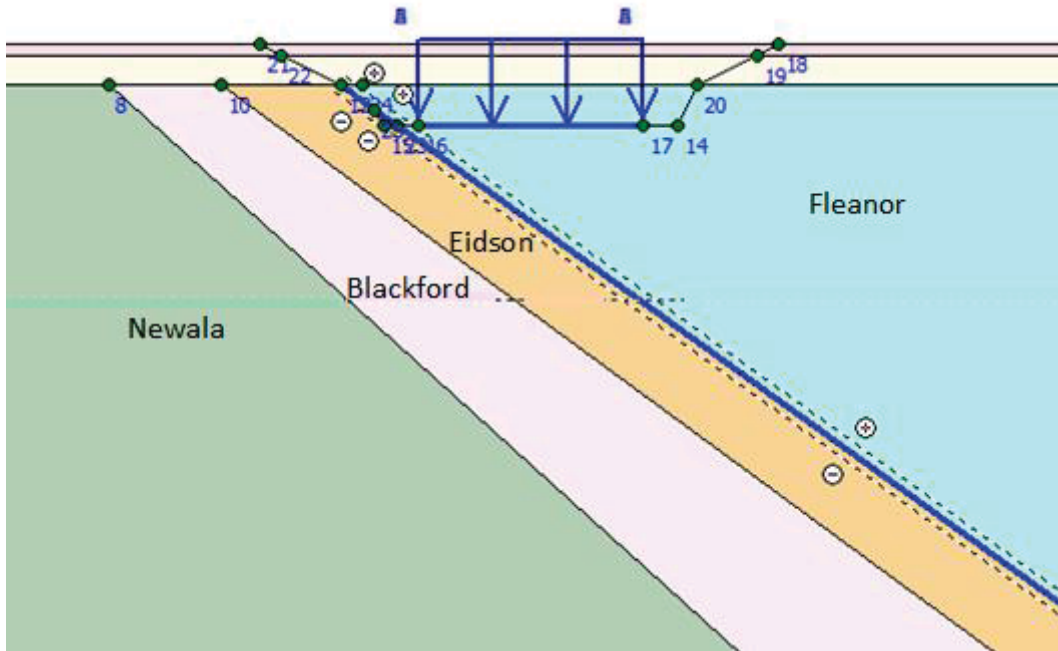


**FIGURE 2-4**  
**SITE B, CROSS SECTION: B-B', EMBEDMENT DEPTH: 80 FT**

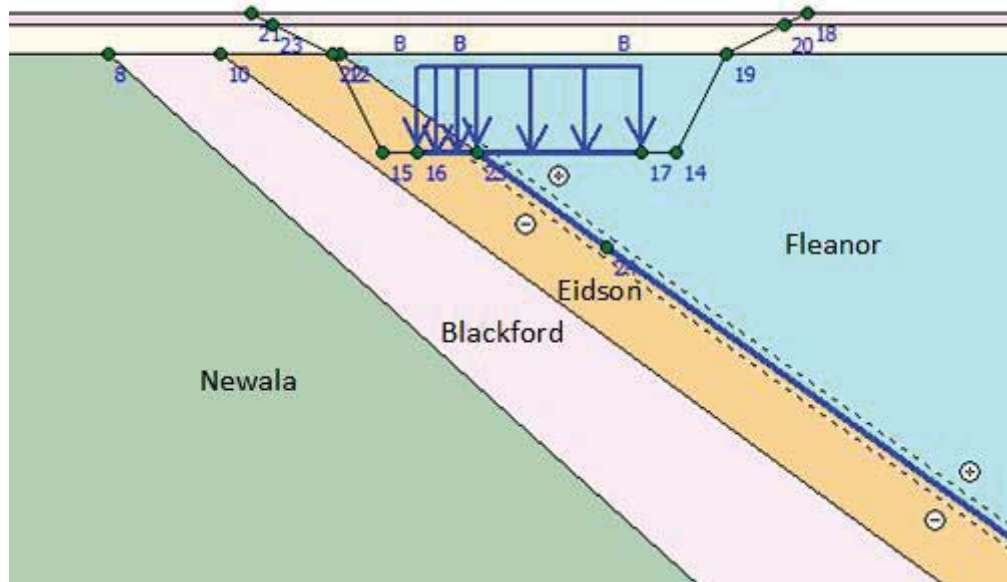


**FIGURE 2-5**  
**SITE B, CROSS SECTION: B-B', EMBEDMENT DEPTH: 138 FT**



### 2.2.2 Finite-Element Mesh

As shown on *Figure 2-6*, 15-node triangle elements are used in the analysis, with a total of approximately 5,000 elements for the design mesh model. The size of the triangular FE is about 2 ft in finely meshed areas near the foundation elevation, and 80 ft in the coarsely meshed areas outside of the excavation zone. In the vertical plane, the element length varies between approximately 2 ft and 80 ft. The effect of mesh size in the bearing capacity results was investigated during the calculations. The sensitivity analysis showed that the estimated bearing capacity values obtained with different mesh configurations would not change significantly. The choice of mesh configuration proved to have more influence on the distribution of the plastic points. However, for the purpose of estimating the ultimate bearing capacity for the foundation, the mesh configuration selected proved to be adequate.

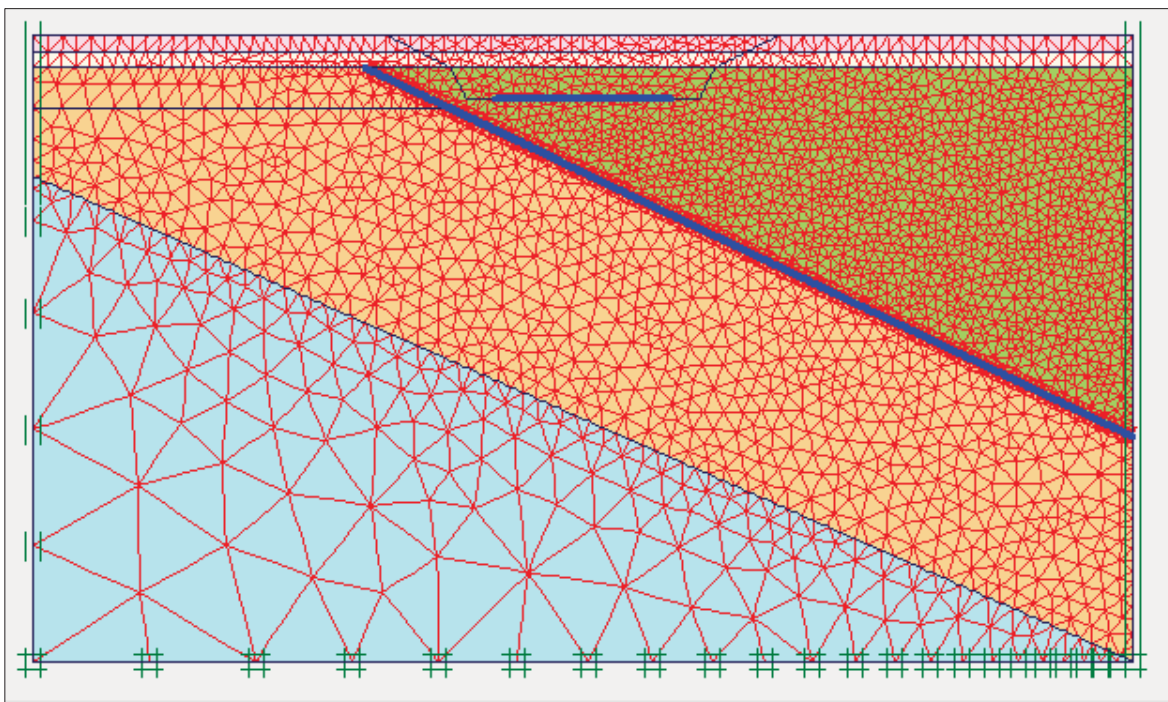


**FIGURE 2-6  
A TYPICAL MODEL WITH REFINED MESH**

### 2.2.3 Loading

PLAXIS 2D simulates dewatering, excavation, and other construction steps as individual phases. Accordingly, differential settlement can be visually examined using contour plots provided for



discrete construction steps. Alternatively, numerical values along any given axis can be extracted using calculated nodal displacements.

The PLAXIS 2D models for Site A and Site B specifically included the following simulation phases:

- Initial Conditions: Initial effective stresses for the Site are obtained.
- Dewatering: The water level, initially assumed to be at the top of existing fill for all models, is lowered to the level of embedment depth considered for the analysis.
- Excavation: Upon dewatering down to embedment depth, the material between ground surface (EL 821 ft) and embedment depth elevation is removed.
- Initial Loading: A load of 10ksf is applied to the foundation basemat. It is important to note that the load on the footprint of the common basemat is applied while the pore pressure is assumed to be zero at the bottom of the foundation. This condition is kept for conservative purposes.
- Incremental Loading: The load on the basemat is increased incrementally up to more than 70 times the initial loading.



### 3.0 RESULTS

The results of the FE models are evaluated with one primary goal: to identify the bearing capacity for the embedment depth and foundation size considered.

The ultimate bearing capacity is determined by inspecting the load-displacement curves for nodes immediately beneath the foundation basemat. The load at which a significant decrease in the stiffness of the subsurface is observed is considered the bearing capacity. At the ultimate bearing capacity, general failure criterion, a plastic zone develops beneath the foundation, typically starting on the corner, and propagates to the other end away from the foundation, as shown on *Figure 3-1*. If this behavior is not yet observed, the assumed bearing capacity level is conservative, as it corresponds to a partially developed general failure surface.

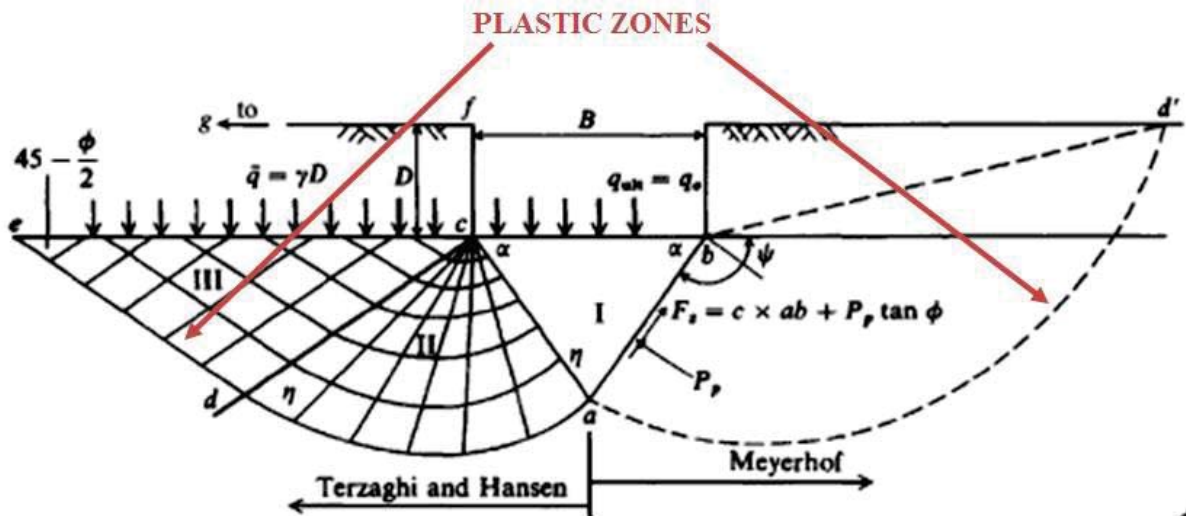


FIGURE 3-1  
TYPICAL BEARING CAPACITY FAILURE WITH PLASTIC ZONES  
(FROM BOWLES, 1997)

Results for the incremental analysis for Site A are shown on *Figure 3-2 and Figure 3-3*. Results for the incremental analysis for Site B are shown on *Figure 3-4 and Figure 3-5*. Results for both Sites are summarized in *Table 3-1*. On *Figure 3-2 through Figure 3-5*, deformation values are not shown in the x-axis, since close to the failure, deformation levels become meaningless.



Instead the drop in the stiffness denoting the initiation of failure is important for bearing capacity purposes.

**TABLE 3-1  
ULTIMATE BEARING CAPACITY FROM PLAXIS 2D**

SITE CROSS SECTION	EMBEDMENT DEPTH (FT)	ULTIMATE BEARING CAPACITY (KSF)
A-A'	80	499
	138	441
B-B'	80	526
	138	320

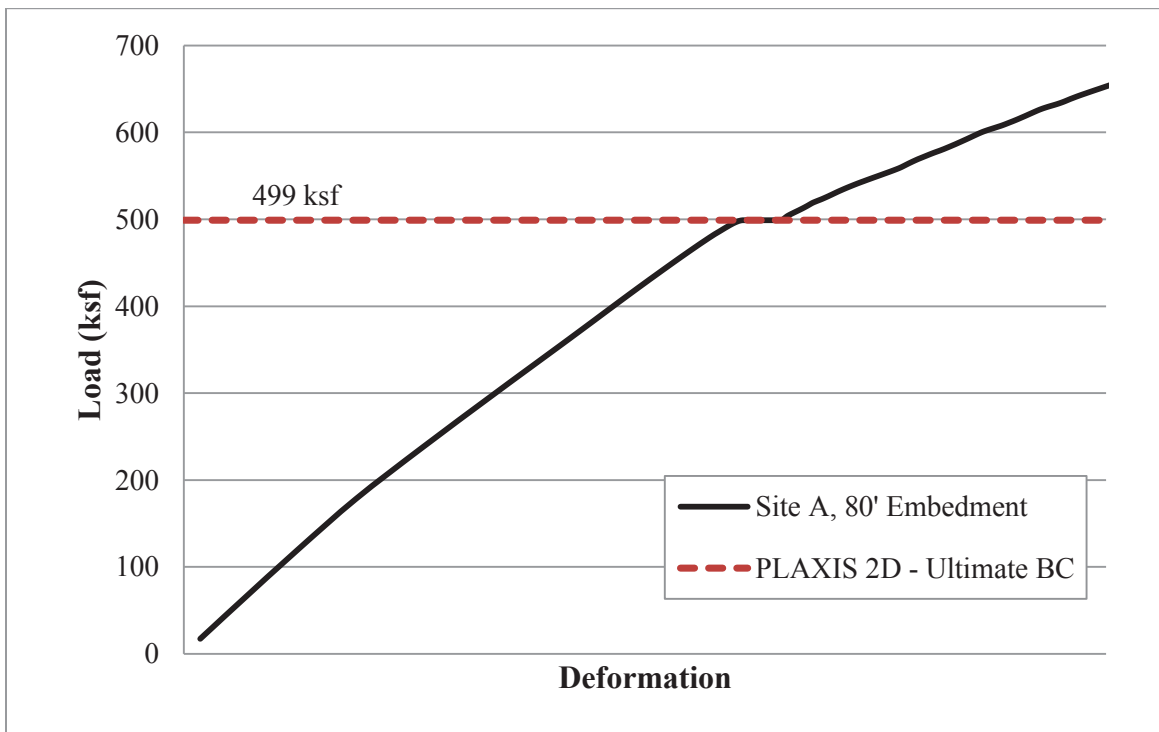


**FIGURE 3-2  
LOAD DEFORMATION CURVE FOR SECTION A-A', 80 FT EMBEDMENT**



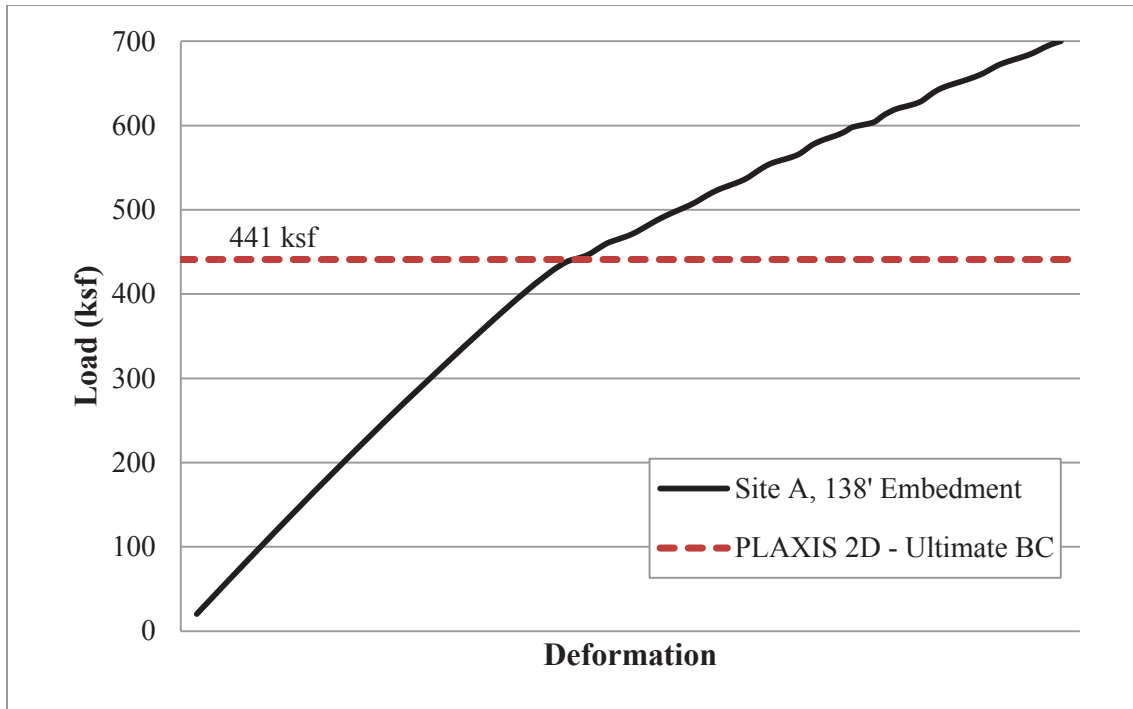


**FIGURE 3-3**  
**LOAD DEFORMATION CURVE FOR SECTION A-A', 138 FT EMBEDMENT**

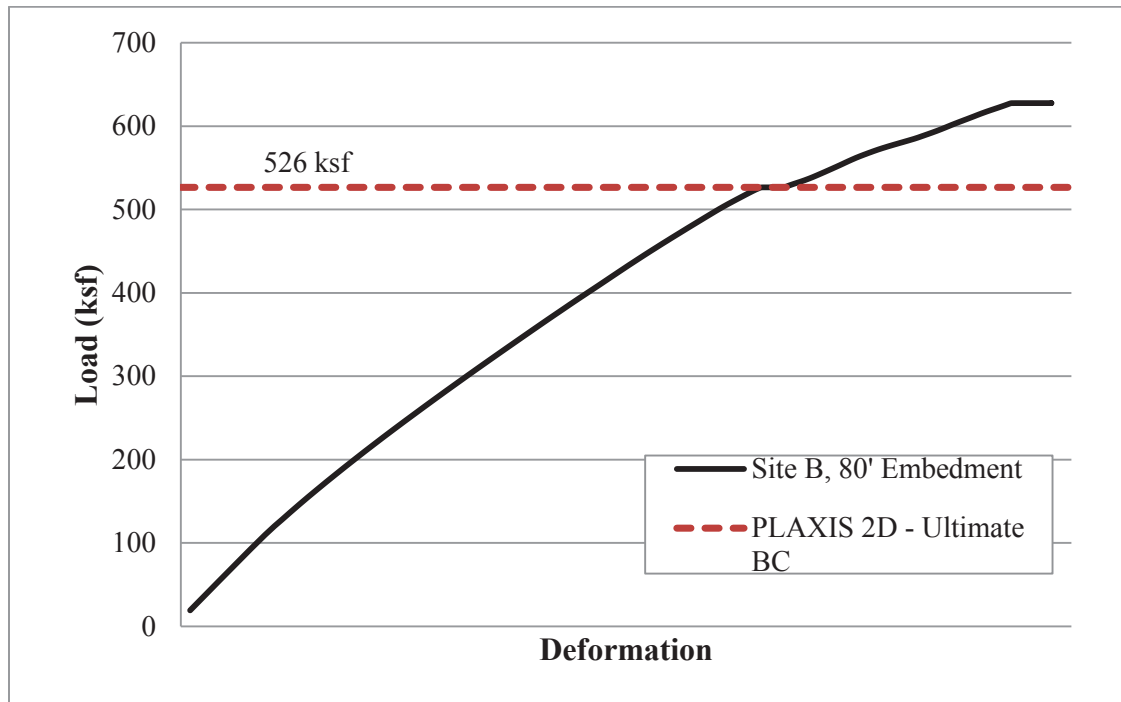


**FIGURE 3-4**  
**LOAD DEFORMATION CURVE FOR SECTION B-B', 80 FT EMBEDMENT**



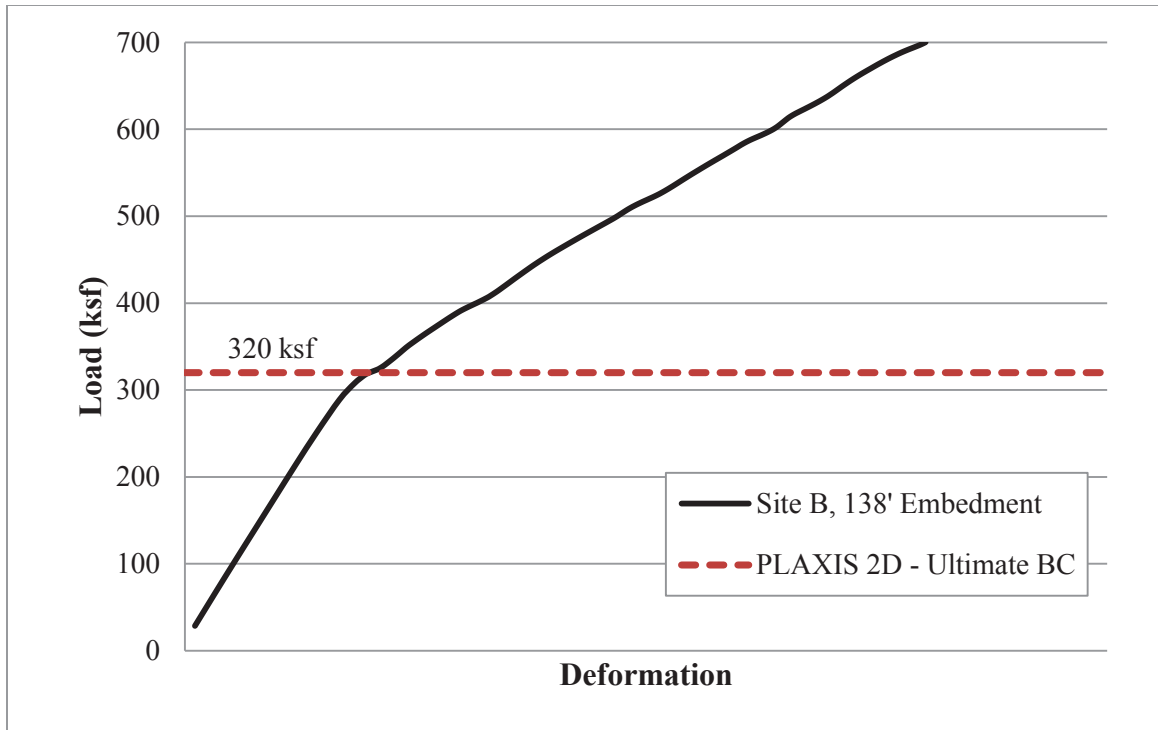


**FIGURE 3-5  
LOAD DEFORMATION CURVE FOR SECTION B-B', 138 FT EMBEDMENT**

*Figure 3-6 through Figure 3-17* present the progression of the failure surface with increasing load, as illustrated by the red Mohr-Coulomb plastic points. For each case evaluated, three figures are presented:

- a view of the plastic points when the load is relatively small and the response is elastic,
- a view of the plastic points at the conservatively defined ultimate bearing capacity load, and
- a view of the plastic points at a load beyond the defined ultimate bearing capacity.

The failure progression for Section A-A' with 80 ft embedment is illustrated on *Figure 3-6* through *Figure 3-8*. *Figure 3-6* corresponds to a 100 ksf loading with an elastic response, *Figure 3-7* corresponds to a 500 ksf load near the conservatively defined ultimate bearing capacity, and *Figure 3-8* corresponds to a 1,500 ksf load beyond the defined ultimate bearing capacity.



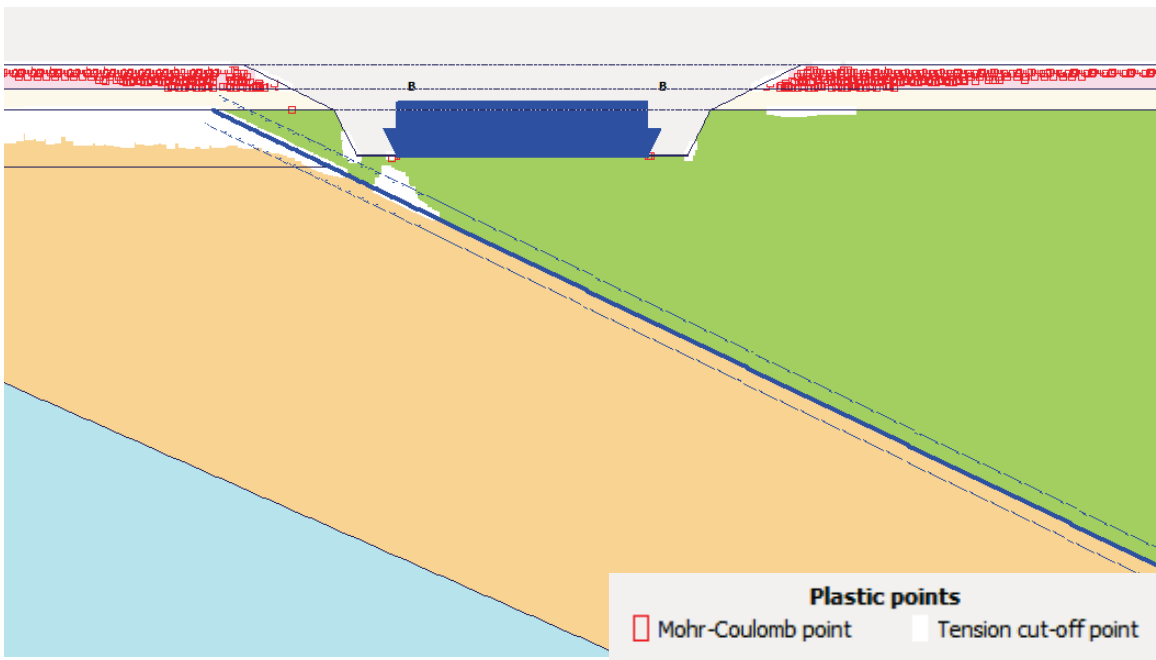


**FIGURE 3-6**  
**PLASTIC POINTS FOR SECTION A-A', 80 FT EMBEDMENT**  
**100 KSF LOAD (ELASTIC RESPONSE)**

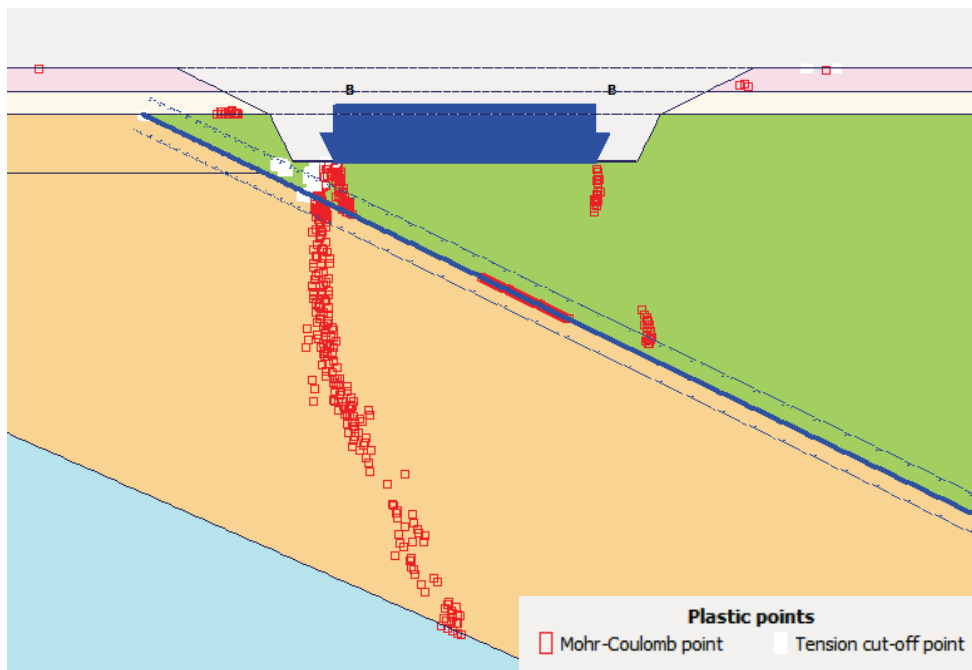


**FIGURE 3-7**  
**PLASTIC POINTS FOR SECTION A-A', 80 FT EMBEDMENT**  
**500 KSF LOAD (DEFINED ULTIMATE BEARING CAPACITY)**



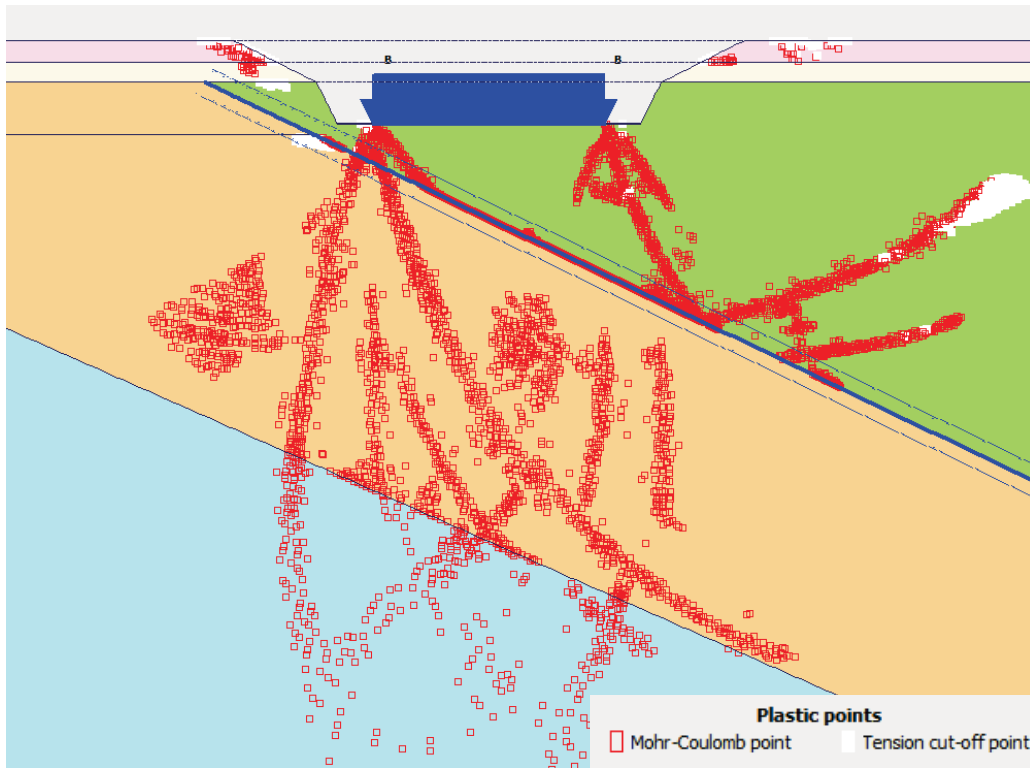


**FIGURE 3-8**  
**PLASTIC POINTS FOR SECTION A-A', 80 FT EMBEDMENT**  
**1500 KSF LOAD (BEYOND ULTIMATE BEARING CAPACITY)**

The failure progression for Section A-A' with 138 ft embedment is illustrated on *Figure 3-9 through Figure 3-11*. *Figure 3-9* corresponds to a 100 ksf loading with an elastic response, *Figure 3-10* corresponds to a 440 ksf load near the assumed ultimate bearing capacity, and *Figure 3-11* corresponds to a 1,200 ksf load beyond the assumed ultimate bearing capacity.



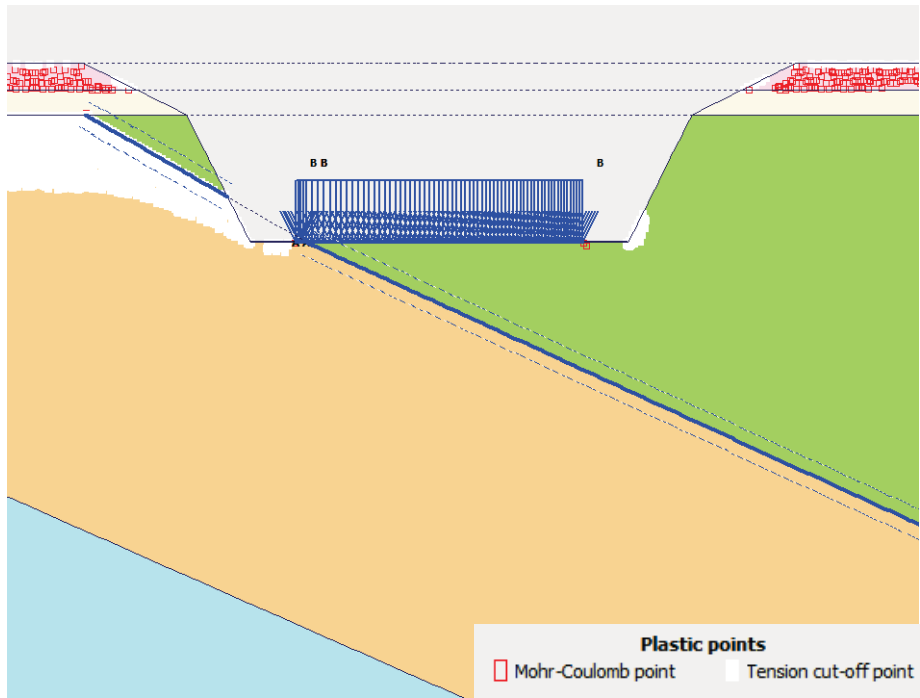


**FIGURE 3-9**  
**PLASTIC POINTS FOR SECTION A-A', 138 FT EMBEDMENT**  
**100 KSF LOAD (ELASTIC RESPONSE)**

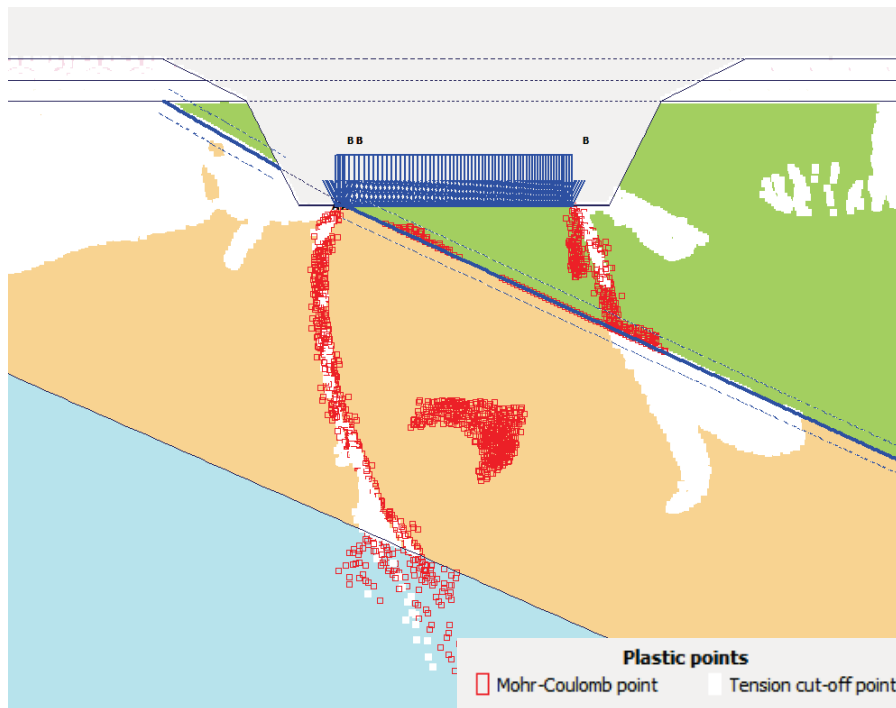


**FIGURE 3-10**  
**PLASTIC POINTS FOR SECTION A-A', 138 FT EMBEDMENT**  
**440 KSF LOAD (DEFINED ULTIMATE BEARING CAPACITY)**



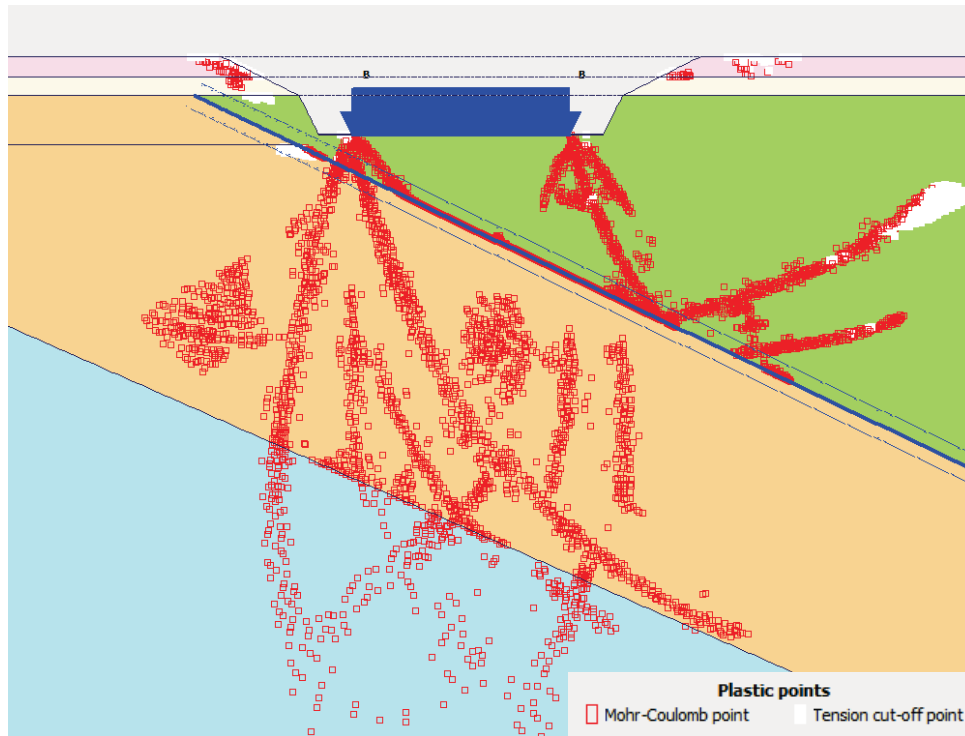


**FIGURE 3-11  
PLASTIC POINTS FOR SECTION A-A', 138 FT EMBEDMENT  
1200 KSF LOAD (BEYOND ULTIMATE BEARING CAPACITY)**

The failure progression for Section B-B' with 80 ft embedment is illustrated on *Figure 3-12* through *Figure 3-14*. *Figure 3-12* corresponds to a 100 ksf loading with an elastic response, *Figure 3-13* corresponds to a 520 ksf load near the conservatively defined ultimate bearing capacity, and *Figure 3-14* corresponds to a 620 ksf load beyond the ultimate bearing capacity.



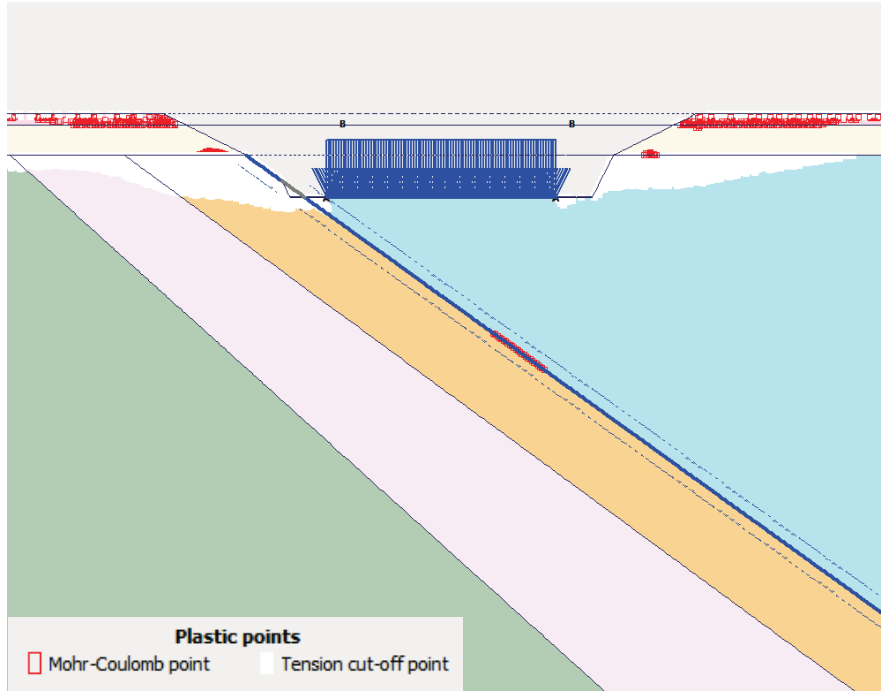


**FIGURE 3-12  
PLASTIC POINTS FOR SECTION B-B', 80 FT EMBEDMENT  
100 KSF LOAD (ELASTIC RESPONSE)**

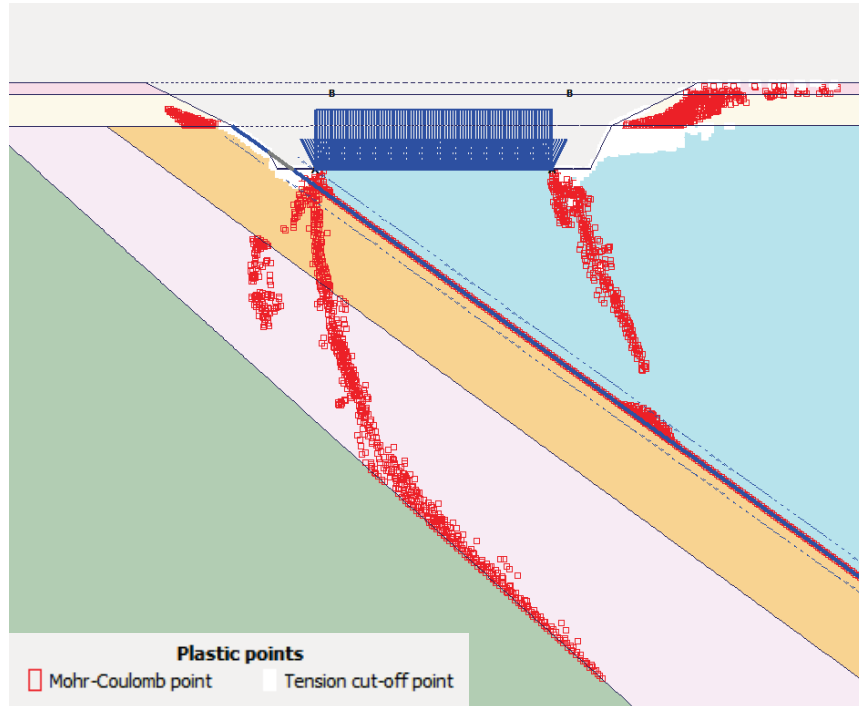


**FIGURE 3-13  
PLASTIC POINTS FOR SECTION B-B', 80 FT EMBEDMENT  
520 KSF LOAD (DEFINED ULTIMATE BEARING CAPACITY)**



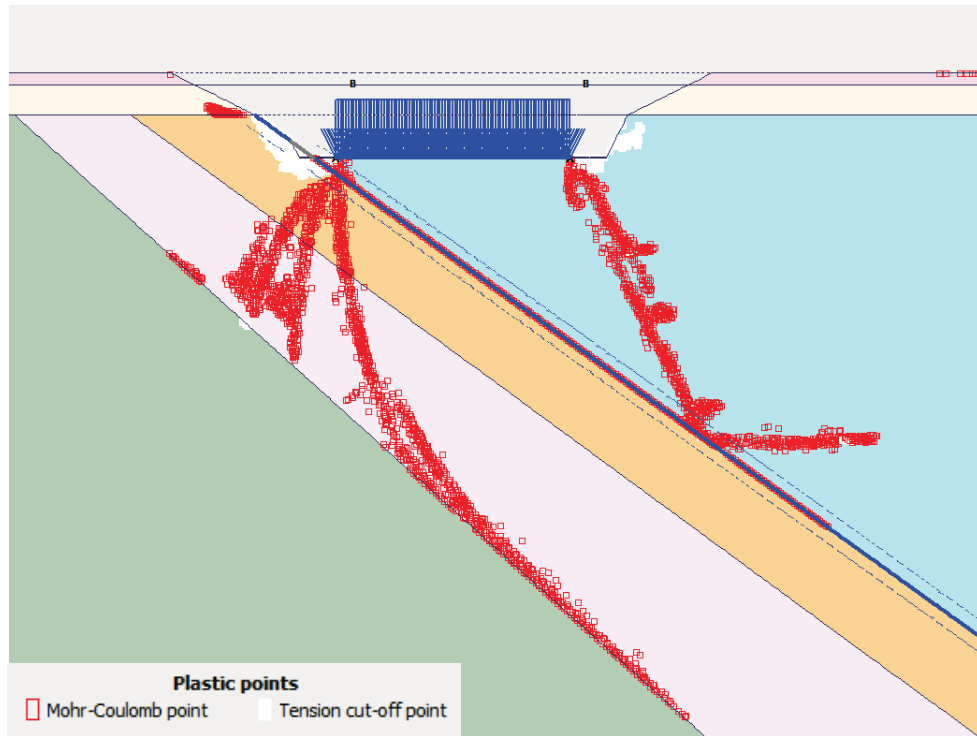


**FIGURE 3-14  
PLASTIC POINTS FOR SECTION B-B', 80 FT EMBEDMENT  
620 KSF LOAD (BEYOND ULTIMATE BEARING CAPACITY)**

The failure progression for Section B-B' with 138 ft embedment is illustrated on *Figure 3-15* through *Figure 3-18*. *Figure 3-15* corresponds to a 100 ksf loading with an elastic response, *Figure 3-16* corresponds to a 320 ksf load near the defined ultimate bearing capacity, and *Figure 3-17* corresponds to a 1,500 ksf load beyond the ultimate bearing capacity.



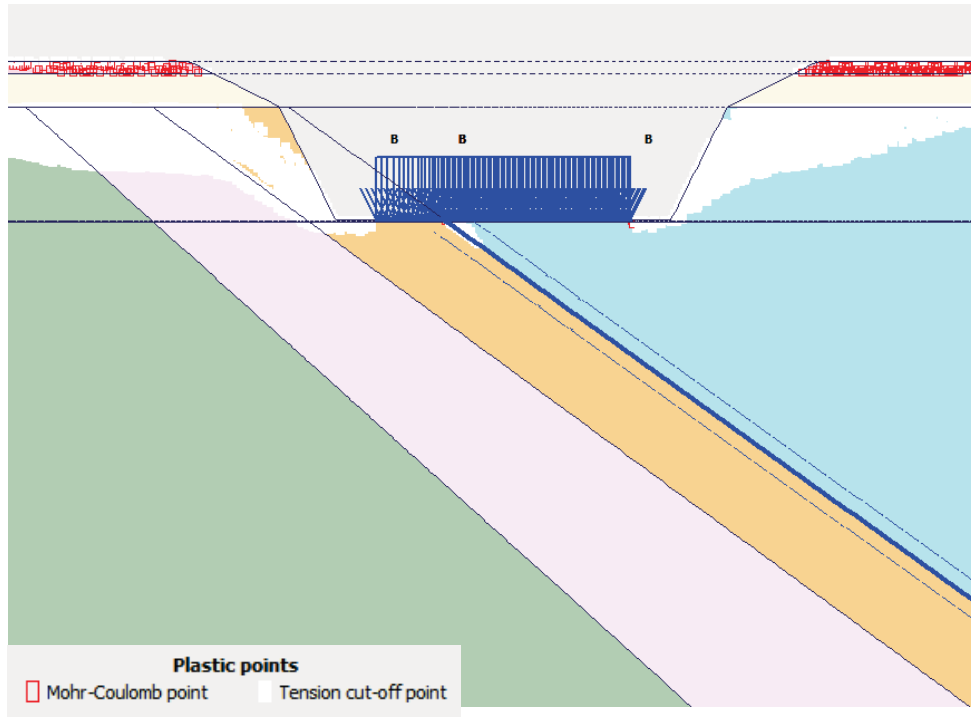


**FIGURE 3-15**  
**PLASTIC POINTS FOR SECTION B-B', 138 FT EMBEDMENT**  
**100 KSF LOAD (ELASTIC RESPONSE)**

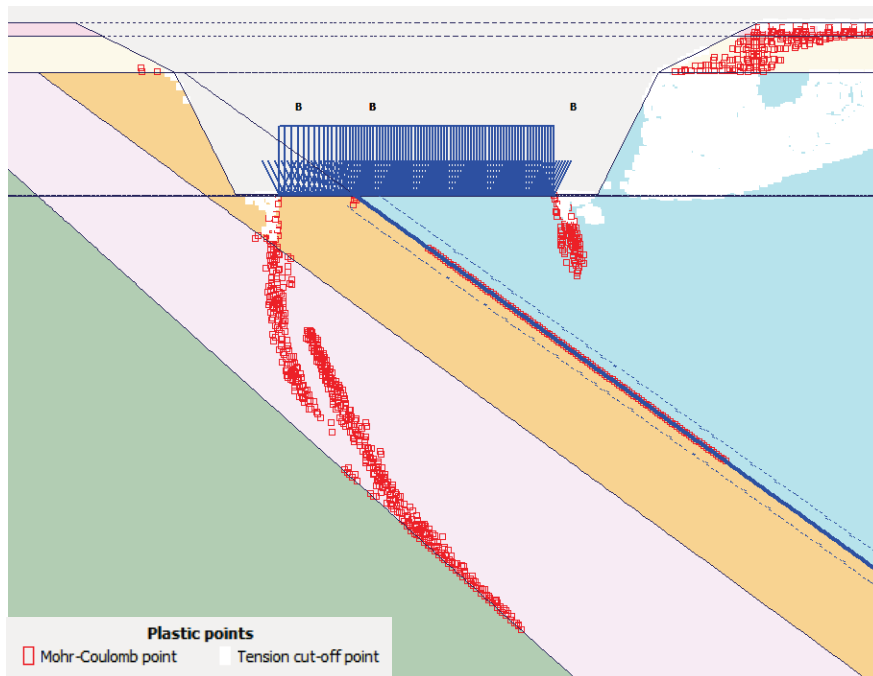


**FIGURE 3-16**  
**PLASTIC POINTS FOR SECTION B-B', 138 FT EMBEDMENT**  
**320 KSF LOAD (DEFINED ULTIMATE BEARING CAPACITY)**



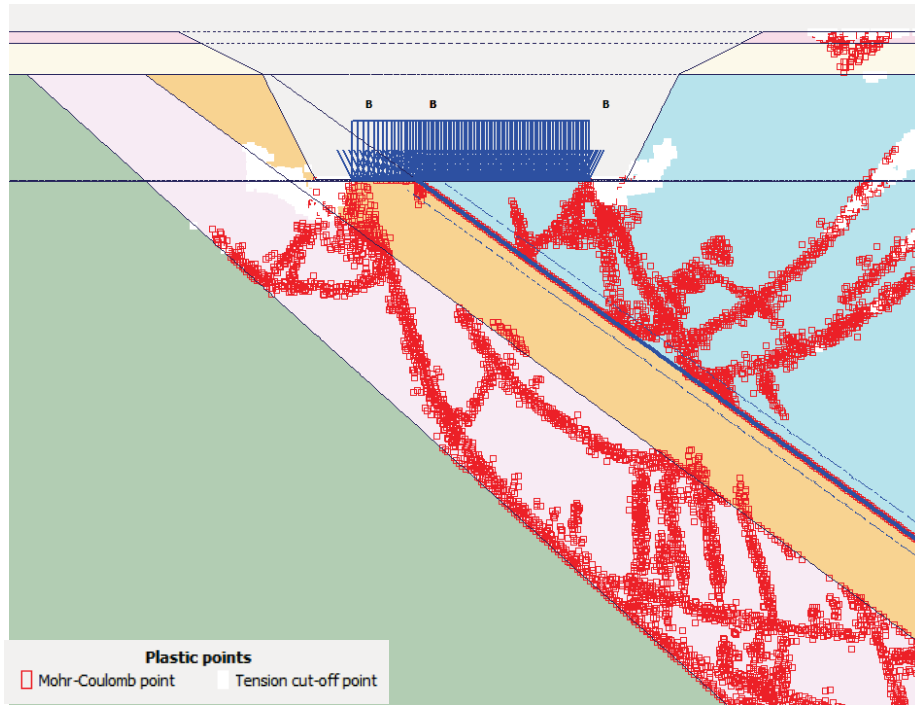


**FIGURE 3-17**  
**PLASTIC POINTS FOR SECTION B-B', 138 FT EMBEDMENT**  
**1500 KSF LOAD (BEYOND ULTIMATE BEARING CAPACITY)**



## 4.0 SUMMARY

A PLAXIS 2D FE model is used to estimate the ultimate bearing capacity at the CRN Site for various embedment depths. As expected from a competent rock foundation, the ultimate bearing capacity for the CRN Site is high, ranging from 320 kips per square foot (ksf) to 526 ksf for the sections and embedment depths evaluated. The ultimate bearing capacity for Site A is estimated as 441 ksf, and the ultimate bearing capacity for Site B is estimated as 320 ksf. Please note that these bearing capacities are estimates with the purpose of showing that the site does not present bearing capacity issues for ESP application. We recommend these calculations to be repeated once the technology is selected, and the following factors are addressed in more detail:

- The foundation embedment depth and foundation
- The lateral location of the foundation with respect to the bedding planes and shear fracture zones
- The shear strength at the bedding planes, and shear fracture zones
- In situ stresses

The PLAXIS model geometry is slightly modified compared to the settlement model in the non-proprietary Report, as summarized in *Section 2.2.1*. The geometry modifications primarily serve to make the bearing capacity model more consistent with the traditional bearing capacity calculations presented in the SSAR. When a factor of safety of 3 is considered to determine the allowable bearing capacity, the values obtained from this analysis compare well with the allowable capacities reported in the SSAR, as shown in *Table 4-1*.

**TABLE 4-1  
COMPARISON OF PLAXIS AND SSAR BEARING CAPACITY**

<b>SITE</b>	<b>MINIMUM PLAXIS ULTIMATE BEARING CAPACITY (ksf)</b>	<b>ALLOWABLE PLAXIS BEARING CAPACITY (ksf)</b>	<b>ALLOWABLE SSAR BEARING CAPACITY, BOWLES METHOD (ksf)</b>
A	441	147	149
B	320	107	108



## 5.0 REFERENCES

Bowles, J. E., *Foundation Analysis and Design*, Fifth Edition, 1997.

ML16144A067 - Part 02 SSAR (Rev. 0) - Part 2 - SSAR - Chapter 2 - Site Characteristics -  
Section 2.5.4 - Stability of Subsurface Materials and Foundations, 2016

RIZZO, 2017, "Non-Proprietary Report, Foundation Assessment, Clinch River Nuclear Site,"  
Rev. 0, May 2017.



**Attachment 3**  
**Site Safety Analysis Report Subsection 2.5 Markups**

**The following SSAR Subsection 2.5.1.2.3.4, “Estimate of Hypothetical Large Void,” is being revised and renamed “Karst Evaluation. A sentence in SSAR Subsection 2.5.1.2.9, under “Conclusions,” is being removed. Underlines indicate text to be added. Strikethroughs indicate text to be deleted.**

**2.5.1.2.3.4    ~~Estimate of Hypothetical Large Void~~Karst Evaluation**

~~An estimate of a hypothetical large void was made based upon existing data from the CRBRP and CRN Site subsurface investigation and consideration of the geologic units immediately beneath the designated power block area. The estimated size is based on the height of the largest cavities encountered in boreholes at and below the elevation of 740 ft NAVD88 (Table 2.5.1-19). This elevation corresponds to the shallowest embedment depth of the range of proposed technologies and also corresponds to the pool elevation of the Watts Bar Reservoir. Additional explanation follows below. The hypothetical large void described is intended to be used for the evaluation of foundation stability to support the demonstration of site suitability and is not a prediction of what may be encountered during excavation.~~

*Data review*

A review of the cavity data from the CRN and CRBRP Site drilling programs reveal several trends illustrated in Figures 2.5.1-75 through 2.5.1-77. The data are segregated by geologic formation to assess the likelihood of the presence of cavities, as well as to estimate cavity size within each geologic unit. Each data plot presents the cavity center-point elevation versus cavity length within the borehole. For this analysis, karst cavity data were partitioned into three elevation intervals. Intervals were as follows: (1) above the CRN Site proposed plant grade of elevation 821 ft NAVD88; (2) between elevations 821 ft NAVD88 and 740 ft NAVD88, the shallowest embedment depth considered and also the Watts Bar Reservoir pool elevation; and (3) lower than elevation 740 ft NAVD88. A comparison of the compiled borehole data shows that the majority of cavities: (1) occur above the elevation 740 ft NAVD88 pool elevation of the Watts Bar Reservoir, and (2) are less than 2 ft in height. The Eidson and Rockdell units show the largest and greatest frequency of cavities. The largest cavity encountered in any borehole has a height of 16.5 ft and occurs at elevation 789 ft NAVD88.

The cavities that occur below the current Watts Bar Reservoir elevation of 740 ft NAVD88, which is the current Watts Bar Reservoir elevation as well as the shallowest embedment depth considered in this investigation, are assumed to reflect dominantly phreatic development below the water table. Cavities in the vadose zone, the area above the water table, may be related to either vadose processes only, or vadose dissolution overprinted on originally phreatic cavities. The relative amount of dissolution attributed to vadose versus phreatic processes in the latter case cannot be determined or quantified from borehole data.

Based on the compiled borehole data, the highest frequency and largest size of cavities occur within the Rockdell and the Eidson units (Table 2.5.1-19, Figure 2.5.1-51). These two units also contain the greatest thicknesses of pure limestone beds relative to other Chickamauga Group strata encountered at the site. More detail regarding the variability of carbonate content by

stratigraphic unit is demonstrated in the geophysical logs for these units (Reference 2.5.1-214). Natural gamma radiation increases with the proportion of silt and clay in the formation and the alternating high and low levels reflect the locations of siltstone and limestone beds, respectively (Figure 2.5.1-78; Reference 2.5.1-9). Additionally, carbonate contents were determined from rock core samples during the CRN subsurface investigation (Figure 2.5.1-49). These methods demonstrate the variability of carbonate content both between and within the stratigraphic units at the CRN Site.

The spatial distribution of cavities is consistent with the trends discussed above. A map of boreholes indicating the presence and elevation interval of cavities is presented in Figure 2.5.1-79. Several boreholes within the Rockdell Formation in the south-center of the power block area exhibit cavities in the middle and lower elevation intervals. The boreholes and cavities occur along strike with bedding. However, elevations of individual cavities within this cluster do not appear to correlate directly. Boreholes B-144 and B-145, spaced approximately 33 ft apart, have cavities at elevation 781 ft NAVD88, although connectivity between cavities is uncertain.

### *Theoretical Conduit Shape*

Karst cavity shapes can vary widely, but their morphology is determined by several basic principles. The three dimensional shape of any cavity is governed by its environment of formation, hydrogeologic setting, and rock characteristics. For example, dissolution within the vadose zone, where water is moving downward toward the water table, tends to create slots, shafts, canyons, and passages oriented down dip or following steep joint planes (Reference 2.5.1-305). By contrast, dissolution within the phreatic zone, where water is moving at and below the water table following the hydraulic gradient, tends to create an integrated conduit system with subhorizontal tubular passages that tend to be circular, the most efficient shape for transmittal of water (Reference 2.5.1-305).

The common phreatic tube shape can be modified by factors such as variations in rock solubility, bed thickness, structural discontinuities, geometry of the fracture pathway where dissolution initiated, and the degree to which the initial fractures have been enlarged (Reference 2.5.1-305). The conduit system follows available fractures in response to the hydraulic gradient and may descend or ascend as needed to respond to that gradient, while at the same time following the more open or connected fractures. The resulting pathway enlarges by dissolution, tending toward a circular cross section as dissolution proceeds assuming uniform solubility of the rock.

### *Hypothetical large void*

~~Based on project data and the understanding that cavities in the phreatic zone comprise portions of an integrated conduit system, the size and shape of a hypothetical large void can be estimated. The estimated size is based on the height of the largest cavities encountered in boreholes at and below the elevation of 740 ft NAVD88 (Table 2.5.1-19). This elevation corresponds to the shallowest embedment depth of the range of proposed technologies and also corresponds to the pool elevation of the Watts Bar Reservoir. The choice of this elevation eliminates voids that would have formed by or been modified by vadose dissolution above the water table and thus captures voids primarily formed by phreatic dissolution below the water table.~~

The shape of the void is based on the understanding that phreatic conduits are portions of an underground drainage system whose function is to transport water. In this capacity, a phreatic conduit ideal shape is tubular or pipe-like although this is conceptual with regards to the CRN site (Reference 2.5.1-305). Based on observations of cave passage orientation in the Knox Group and older carbonate strata in the Oak Ridge area (Reference 2.5.1-254), and documented strata-bound movement of contaminants in groundwater through the Chickamauga Group at the ORNL site (Reference 2.5.1-304), the dominant direction of flow is expected to follow the strike of bedding.

The characteristics of the hypothetical large void are shown in Table 2.5.1-20. The geometric characteristics are provided as a simple shape, both for ease of subsequent analysis, and to acknowledge a lack of direct observations that support further detail. A hypothetical large void that could occur below foundation level has a cylindrical shape with the long axis oriented N52°E, parallel to strike. The cross section is circular, with a diameter (height and width) of 10 ft, approximately the largest void encountered in the boreholes at or below elevation 740 ft NAVD88, rounded up to the nearest foot (MP-418 in Table 2.5.1-19). Voids encountered above elevation 740 ft NAVD88 are located above the shallowest embedment depth of the range of proposed technologies and may have been modified by vadose dissolution not expected below elevation 740 ft NAVD88. The length may be a few or several tens of feet at the scale of the proposed plant foundation based on the site borehole data, and geologic mapping of the CRBRP excavation (Reference 2.5.1-303).

The hypothetical large void described is intended to be used for the evaluation of foundation stability to support the demonstration of site suitability and is not a prediction of what may be encountered during excavation. The shape and size are based on an interpretation of the documented borehole data, informed by observations of cavities mapped within the Rockdell Formation in the CRBRP excavation, and on professional judgment considering the combined site data and the understanding of karst processes at the CRN Site and within the region.

### **2.5.1.2.9 Relational Analysis**

#### *Conclusions*

The aforementioned relational analysis provides a comparison of the CRN Site with the CRBRP Site with respect to geologic formation, rock type, geologic structure and occurrence and character of karst and voids/cavities encountered at and below the depth of foundations. The results of the relational analysis form the basis for using subsurface data from both sites to formulate an estimate of a hypothetical large void that may be encountered below the proposed power block, which is included as the second item within this response. The geologic units mapped in the CRBRP Site excavation (Fleanor member and Rockdell Formation) are the same as those occurring in Location B of the CRN Site power block area. Except for the Mascot Formation, the karst depression densities and area ratios for the other stratigraphic units within the power block area are all less than those in the stratigraphic units noted above as occurring to the northwest and southeast of the power block area; indicating that the power block area carbonates appear to have similar dissolution characteristics to the Rockdell Formation.

**As a result of removing Subsection 2.5.1.2.3.4, the reference 2.5.1-304 is being removed from SSAR Subsection 2.5.1.3 and the note “Reference number 2.5.1-304 is not used” is being added:**

- 2.5.1-303. Drakulich, N. S., Geologic mapping of the Clinch River Breeder Reactor plant excavations, prepared for the U. S. Department of Energy and CRBRP Project Management Corporation: Stone and Webster Engineering Company, Cherry Hill, NJ, Report No. 12720.50-G(C)-1, 1984
- ~~2.5.1-304. Ketelle, R. J., and R.R. Lee, Migration of a groundwater contaminant plume by stratabound flow in waste area grouping 1 at Oak Ridge National Laboratory, Oak Ridge, Tennessee: ORNL/ER-126, prepared by Martin Marietta Energy Systems, Inc., 21 p., 1992. Reference number 2.5.1-304 is not used.~~
- 2.5.1-305. Lauritzen, S.E., and J. Lundberg, Solutional and erosional morphology, Chapter 6.1 in: Speleogenesis, Evolution of Karst Aquifers, A. B. Klimchouk, D. C. Ford, A. N. Palmer, W. Dreybrodt, National Speleological Society, Inc., p. 408-426, 2000.

**As a result of removing Subsection 2.5.1.2.3.4, the following tables are being removed from SSAR Subsection 2.5.1:**

Table 2.5.1-20            Hypothetical Large Void below Foundation Level

**SSAR Subsection 2.5.4.13, “References,” is being renamed “Foundation Assessment Model,” and new text is being added. Current Subsection 2.5.4-13, “References,” is being renumbered 2.5.4-14. Strikethroughs indicate text to be deleted. Underlines indicate text to be added.**

#### **2.5.4.13      References**Foundation Assessment Model****

A PLAXIS 2D model was developed to determine potential karstic cavity impacts on SMR foundations. The details of the analysis are contained within Reference 2.5.4-59. Cases were performed at 40 ft, 90 ft and 140 ft depths for 5 foot, 10 foot and 15 foot cavity sizes at varying locations under the foundation. Table 2.5.4-33 provides the cases for Location A and B.

The PLAXIS model for Location A and B was performed at two different cross-sections, to account for varying dip of the stratigraphic layers. The model included a disturbed zone around the simulated cavity to include the appropriate material properties for cohesion and friction angle. The model also included initial conditions, dewatering assumptions, excavation assumptions and loading similar to currently approved Large Light Water Reactor designs. The results of the foundation assessment model are provided in Table 2.5.4-34.

The results of the FE models were evaluated with one primary goal: to identify a cavity size that may potentially collapse under static excavation, dewatering, and structural loads. Anticipated foundation host rocks, namely the Fleanor Member of the Lincolnshire Formation and the Benbolt and Rockdell formations, are all relatively stiff/competent rocks. Excluding potential cavity collapses, these rock formations are not expected to undergo large strains or deformation under excavation, dewatering, or structural static loads (i.e., foundation deformations are expected to be negligible). As such, the foundations should be safe provided that potential postulated critical (large enough size) cavities do not collapse.

The collapse potential of cavities is evaluated in terms of relative shear. Relative shear is the ratio of induced shear stress (due to static loads) to shear strength. If this ratio reaches 100 percent, a plastic zone (Mohr-Coulomb failure) starts to develop around a cavity, and collapse is initiated. Initiation of plastic zone does not denote impending failure, and further loading is needed to propagate the failure zone to the surface. Therefore, this approach provides additional conservatism. For Location A and B modeling purposes, a critical relative shear ratio value of 0.85 (85 percent) was conservatively selected to provide a margin of safety of at least 15 percent.

All model results after loading phase were specifically evaluated in terms of relative shear and vertical deformation, with consideration for cavity diameters, depths, and locations, and foundation embedment depths.

For model scenarios featuring 15 ft cavity diameters, relative shear values are about 10 percent higher relative to models utilizing 5 ft cavity diameter. Vertical deformation resulting from a 15 ft cavity diameter is also about 2 percent higher than the vertical deformations resulting from a 5 ft diameter cavity.

The computational results suggest that models of 15 ft cavity diameters represent the most critical case of failure, relative to models of 10 ft and 5 ft cavity diameters. However, the effect of cavity size on deformation is negligible given that calculated critical ratios indicate that collapse is not initiated, and is only near the critical limit for the 15 ft cavity size.

Relative shear values are about 10 percent higher for PLAXIS 2D models of cavities located 30 ft below foundation basemat, relative to models featuring cavity depths 5 ft below the basemat. However, vertical deformations resulting from cavities located 5 ft below the foundation basemat are approximately 6% higher than vertical deformations resulting from cavities located 30 ft below the foundation basemat.

Models of cavities located below the center of the foundation or below the edge of foundation exhibit nearly comparable relative shear values. In contrast, models featuring cavities positioned on a stratigraphic contact (i.e., a bedding plane) demonstrate relative shear values about 40% higher. With regards to vertical deformations, models of cavity location 5 ft below foundation basemat levels exhibit deformations roughly 50% higher than models of cavities located on bedding plane discontinuities.

Postulated collapse of karstic cavities is a geologic hazard to be addressed for the proposed SMR Units 1 and 2 and 3 and 4 at the CRN Site. Accordingly, the impact of various postulated cavity sizes and locations on SMR foundation performance were evaluated using a PLAXIS 2D model. Specifically, the PLAXIS 2D model developed for Location A and Location B considered:

- cavity diameters equal to 5 ft, 10 ft, and 15 ft (selected based on what size is likely to fail and based on observed cavity sizes),
- cavity depths of 5 ft and 30 ft below foundation embedment depths,
- foundation embedment depths of 40 ft, 90 ft, and 140 ft, and
- cavity locations on the edge of the nuclear island, the center of the nuclear island, and on or along bedding planes conservatively assumed to feature significant discontinuities or fracture zones.

For all cases considered, the following main conclusions can be drawn:

1. For all model simulations, the largest cavity diameter (15 ft) was determined to be most critical as expected.
2. Deeper cavities produce increased relative shear around the cavity, which is attributed to the larger initial in situ stresses.
3. Relative shears around the cavities are comparable for individual embedment depths. However, vertical deformation increases with decreasing depth of a cavity relative to foundation embedment depths/excavation surfaces.
4. Cavities located on bedding plane discontinuities or in bedding plane fracture zones are most critical and result in highest relative shear around the cavity.

Approximately 99 percent of the cavities observed in Location A and B borings are significantly less than 11 ft in inferred height. Maximum observed cavity height does not exceed 17 ft. Moreover, cavity development in CRN Site areas is generally limited to the most markedly weathered zone immediately below ground surface, to depths less than 100 ft; 75 percent of reported cavities in Location A and B borings occur at depths less than 55 ft. Consequently, cavity-related failure has a higher potential to occur at relatively shallow depth, less than about 30 ft. Given that foundation embedment depths are deeper than 30 ft and that the 15 ft critical cavity diameter determined by PLAXIS 2D modeling is significantly larger than the 11 ft height that bounds 99 percent of the cavities observed in CRN Site borings, Location A and B are generally suitable for SMR foundation.

Nonetheless, at COLA, foundation performance will be re-evaluated on selection of a final technology, taking into account specific plant design, specific plant loads, and any potential ground improvement or grouting plans. Final foundation locations will also be re-evaluated using specific plant information, with consideration for specific site stratigraphy, subsurface layering orientation, and specific fracture or bedding plane discontinuity zonation.

In addition to the karst evaluation performed in the PLAXIS 2D analysis, an additional analysis of the site bearing capacity was performed for Location A and B at 80 and 138 foot depths. This analysis included a finite-element model to determine the ultimate bearing capacity at the CRN Site. The analysis is provided in Reference 2.5.4-60. The ultimate bearing capacity for the CRN Site is high, ranging from 320 kips per square foot to 526 kips per square foot for the sections and embedment depths evaluated. The ultimate bearing capacity for Location A is estimated as 441 kips per square foot, and the ultimate bearing capacity for Location B is estimated as 320 kips per square foot. Geometry modifications were made to allow the PLAXIS model to be more consistent with the bearing capacity calculations presented in Subsection 2.5.4.10.1.2 and Table 2.5.4-27. When a factor of safety of 3 is considered to determine the allowable bearing capacity, the values from this analysis compare very well with the previously performed allowable bearing capacity analysis as presented in Subsection 2.5.4.10. For Location A, the PLAXIS bearing capacity is 147 kips per square foot as compared to the SSAR bearing capacity of 149 kips per square foot. For Location B, the PLAXIS bearing capacity is 107 kips per square foot as compared to the SSAR bearing capacity of 108 kips per square foot. In general, the comparison of these two methodologies and the subsequent results demonstrates a reasonable agreement for the allowable bearing capacity.

New references 2.5.4-59 and 2.5.4-60, new tables 2.5.4-33 and 2.5.4-34, and new figures 2.5.4-27 through 2.5.4-30 are being added.

**2.5.4-14**      **References**

2.5.4-59.      Rizzo Associates, "Non-Proprietary Report Foundation Assessment Clinch River Nuclear Site," Revision 0, June 16, 2017

2.5.4-60      Rizzo Associates, "Addendum to Non-Proprietary Report Foundation Assessment Clinch River Nuclear Site," Revision 0, June 15, 2017

**Table 2.5.4-33  
Analyzed Cases for Location A and B**

LOCATION <sup>(1)</sup>	SECTION <sup>(2)</sup>	FOUNDATION DEPTH <sup>(3)</sup>	CAVITY SIZE <sup>(4)</sup>	CAVITY LOCATION <sup>(5)</sup>	REMARKS <sup>(6)</sup>				
		(ft)	(ft)						
A	A-A'	40	5,10,15	Center of common basemat	5 ft below basemat				
				Center of common basemat	30 ft below basemat				
				Bedding (Benbolt-Rockdell)	1 Interface				
				Bedding (Benbolt-Rockdell)	2 interfaces				
				Edge of common basemat	5 ft below basemat				
				Center of common basemat	5 ft below basemat				
	E-E'	90	5,10,15	Center of common basemat	5 ft below basemat				
				Bedding (Benbolt-Rockdell)	1 Interface				
				140	5,10,15	Bedding (Benbolt-Rockdell)	1 Interface		
						40	5,10,15	Center of common basemat	5 ft below basemat
								Center of common basemat	30 ft below basemat
						90	5,10,15	Center of common basemat	5 ft below basemat
Bedding (Benbolt-Rockdell)	1 Interface								
140	5,10,15	Bedding (Benbolt-Rockdell)	1 Interface						
		B	B-B'	40	5,10,15	Center of common basemat	5 ft below basemat		
Center of common basemat	30 ft below basemat								
Bedding (Fleanor-Eidson)	1 Interface								
Edge of common basemat	5 ft below basemat								
90	5,10,15					Center of common basemat	5 ft below basemat		
						Bedding (Fleanor-Eidson)	1 Interface		
			Bedding (Fleanor-Eidson)	1 Interface					
F-F'	40		5,10,15	Center of common basemat	5 ft below basemat				
				Center of common basemat	30 ft below basemat				
				90	5,10,15	Center of common basemat	5 ft below basemat		
						Bedding (Fleanor-Eidson)	1 Interface		
						140	5,10,15	Bedding (Fleanor-Eidson)	1 Interface
		Bedding (Fleanor-Eidson)						1 Interface	

Reference 2.5.4-59 Table 2-1

**Notes:**

- (1) The CRN Site contains two potential locations for safety related structures.
- (2) Typical Modeled Location A and B cross sections, shear values and vertical deformations (see Figure 2.5.4-27 through Figure 2.5.4-30).
- (3) Modeled foundation embedment depth (ft below ground surface).
- (4) Modeled cavity diameters.
- (5) Modeled cavity locations.
- (6) Additional detail related to cavity location. For Location A, "1 interface" indicates a single interface element introduced on both sides of the contact between the Benbolt and Rockdell formations. In turn, "2 interfaces" indicates simulation of an interface element on both sides of the Benbolt Formation and Rockdell Formation contact, and simulation of a second interface element located approximately 15 ft above the contact between the Benbolt and Rockdell formations. For Location B, "1 interface" indicates a single interface element introduced on both sides of the contact between the Fleanor and Eidson members of the Lincolnshire Formation.

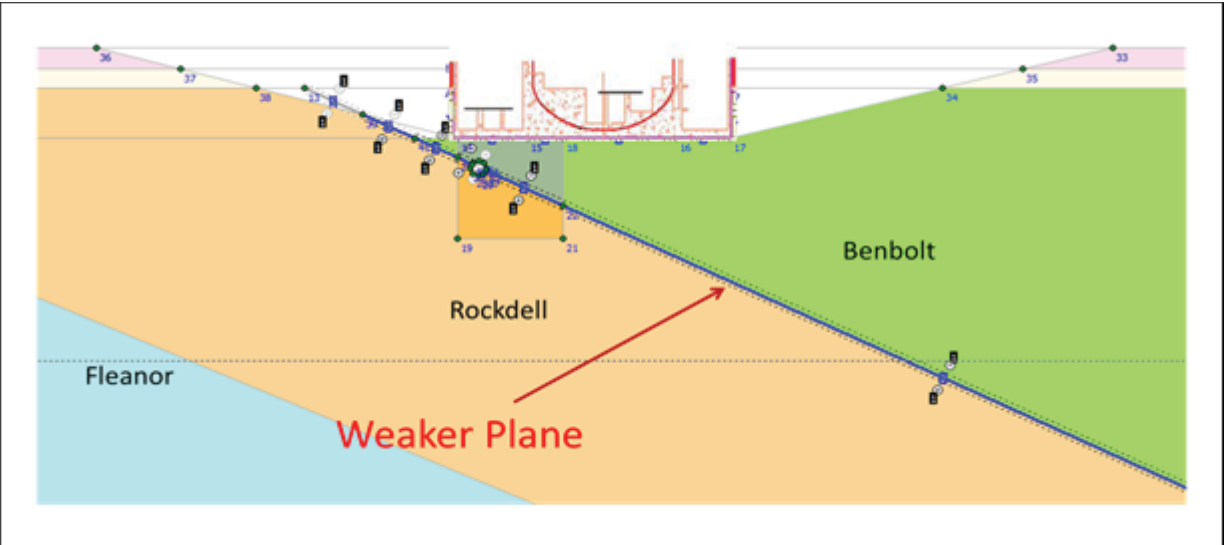
**Table 2.5.4-34  
Model Results in Loading Phases for Location A and B**

LOCATION <sup>(1)</sup>	SECTION <sup>(2)</sup>	FOUNDATION DEPTH <sup>(3)</sup> (ft)	CAVITY SIZE <sup>(4)</sup> (ft)	CRITICAL CAVITY LOCATION <sup>(5)</sup>	REMARKS <sup>(6)</sup>	RELATIVE SHEAR <sup>(7)</sup>	DEFORMATION <sup>(8)</sup> (ft)
Location A	A-A'	40	15	Center of common basemat Bedding (Benbolt-Rockdell)	5 ft below basemat 1 Interface	0.60	0.008
		90	15	Center of common basemat Bedding (Benbolt-Rockdell)	5 ft below basemat 1 Interface	0.70	0.008
		140	15	Bedding (Benbolt-Rockdell)	1 Interface	0.90	0.006
Location A	E-E'	40	15	Center of common basemat Center of common basemat	5 ft below basemat 5 ft below basemat	0.60	0.008
		90	15	Center of common basemat Bedding (Benbolt-Rockdell)	5 ft below basemat 1 Interface	0.60	0.008
		140	15	Bedding (Benbolt-Rockdell)	1 Interface	0.90	0.005
Location B	B-B'	40	15	Center of common basemat Bedding (Benbolt-Rockdell)	5 ft below basemat 1 Interface	0.80	0.008
		90	15	Center of common basemat Bedding (Benbolt-Rockdell)	5 ft below basemat 1 Interface	0.95	0.009
		140	15	Bedding (Benbolt-Rockdell)	1 Interface	0.75	0.011
Location B	F-F'	40	15	Center of common basemat Center of common basemat	5 ft below basemat 5 ft below basemat	0.90	0.007
		90	15	Center of common basemat Bedding (Benbolt-Rockdell)	5 ft below basemat 1 Interface	0.92	0.011
		90	15	Bedding (Benbolt-Rockdell)	1 Interface	0.75	0.007
		90	15	Center of common basemat Bedding (Benbolt-Rockdell)	5 ft below basemat 1 Interface	0.70	0.010
					1 Interface	0.90	0.006

Reference 2.5.4-59 Table 3-1

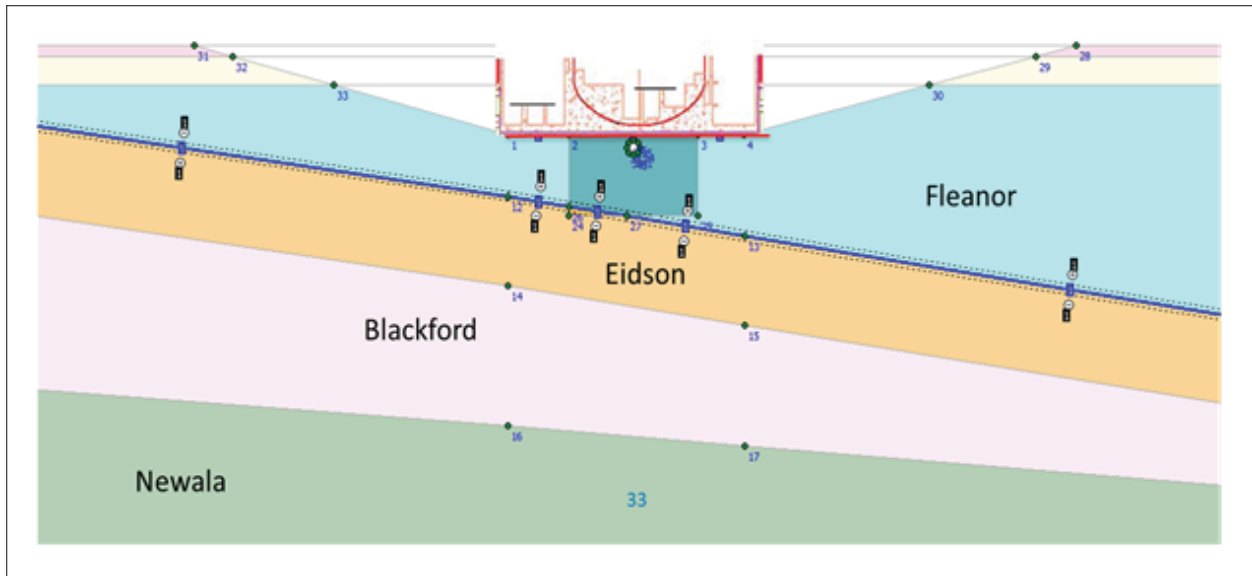
**Notes:**

- (1) The CRN Site contains two locations for safety related structures.
- (2) Typical Modeled Location A and B cross sections, relative shear values and vertical deformations (see Figure 2.5.4-27 through Figure 2.5.4-30).
- (3) Modeled foundation embedment depth (ft below ground surface).
- (4) Critical cavity diameter.
- (5) Critical cavity locations.
- (6) Additional detail related to cavity location. For Location A, "1 interface" indicates a single interface element introduced on both sides of the contact between the Benbolt and Rockdell formations. For Location B, "1 interface" indicates a single interface element introduced on both sides of the contact between the Fleanor and Eidson members of the Lincolnshire Formation.
- (7) Calculated relative shear.
- (8) Calculated vertical deformation.



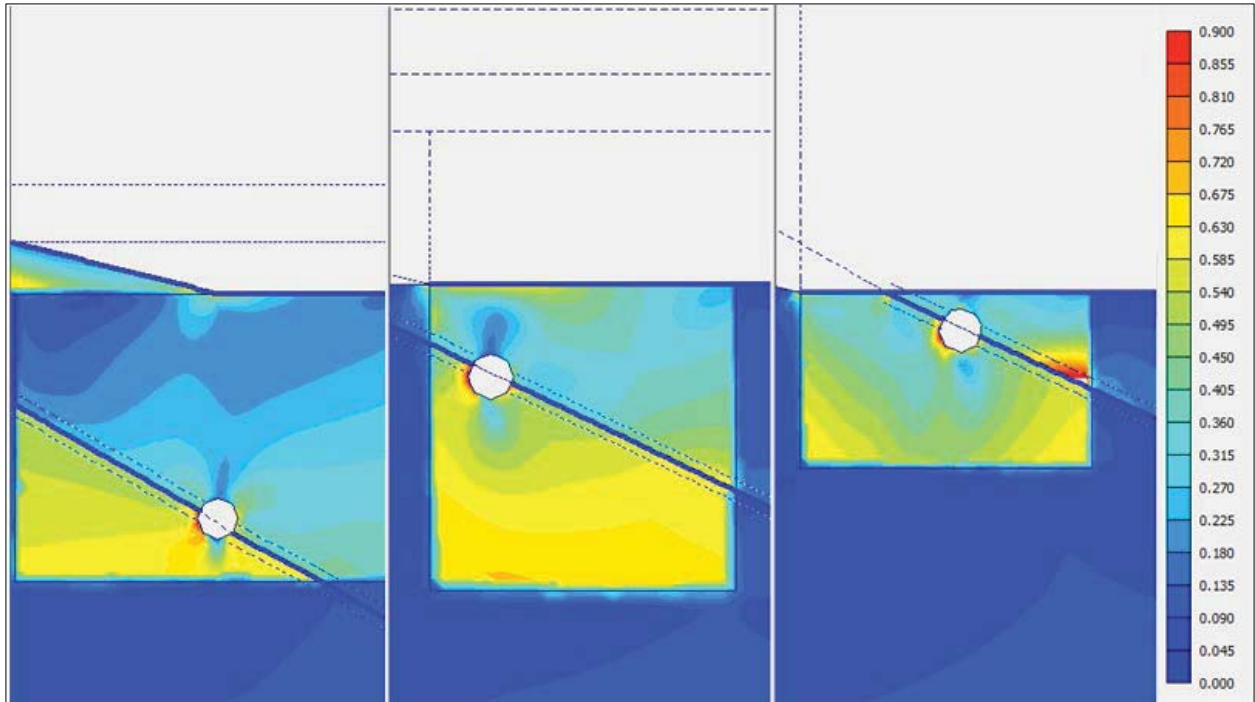
Note: Reference 2.5.4-59 Figure 2-14

**Figure 2.5.1-27**  
**Location A, Cross Section: A-A'**  
**Cavity Diameter: 15 ft, Embedment Depth: 90 ft**  
**Cavity Location: 30 ft Below Edge of Common Basemat, Bedding Plane,**  
**Shear Joint Interface**



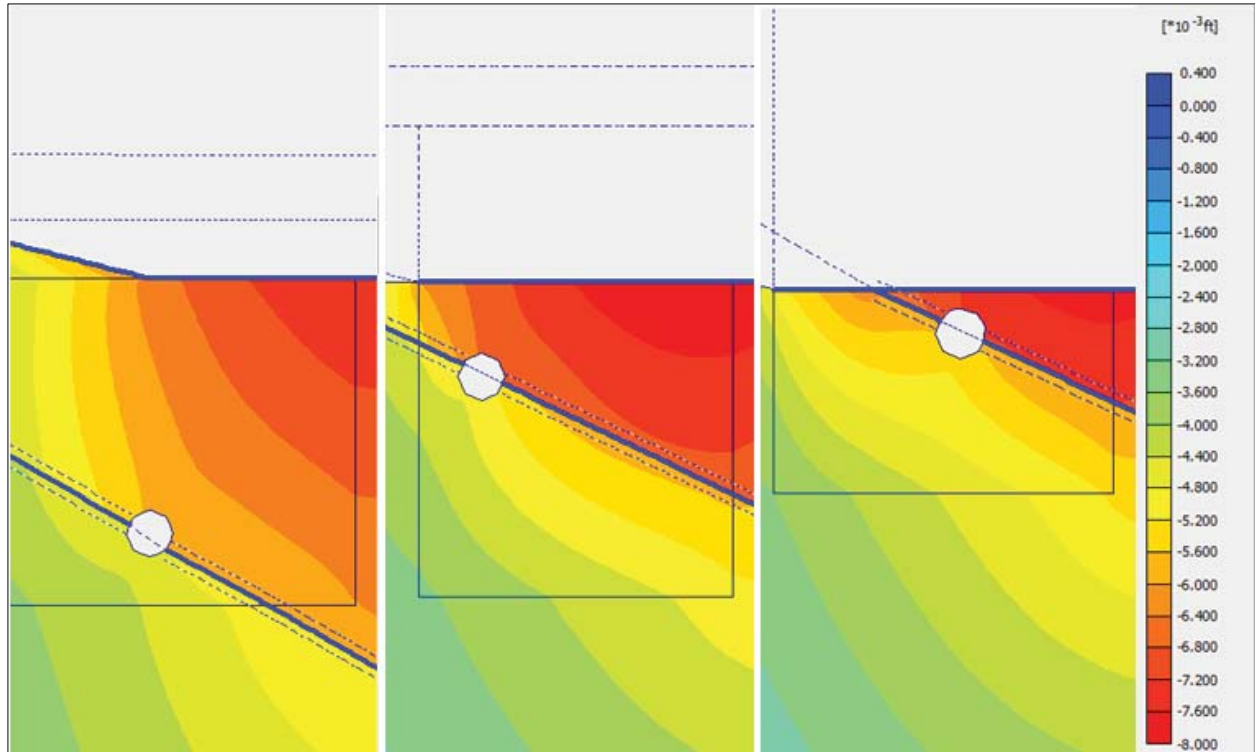
Note: Reference 2.5.4-59 Figure 2-29

**Figure 2.5.4-28**  
**Location B, Cross Section: F-F'**  
**Cavity Diameter: 15 ft, Embedment Depth: 90 ft, Cavity Depth: 5 ft Below Foundation,**  
**Cavity Location: Center of Common Basemat with Shear Fracture Zone Interface**



Note: Reference 2.5.4-59 Figure 3-7

**Figure 2.5.4-29**  
**Example Relative Shear Value Results for Foundation Embedment depths of 140 ft (Left), 90 ft (Center), and 40 ft (Right)**



Note: Reference 2.5.4-59 Figure 3-8

**Figure 2.5.4-30**  
**Example Results for Vertical Deformations for Foundation Embedment depths of 140 ft (Left), 90 ft (Center), and 40 ft (Right)**